



National Library
of Canada

Bibliothèque nationale
du Canada

Canadian Theses Service

Services des thèses canadiennes

Ottawa, Canada
K1A 0N4

CANADIAN THESES

THÈSES CANADIENNES

NOTICE

The quality of this microfiche is heavily dependent upon the quality of the original thesis submitted for microfilming. Every effort has been made to ensure the highest quality of reproduction possible.

If pages are missing, contact the university which granted the degree.

Some pages may have indistinct print especially if the original pages were typed with a poor typewriter ribbon or if the university sent us an inferior photocopy.

Previously copyrighted materials (journal articles, published tests, etc.) are not filmed.

Reproduction in full or in part of this film is governed by the Canadian Copyright Act, R.S.C. 1970, c. C-30. Please read the authorization forms which accompany this thesis.

AVIS

La qualité de cette microfiche dépend grandement de la qualité de la thèse soumise au microfilmage. Nous avons tout fait pour assurer une qualité supérieure de reproduction.

S'il manque des pages, veuillez communiquer avec l'université qui a conféré le grade.

La qualité d'impression de certaines pages peut laisser à désirer, surtout si les pages originales ont été dactylographiées à l'aide d'un ruban usé ou si l'université nous a fait parvenir une photocopie de qualité inférieure.

Les documents qui font déjà l'objet d'un droit d'auteur (articles de revue, examens publiés, etc.) ne sont pas microfilmés.

La reproduction, même partielle, de ce microfilm est soumise à la Loi canadienne sur le droit d'auteur, SRC 1970, c. C-30. Veuillez prendre connaissance des formules d'autorisation qui accompagnent cette thèse.

**THIS DISSERTATION
HAS BEEN MICROFILMED
EXACTLY AS RECEIVED**

**LA THÈSE A ÉTÉ
MICROFILMÉE TELLE QUE
NOUS L'AVONS REÇUE**



National Library
of Canada

Bibliothèque nationale
du Canada

Ottawa, Canada
K1A 0N4

TC -

IS

0-315-23245-5

CANADIAN THESES ON MICROFICHE SERVICE - SERVICE DES THÈSES CANADIENNES SUR MICROFICHE

PERMISION TO MICROFILM - AUTORISATION DE MICROFILMER

• Please print or type - Écrire en lettres moulées ou dactylographier

AUTHOR - AUTEUR

Full Name of Author - Nom complet de l'auteur

DEAN LORNE CUMSTAD

Date of Birth - Date de naissance

JAN 19 / 1958

Canadian Citizen - Citoyen canadien

☒ Yes / Oui

☐ No / Non

Country of Birth - Lieu de naissance

CANADA

Permanent Address - Résidence fixe

5204 - 111 A Street
Edmonton Alberta
T6H 3G9

THESIS - THÈSE

Title of Thesis - Titre de la thèse

A Microprocessor-based Corneal Blood
Flow Measurement System

Degree for which thesis was presented
Grade pour lequel cette thèse fut présentée

Master of Science

Year this degree conferred
Année d'obtention de ce grade

1985

University - Université

University of Alberta

Name of Supervisor - Nom du directeur de thèse

Dr Z J Koles

AUTHORIZATION - AUTORISATION

Permission is hereby granted to the NATIONAL LIBRARY OF CANADA to
microfilm this thesis and to lend or sell copies of the film.

The author reserves other publication rights, and neither the thesis nor extensive extracts from it may be printed or otherwise reproduced without the author's written permission.

L'autorisation est, par la présente, accordée à la BIBLIOTHÈQUE NATIONALE DU CANADA de microfilmer cette thèse et de prêter ou de vendre des exemplaires du film.

L'auteur se réserve les autres droits de publication; ni la thèse ni de longs extraits de celle-ci ne doivent être imprimés ou autrement reproduits sans l'autorisation écrite de l'auteur.

ATTACH FORM TO THESIS - VEUILLEZ JOINDRE CE FORMULAIRE À LA THÈSE

Signature

Dean Lorne Cumstadi

Date

Oct 1 / 85

THE UNIVERSITY OF ALBERTA

A Microprocessor-based Cerebral Blood Flow Measurement
System

by

Dean Lorne Olmstead

A THESIS

SUBMITTED TO THE FACULTY OF GRADUATE STUDIES AND RESEARCH
IN PARTIAL FULFILMENT OF THE REQUIREMENTS FOR THE DEGREE
OF Master of Science

Department of Electrical Engineering

EDMONTON, ALBERTA

Fall, 1985

THE UNIVERSITY OF ALBERTA

RELEASE FORM

NAME OF AUTHOR Dean Lorne Olmstead
TITLE OF THESIS A Microprocessor-based Cerebral Blood
 Flow Measurement System
DEGREE FOR WHICH THESIS WAS PRESENTED Master of Science
YEAR THIS DEGREE GRANTED Fall, 1985

Permission is hereby granted to THE UNIVERSITY OF ALBERTA LIBRARY to reproduce single copies of this thesis and to lend or sell such copies for private, scholarly or scientific research purposes only.

The author reserves other publication rights, and neither the thesis nor extensive extracts from it may be printed or otherwise reproduced without the author's written permission.

(SIGNED) *Dean L. Olmstead*

PERMANENT ADDRESS:

..... 5204 - 111A Street
.....
..... Edmonton, Alberta
.....
..... T6H 3G9
.....

DATED September 19 1985

THE UNIVERSITY OF ALBERTA
FACULTY OF GRADUATE STUDIES AND RESEARCH

The undersigned certify that they have read, and recommend to the Faculty of Graduate Studies and Research, for acceptance, a thesis entitled A Microprocessor-based Cerebral Blood Flow Measurement System submitted by Dean Lorne Olmstead in partial fulfilment of the requirements for the degree of Master of Science.

.....Z. J. Koles.....
Supervisor
.....Dennis M. Penon.....
.....M. J. Timoney.....
.....L. L.dk.....

Date...September.19..1985.....

Abstract

A microprocessor-based data acquisition, display, and analysis system, was developed to measure cerebral blood flow, by means of the ^{133}Xe inhalation method. It is used in conjunction with a Medimatic Inhamatic rCBF System, which contains the scintillation detectors, the amplifier and counting circuits, and the ^{133}Xe administration system. The microprocessor system was developed in order that the acquisition of cerebral blood flow data could be monitored in real-time, stored on floppy disk, and subsequently graphically displayed and analyzed. The data analysis utilizes a two-compartment exponential model in which a faster clearing compartment, considered to be cerebral grey matter, is separated from a slower clearing compartment, considered to be white matter and extracerebral tissue. This mobile system is relatively simple to operate, and provides accurate and onsite analysis of data and results. The application of this cerebral blood flow system will potentially benefit studies of a variety of cerebral circulatory conditions, and assist the clinician in developing accurate prognoses to improve the condition of the patient.

This thesis is intended to describe the design and development of this microprocessor-based system, and to review the theory of cerebral blood flow measurement as it relates to this project.

Acknowledgements

As with most multidisciplinary projects, the development of this system involved the efforts of many individuals other than myself. In particular, I would like to thank Mr. Narc Ouellette and Mr. Elias Haska for their considerable technical advice and assistance. Also, the input and advice of Dr. Devidas Menon, particularly with regards to the theory and methodology of cerebral blood flow, was greatly appreciated. I would also like to thank Dr. L. Disney, of the Department of Neurosurgery, for his cooperation and patience as the bugs of this system were gradually worked out.

I would especially like to recognize the contribution of my supervisor, Dr. Zoly Koles, who provided constant advice and encouragement during the duration of my master's program. I would also like to thank Dr. Koles for his financial support. And to all my other friends in the Department of Applied Sciences in Medicine, I would like to offer my appreciation for their assistance given from time to time, and for making my stay a pleasurable one.

And lastly, but not least, I would like to thank my wife, Deb, for her constant love and encouragement throughout the period of time I spent in classes and working on this thesis, and also, for the considerable time and effort she spent on typing and proofreading this thesis.

Table of Contents

Chapter	Page
1. Introduction	1
1.1 Raisons d'être	1
1.2 Anatomy	4
1.3 Physiology	8
1.4 Applications	10
2. Methods of Cerebral Blood Flow Measurement	16
2.1 Non-Diffusible Indicator Methods	17
2.1.1 Transit Time	17
2.1.2 Indicator Dilution Technique	19
2.2 Freely Diffusible Indicator Methods	19
2.2.1 Heat Clearance	20
2.2.2 Hydrogen Clearance	20
2.2.3 Kety-Schmidt Method	20
2.2.4 Intra-Arterial ^{133}Xe Xenon Method	25
2.2.4.1 Calculation of Regional Cerebral Blood Flow	27
2.2.4.2 Advantages and Disadvantages	33
2.2.5 Inhalation ^{133}Xe Xenon Method	34
2.2.5.1 Sources of Error	35
2.2.5.2 Initial Slope Index	42
2.2.5.3 Advantages and Disadvantages	44
2.2.6 Intravenous ^{133}Xe Xenon Method	45
2.3 Three-Dimensional Methods	46
3. System Hardware	50
3.1 Inhamatic System	50
3.1.1 Detectors	53

3.1.2	Electronics	57
3.1.2.1	Amplifier Modules	57
3.1.2.2	High Voltage Module	58
3.1.2.3	Ratemeter Modules	59
3.1.2.4	Counting System Module	59
3.1.2.5	Interface Module	62
3.1.3	Xenon Administration System	66
3.2	Microprocessor System	68
3.2.1	Microcomputer	68
3.2.1.1	System Structure	70
3.2.1.2	Microprocessor Architecture	72
3.2.1.3	Programmable Systems Interface	74
3.2.1.4	Asynchronous Communications Controller	78
3.2.1.5	Memory	79
3.2.2	Floppy Disk Drive	80
3.2.3	Terminals	81
4.	System Software	83
4.1	Software Organization	83
4.1.1	Terminal Software Support	88
4.2	Data Acquisition	92
4.3	Data Display	107
4.3.1	Viewpoint Terminal Display	109
4.3.2	Tektronix 4010 Graphical Display	109
4.4	Data Analysis	114
4.4.1	Air Curve Analysis	115
4.4.2	Head Curve Analysis	117

5. System Evaluation	121
5.1 Performance	121
5.2 Possible Improvements	130
5.3 Conclusion	132
References	135
Appendix A. Radiation Dosage and Decay Scheme of ¹³³ Xenon	150
Appendix B. ¹³³ Xenon Filling and Measuring Procedure	154

List of Tables

Table	Page
4.1 Data Acquisition Mode Command Menu	86
4.2 Analysis Mode Command Menu	87
A.1 Emissions in the Decay Scheme of ^{133}Xe	151
A.2 Radiation Dosage Levels	153

List of Figures

Figure	Page
2.1 Arteriovenous N ₂ O Concentration Curves	23
2.2 Exponential Stripping Procedure	31
2.3 Inhalation Method Clearance Curves	36
3.1 System Block Diagram	51
3.2 Scintillation Detector and Amplifier Module Diagram	55
3.3 Block Diagram of Counting System	60
3.4 Block Diagram of Interface Module	64
3.5 Handshaking Protocol	66
3.6 Inhamatic/Microprocessor Interface	67
3.7 ¹³³ Xenon Administration System	69
3.8 Microcomputer, Block Diagram	71
4.1 Basic System Task Flowchart	85
4.2 Data Acquisition Flowchart	93
4.3 Data Interrupt Service Routine Flowchart	99
4.4 Real-Time Data Display Subroutine Flowchart	104
4.5 Display Subroutine Flowchart	108
5.1 Large Graphic Display of Head Data	123
5.2 Small Graphic Display of Head Data	124
5.3 Raw Air Curve Data	125
5.4 Calculated Air Curve Data	126
A.1 Decay Scheme of ¹³³ Xenon	150

List of Plates

Plate	Page
3.1 Front Panel of Inhamatic System	52
3.2 Microprocessor-based Cerebral Blood Flow System	52

1. Introduction

The intent of this thesis is to review the theory of cerebral blood flow (CBF) measurement as it relates to this project and to describe the design and development of a microprocessor controlled system to measure cerebral blood flow. This chapter includes a description of the requirements and *raisons d'être* of such a system in terms of the University of Alberta Hospitals, as well as the applications of cerebral blood flow measurement techniques universally. In addition, a brief introduction to the anatomy and physiology of the brain and its blood flow is included to aid the reader in understanding some of the subsequent discussions and descriptions. Chapter two is a review of the theory of cerebral blood flow methodology with an emphasis on that which relates specifically to this system. The hardware and software aspects of the microprocessor controlled system are described in chapters three and four, respectively. An evaluation of the existing system along with recommendations for possible improvements is presented in chapter five.

1.1 Raisons d'être

The original objectives of the proposed system were to provide accurate and reliable quantitative measurements of cerebral blood flow that were atraumatic (ie. non-invasive) to the patient. The system was to be mobile in order that it could be utilized throughout the hospital, and it was to

provide rapid and onsite analysis of data and results. The operation of the system needed to be designed for non-technical users, and therefore it had to be relatively simple to operate and yet still allow flexible use of the system.

Furthermore, it was proposed that the overall system should incorporate an existing commercially obtained system which the hospital had previously purchased'. This system had the capabilities of collecting data and storing it on paper tape, and administering the radioisotope gas to the patient but it was not able to effectively monitor the data collection in real-time, graphically display or analyze the data. What was required, therefore, was a system which could be easily interfaced with the Inhamatic system and provide rapid and onsite data analysis and data display functions that the Inhamatic system could not previously perform.

The system that was designed to fulfill these requirements utilizes a 16-bit Texas Instrument TMS-9900 microprocessor, along with two 8-inch floppy disk drives and either a Tektronix 4010 or an ADDS Viewpoint terminal. The operator is able to run the entire system via the terminal's keyboard using menu-driven software. This microprocessor controlled system performs four primary functions:

1. The system collects data from the Inhamatic via its papertape punch interface port and stores it in RAM.
2. Subsequently, the user may store the collected data on

'Medimatic Inhamatic rCBF System (Denmark)

floppy disk for later analysis and/or display.

3. The data can be displayed on the Viewpoint terminal in bar graph form or on the Tektronix terminal in graphical form.
4. The data can be analyzed onsite according to a two-compartment exponential decay model and the regional blood flow values calculated and displayed.

In addition, the system has the capability of uploading the data to a VAX 11-750 computer where further data analysis may occur.

A commercially available system does exist that can be interfaced with the Inhamatic system but it was considered too expensive and inflexible for the clinical and research purposes envisioned. An advantage of an in-house designed system is that it can be customized and modified to suit the specific requirements of the individual users' or research programs.

The method of administering the radioisotope gas was chosen to be inhalation primarily because of its atraumatic nature. For the class of patients that the cerebral blood flow measurements were expected to be performed on, an invasive procedure, such as the intra-arterial technique, was not considered to be a desirable option. The algorithm that is used to calculate the blood flow is one that is commonly in use in other cerebral blood flow facilities, and is based upon the algorithm employed by Obrist et al.[59] with modifications by Risberg et al.[66]. Its wide

acceptance and extensive investigations, which have shown it to produce stable and reliable regional cerebral blood flow data, are some of the reasons why this algorithm was chosen.

1.2 Anatomy

The nervous system is composed of two parts, the central nervous system and the peripheral nervous system. The peripheral nervous system consists of the cranial and spinal nerves, while the central nervous system is represented by the brain and spinal cord. The human brain is a relatively small structure weighing about 1400 grams, constituting about 2% of the total body weight, and yet it receives about 15% of the cardiac output of blood. This is indicative of the high metabolic rate of the brain tissues.

The brain consists of three basic subdivisions, the cerebrum, the brainstem, and the cerebellum. The brain stem is composed of the medulla, pons and midbrain. It is the stalk of the brain, through which pass all the nerve fibers relaying signals between the spinal cord and the higher brain centers. The brainstem also contains numerous neuronal circuits which control respiration, cardiovascular function, gastrointestinal function, eye movement, equilibrium, and other special movements of the body. The cerebellum sits on top of the brainstem. It does not initiate movement but acts by influencing other regions of the brain responsible for motor activity. The cerebellum is especially vital to the control of very rapid muscular activities.

The large part of the brain that remains is the cerebrum, or the cerebral hemispheres. The two highly convoluted hemispheres are partially separated by a prominent longitudinal fissure. Each of these hemispheres is covered with a cellular mantle of grey matter, the cerebral cortex. The cortex is a shell approximately a half centimeter thick, containing upwards of 50 billion neurons and having a total surface area of about one-quarter square meter. Its purpose is multifaceted but includes providing a high degree of sensory analysis of the spatial, temporal and associative aspects of sights, sounds, body sensations, tastes and smells. Through interactions with other areas of the brain, the cortex acts to organize skilled responses and movements, and also provides for memory. The topography of the cortex is defined by convolutions (or gyri) separated by sulci (shallow grooves) and fissures (deeper grooves) which divide it into several identifiable lobes: frontal, parietal, occipital and temporal. The occipital lobe deals with visual processing. The temporal lobe is involved in analyzing sounds, vestibular messages, and smells; it also appears to store memories. The parietal lobe is the domain of the somatosensory cortex and the sense of taste. In the frontal lobe lie the motor cortex and speech area.

The cortex is an area of grey matter, so called because of the predominance of cell bodies. In other parts of the cerebrum, underlying the cortex, nerve-fiber tracts predominate, their whitish myelin coating distinguishing

them as white matter. There is, however, another area of grey matter which lies beneath the cortex, known as the subcortical nuclei.

The blood supply of the contents of the cranial cavity is derived from two pairs of arteries in the neck. These are the common carotid and the vertebral arteries. The paired carotid arteries carry 85% of the cerebral blood flow, with the remaining 15% passing through the vertebral arteries.

The common carotid arteries originate at the aortic arch and ascend through the neck. Below the base of the skull, each divides into an external and internal carotid artery. Each internal carotid artery enters the cranial cavity and divides into an anterior and middle cerebral artery. The rate of vascular flow through each internal carotid artery is rapid (350 millilitres/minute), and the diameter of the vessel is large (3.7 to 4.5 millimetres). The external carotid artery supplies primarily the facial and scalp regions of the head.

The vertebral arteries ascend along the cervical vertebrae and enter the cranial cavity through the foramen magnum. They join on the surface of the brainstem to form the basilar artery which ends dividing into two posterior cerebral arteries. The vertebral arteries also supply the brainstem and cerebellum.

The carotid and vertebral arteries unite at the base of the brain to form the circle of Willis. This vascular loop connects the two carotid arteries with each other and with

the basilar artery, thus providing collateral circulatory routes to protect the vulnerable brain tissue from ischemia (ie. low blood flow). Normally little blood is exchanged between the two sides of the circle, due to the equality of blood pressure, however, if the blood from one of the three vessels entering the circle is occluded or reduced, then the circle of Willis helps to equalize blood flow to various brain regions.

The brain is drained by two sets of veins. One is the deep or great cerebral venous system which eventually empties into dural venous sinuses, and thereby reaches the internal jugular veins. Another set drains the superficial part of the brain and also empties into dural venous sinuses.

The capillary network of the central nervous system is extensive, especially in the grey matter. What is of unique importance, however, is that these capillaries have permeability characteristics that are fundamentally different from those of capillaries elsewhere in the body. The tight junctions between the endothelial cells of the cerebral capillaries form the *blood-brain barrier*. This relatively impermeable barrier limits the diffusion of most substances, except for lipid-soluble compounds and water. This barrier may also prevent potentially therapeutic drugs from reaching the brain.

1.3 Physiology

The normal blood flow through brain tissue averages 50 to 55 millilitres per 100 grams of brain per minute.² The blood flow through the grey matter appears to average about 80 millilitres per 100 grams per minute, with the flow through the white matter about one-quarter of this.

The regulation of cerebral blood flow is closely related to at least three metabolic factors. These are carbon dioxide concentration, hydrogen ion concentration, and oxygen concentration. An increase in either the carbon dioxide or the hydrogen ion concentration increases cerebral blood flow, whereas a decrease in oxygen concentration increases the flow. Carbon dioxide increases cerebral blood flow by combining with water to form carbonic acid, with subsequent dissociation to form hydrogen ions. The hydrogen ions then cause vasodilatation of the cerebral vessels. In normal tissue, changing the carbon dioxide or hydrogen ion concentration has a dramatic effect on the cerebral blood flow. The effect of lowering the concentration of oxygen, in normal tissue, is much less marked. However, if the blood flow to the brain decreases sufficiently to allow cerebral hypoxia, the lack of oxygen causes vasodilatation to occur, thus returning the blood flow and the transport of oxygen to the cerebral tissues near to normal.

²Note that these flow values represent *tissue* blood flow as opposed to *vascular* blood flow mentioned in the previous section. The techniques described in this thesis measure brain tissue blood flow.

The aspect of the above discussion with which we must be concerned is that it is important when measuring cerebral blood flow by whatever method to also record the partial pressures of carbon dioxide and oxygen. The reactivity of cerebral blood flow to changes in carbon dioxide concentration is particularly important. Oleson, et al. [60], determined that correction of a flow value of a previous study should be carried out according to the equation:

$$CBF' = CBF^2 \cdot \exp(0.041) \cdot (PaCO_2' - PaCO_2^2) \quad (1.1)$$

where CBF' and $PaCO_2'$ represents, respectively, the cerebral blood flow and partial pressure of carbon dioxide of a current study, and CBF^2 and $PaCO_2^2$ represents that of a previous study. This corresponds to approximately a 4% change in blood flow per mm Hg in the partial pressure of carbon dioxide.

The cerebral blood vessels, in the normal brain, have the ability to alter their caliber in order to maintain a constant blood flow despite moderate alterations in arterial blood pressure (autoregulation). Cerebral blood flow is autoregulated very well between the pressure limits of 50 and 140 mm Hg. However, if the pressure falls below 50 or rises above 140 mm Hg, the flow will fall or rise accordingly.

In pathologic states, however, the physiological factors regulating blood flow, including autoregulation, may be modified or severely impaired. For example, in persons with hypertension, the range of arterial pressures within

which normal autoregulation occurs may be shifted upward. Also, following subarachnoid hemorrhage, the ability to maintain constant blood flow is probably decreased to some extent [81].

1.4 Applications

The dependence of the brain on a steady supply of oxygen and on the continuous removal of metabolites makes it uniquely vulnerable to circulatory insufficiency. The clinician's concern with the cerebral circulation extends beyond the field of cerebrovascular disease because the brain damage associated with a wide range of intracranial conditions, including head injuries, tumors, and infections, proves in the final analysis to be the consequence of some local circulatory disturbance. The demand, therefore, for more reliable and effective methods of assessing various aspects of the cerebral circulation are constantly increasing.

Many significant advances have been made in recent years in the development of techniques for measuring cerebral blood flow. Some of the more important developments in bringing cerebral blood flow measurement to its present state of the art have been the development of three-dimensional methods, the use of short-lived isotopic tracers, and the introduction of computer systems [49]. The use of microcomputers, in particular, has increased the applicability of the various cerebral blood flow methods.

The mobility of cerebral blood flow measuring systems are such that they now may be used in operating suites, intensive care units, emergency departments and other areas of the hospital [10,29].

Computers have especially facilitated the development of regional cerebral blood flow multi-detector systems. Regional CBF systems have been developed which record blood flow in as many as 256 isolated segments of the human cerebral cortex simultaneously [43]. The relative levels of blood flow are then imaged using colours or varying shades of gray. These large systems are often used to study the *localization of function* in the cerebral cortex. In normal tissue, changes in the level of blood flow in areas of the cortex reflect changes in the metabolism and activity of those tissues which correspond to specific sensory and motor functions.

An understanding of the cerebral circulation is fundamental to comprehension of the pathogenesis of *stroke*, an acute disease of the central nervous system caused by the occlusion or rupture of a brain artery. It is understandable, then, that cerebral blood flow techniques are essential to the prognosis and management of stroke [50,70]. Measurement of cerebral blood flow often provides the clinician with an indication of cerebrovascular responsiveness, which might provide a basis for selecting the proper treatment for a stroke patient. That is, it is often desirable to stress the cerebral circulatory system in

— some way, in order to measure its ability to respond to changing physiological conditions [73]. Examples of typical manoeuvres include changing the level of oxygen or carbon dioxide inhaled, raising or lowering the blood pressure, or by changing the blood volume, after which the change in cerebral blood flow is measured.

One of the earliest applications of cerebral blood flow measurement was in the prediction of the outcome of *carotid ligation* [73]. This operation is an established neurosurgical procedure for certain types of intracranial aneurysms. Measurements of CBF before and after trial carotid clamping make it possible to identify patients liable to develop ischemia. It has been established that when clamping of the carotid artery during surgery reduces regional cerebral blood flow below 18 mls to 20 mls/100 gms/minute for five minutes or longer, cerebral infarction with permanent neurologic deficit is likely to ensue [70].

Measurements of cerebrovascular reactivity might also provide a basis for selecting which patients suspected of *carotid arteriosclerosis* and other occlusive cerebrovascular diseases should have angiograms and what treatments may be most beneficial [73]. Analysis of cerebral blood flow measurements indicate that an increase in CBF after a carotid endarterectomy can be expected when the degree of stenosis has exceeded 90% [70]. Intra-operative cerebral blood flow measurements can also indicate when a shunt is appropriate.

By utilizing both cerebral blood flow measurements and therapeutic evaluation techniques, the medical complications of *subarachnoid hemorrhage* due to ruptured intracranial aneurysms can be diagnosed, and a program of treatment planned [53,70,82]. Attempts are being made to use cerebral blood flow measurements to identify patients, either before or during an intracranial operation, who are at risk of developing delayed cerebral ischemia. If a patient is neurologically well after a subarachnoid hemorrhage but shows a low blood flow, this may reflect severe cerebral arterial vasospasm. In such patients it may be advisable to delay intracranial surgery [16,73]. Weir et al. [82], however, have found that there is a poor correlation between vasospasm and reduced cerebral blood flow except when there is severe spasm. Nevertheless, cerebral blood flow measurements can still assist the clinician with decisions as to the timing of surgical treatment such as clipping aneurysms, evacuating hematomas, or relieving hydrocephalus.

Cerebral blood flow measurements are often used in determining the *effect of pharmaceutical drugs* on the cerebral circulation. Indeed, the cerebral blood flow system described in this thesis is being used by the Division of Neurosurgery at the University of Alberta to measure the effectiveness of the calcium antagonist drug Nimodipine in minimizing the occurrence of cerebral vasospasm [2]. Vasospasm often occurs in stroke patients four to twelve days following a subarachnoid hemorrhage.

Cerebral blood flow measurement techniques are also utilized in the study of various other cerebral disorders such as *dementia, migraine, epileptic seizures* and *severe head injuries*. In particular, it has been found that cerebral blood flow is reduced in dementia and the degree of flow alteration correlates well with the severity of the disorder [70]. Also, following an epileptic seizure, cerebral blood flow is usually decreased, while during a seizure, it increases by 100% or more.

Measuring cerebral blood flow in *secondary polycythemia* is currently taking place in the Department of Pulmonary Medicine using the described CBF system. Secondary polycythemia is a physiologic condition in which there is an excess production of red blood cells, resulting from a decreased oxygen supply to the tissues such as that occurring in association with pulmonary abnormalities. Because of the increase in the viscosity of the blood and the total blood volume, the blood flow becomes extremely sluggish. The measurement of cerebral blood flow in patients before and after venesection (letting of blood) has shown that this procedure leads in general to a significant increase in cerebral blood flow [69,89].

The potential applications of cerebral blood flow measurement techniques particularly in the area of stroke management, is plainly visible. The extent of utilization of these techniques, however, depends on the accuracy and reliability of the method employed and the degree of

traumatic effect it has on the patient. Also, the success of cerebral blood flow techniques will be measured, in part, by how well they can assist the clinician in prescribing preventive treatment to avoid ischemic brain damage. Or, as Teasdale and Mendelow [73] state:

"The key to improved clinical results lies in the devising of tests to identify patients whose cerebral circulatory reserve, although impaired, has not yet become critically exhausted. These patients might then be treated in ways that either avoid such stresses as hypoxia and hypotension or that increase the capacity of the cerebral circulation available to cope with adverse changes."

2. Methods of Cerebral Blood Flow Measurement

Quantitative studies of cerebral blood flow (CBF) have been possible for almost forty years. In this time, various methods and techniques have been developed to assist the researcher and physician in their quest for information as to the state of the cerebral circulation. These quantitative measurements can be of diagnostic importance or can assist the researcher in understanding the functions of the brain.

In general terms, methods of measuring cerebral blood flow can be divided into two basic groups:

1. methods using diffusible indicators, and
2. methods using non-diffusible indicators.

In principle, the indicator is, in some manner, introduced to the brain and subsequently removed by the bloodstream.

The blood flow is measured by recording the rate of indicator clearance, or by its dilution, either directly in the tissue, or by sampling arterial and venous blood. The indicator can be non-diffusible in that it remains within the cerebral vascular bed, or it can be freely diffusible, in which case it can easily cross the brain capillary wall, the so-called blood-brain barrier [40,78].

Measurement of vascular flow in neck arteries and veins can be accomplished using electromagnetic flow meters, ultrasound, thermovelocimetry, and thermodilution techniques. However, due to the multiplicity of arteries supplying the brain and the efficiency of the circle of Willis, the measurement of flow in a single cerebral blood vessel does

not permit conclusions to be drawn about brain tissue blood flow. In fact, one may find that one or more of the four major arteries that are anastomosed in the circle of Willis are occluded, and yet the cerebral blood flow remains at its normal level [23,40]. Nevertheless, techniques used in measuring blood flow in the neck are useful in yielding information as to the patency of these vessels, such as before and after reconstructive vascular surgery.

2.1 Non-Diffusible Indicator Methods

The use of non-diffusible indicators (indicators that do not leave the bloodstream) is among the oldest means of studying the cerebral circulation. The most commonly used is cerebral angiography, which can indicate not only the intracranial distribution of the radiopaque indicator but also the transit time from artery to vein. Cerebral angiograms provide excellent anatomical detail, allowing visual identification of blood vessels down to an inner diameter of approximately 0.1 millimeters [40].

2.1.1 Transit Time

Radioactive isotopes have been used to measure cerebral circulation time as early as 1929 when Wolff and Blumgart used radium C in cats [74]. The earlier techniques measured carotid-to-brain and brain-to-jugular vein transit times using detectors mounted over the neck and head and an intravenous injection of ^{131}I Iodine albumin. More recent

modifications have simplified this technique by mounting a detector over the head only. Following a rapid intravenous injections of ^{131}I -Iodine Hippuran, the passage of the indicator through the head is monitored over time, and the resulting curve is differentiated. The time between the maximum points on the differentiated uptake and clearance curve represents the mode circulation time. That is, it is the time between the maximum rate of entry and the maximum rate of exit (approximately 6.5 to 10 seconds in normal man) [23].

This method, although simple and perhaps attractive to the clinician, is a measurement of blood flow *velocity* and cannot yield quantitative information about cerebral blood flow unless the cerebral blood volume is known. A number of attempts to correlate mean transit time with cerebral blood flow have been made including one by Fieschi et al. [17], who found that

"the mean transit time in cerebral vessels of a bolus of non-diffusible indicator is a linear, though approximate, index of regional cerebral blood flow."

Other researchers, however, have found situations in which the cerebral blood flow was reduced but the circulation time of a non-diffusible indicator remained normal [12]. Most researchers today concur that while the transit time can be an index of cerebral blood flow, the correlation must be made within strict limits and conditions [23].

2.1.2 Indicator Dilution Technique

The Stewart-Hamilton dye dilution principle, which is used to measure cardiac output, can be adapted to measure cerebral blood flow. By injecting a known quantity of indicator into the internal carotid artery and sampling continuously from the internal jugular vein, a venous dilution curve can be obtained. Total cerebral blood flow can then be calculated from the formula

$$F(\text{ml/min}) = Q/(C \cdot t) \quad (2.1)$$

where Q is the quantity of indicator injected, C is the average concentration of the indicator, and t is the time of sampling [23].

This technique is cumbersome and invasive, and to get accurate results it is necessary to sequentially inject the indicator into both internal carotid arteries and sample from both internal jugular veins. As a result the dilution technique is considered impractical for routine clinical use.

2.2 Freely Diffusible Indicator Methods

The use of freely diffusible indicators in determining cerebral blood flow is currently, by far, the most common. The indicator used is primarily the radioisotope $^{133}\text{Xenon}$, although indicators such as heat, hydrogen gas, and other inert gases and radioisotopes are utilized in limited applications.

2.2.1 Heat Clearance

In this context heat may be considered as an inert freely diffusible indicator. Heat is applied locally by heated thermistors implanted in the brain tissue and then cleared by the bloodstream. Although this approach is widely used in studies in experimental animals [40], the highly invasive nature of this method limits its applicability in human studies.

2.2.2 Hydrogen Clearance

Hydrogen gas can be introduced to the brain by inhalation or an injection of hydrogen dissolved in saline into the internal carotid artery. A hydrogen clearance curve can then be obtained by either polarography using a platinum electrode inserted in the tissue [40] or by a catheter placed into each lateral sinus via the cephalic veins [70]. This method is equally traumatic as heat clearance, but has the advantage that quantitative cerebral blood flow can be more readily obtained.

2.2.3 Kety-Schmidt Method

This classical method, published in 1945 by Dr. Seymour S. Kety and Dr. Carl F. Schmidt, was the first which could quantitatively measure cerebral blood flow and cerebral metabolism in man [23,37,40,72]. It was based on the Fick principle which is a restatement of the law on conservation of matter. In its simplest form, it may be stated as

follows:

"The quantity of an inert gas taken up by a tissue is equal to the quantity entering the tissue via the arterial blood minus the quantity leaving in the venous blood." [70]

Kety and Schmidt [37], in applying this principle to blood flow in the brain, restated it in the following manner:

"the rate at which the cerebral venous blood content of an inert gas approaches the arterial blood content depends upon the volume of blood flowing through the brain."

The specific substance which is employed need not necessarily be a gas, but it must be physiologically inert, capable of diffusing rapidly across the blood-brain barrier, and susceptible of accurate analysis in the blood [37]. These qualifications are met by inert gases such as nitrous oxide, hydrogen, argon, krypton, and xenon.

The classical Fick formula may be written as

$$F = \frac{Q}{\int_0^t (C_a - C_v) dt} \quad (2.2)$$

where F is the blood flow (in millilitres/minute) through the organ of interest, Q is the amount of tracer removed from the bloodstream by the organ, and C_a and C_v are the concentrations of the tracer in arterial and venous blood, respectively. Because the brain is enclosed in skull and it is supplied by several collateral arteries, and drained primarily by two venous outputs, it is not possible to measure Q directly. In place of Q , Kety and Schmidt substituted the average *concentration* of the tracer in the

brain resulting in an estimate of the brain perfusion rate or blood flow per unit mass of tissue. If the assumption is made that the tracer reaches equilibrium between blood and brain tissue rapidly, the average concentration of the tracer in the brain tissue can be derived from the venous concentration. Thus, equation (2.2) may be modified as

$$CBF = \frac{100 \cdot \lambda \cdot C_v(t)}{\int_0^t (C_a - C_v) dt} \quad (2.3)$$

where CBF is the cerebral blood flow in millilitres/100 grams/minute, $C_v(t)$ is the venous concentration of the tracer at time t , and λ is the partition coefficient.

The partition coefficient λ is defined as the equilibrium concentration ratio of the tracer in brain tissue and blood. When using inert gases as tracers, this ratio equals the ratio of the solubility coefficients, using one gram and one millilitre as the unit of mass for tissue and blood, respectively. The solubility of many inert gases is somewhat less in grey matter (cortex) than in white matter, but within these two tissues no great variability is found. However, some variation does exist with respect to the inert gas solubility in blood because the percent volume of red cells (hematocrit) influences this factor. In normal tissue, this effect is easy to measure and correct [40,78]. In pathological tissue, however, the value of the partition coefficient may vary.

The Kety-Schmidt technique originally entailed having an individual inhale a 15% mixture of nitrous oxide and air for a period of ten minutes. During this saturation interval, blood samples were periodically taken from the femoral artery and jugular vein and analysed for nitrous oxide content. The arteriovenous concentrations were plotted over time (figure 2.1) and the cerebral blood flow subsequently calculated. Kety and Schmidt found average cerebral blood flow to be 54 millilitres/100 grams/minute in man [50,72].

Several modifications of the Kety-Schmidt technique have developed over the years. Most of the modifications have arisen in attempts to overcome the disadvantages of the original method. These disadvantages include: (1) the inability to measure *regional* cerebral blood flow, (2) the

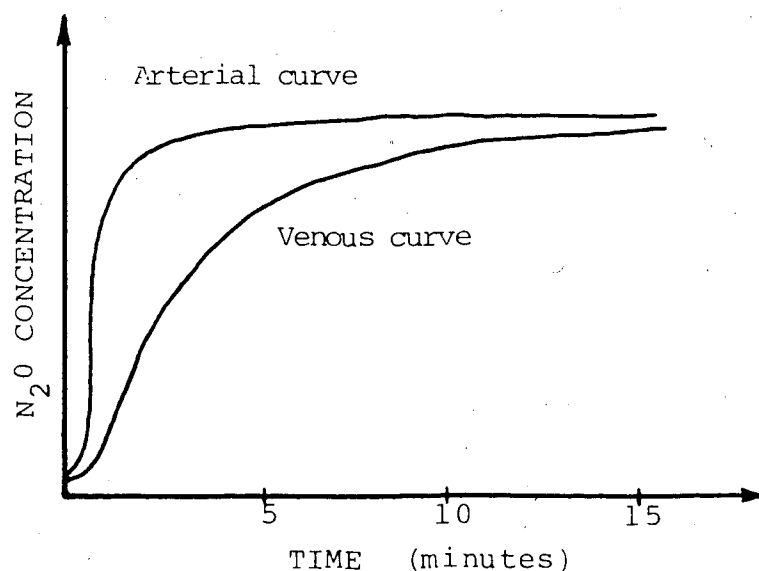


Figure 2.1 Arteriovenous N₂O Concentration Curves

invasive nature of the procedure, (3) the inability to differentiate between blood flow in grey and white matter and extracerebral tissue (only *mean* cerebral blood flow is measured), and (4) the cumbersome measurement techniques of nitrous oxide.

In 1955, Lassen and Munck substituted the radioactive inert tracer, $^{86}\text{Krypton}$, for nitrous oxide. The main advantages of this were avoiding the tedious analysis of nitrous oxide in blood and also $^{86}\text{Krypton}$ is completely physiologically inert. The same calculations were used as in the Kety-Schmidt procedure, but the period of saturation was extended to fifteen minutes and, in addition, the arteriovenous curves were extrapolated to infinity. The extrapolation was based on the observation that at the end of the saturation period, the arterial concentration is relatively constant and the venous concentration approaches the arterial in a monoexponential fashion. Extrapolation to infinity eliminates the systematic errors of incomplete saturation and the lack of equilibrium at the end of the period of study [50].

The success of the Kety-Schmidt technique depends to some extent on a constant concentration of the indicator that is being delivered to the patients' lungs. McHenry suggested, in 1963, that the need for precise control during inhalation would be eliminated if the *desaturation* curve, as opposed to the saturation curve, was used for the determination of cerebral blood flow [50,72]. Similar

calculations as with the saturation curve were used but, assuming the brain was fully saturated initially, more accurate estimates of cerebral blood flow could be obtained while making the procedure simpler.

While the Kety-Schmidt technique and its modifications are limited to measuring average cerebral blood flow, it is still considered as the reference method for studies in man [40]. A major advantage of this method is that the cerebral metabolism can be readily assessed by multiplying the flow with the corresponding arteriovenous differences of oxygen, glucose, and other metabolites [23,40].

2.2.4 Intra-Arterial ^{133}Xe Xenon Method

The Kety-Schmidt method and its modifications provides an average cerebral blood flow value. It is often necessary, however, to know *regional* cerebral blood flow (rCBF) values. That is, measurements of blood flow through circumscribed areas of the brain.

In the early 1960s, Ingvar and Lassen (1961) tackled the problem of quantitative measurement of regional cerebral blood flow by recording the rate of clearance from the exposed cerebral cortex of the beta emissions of ^{86}Kr following its injection into the carotid artery. This method was subsequently adapted by Glass and Harper (1963) who recorded the gamma emissions of ^{133}Xe through the intact skull and by Lassen and his co-workers (1963), who measured the gamma emissions of ^{86}Kr [23,40,42,50,72]. This

intra-arterial method has been refined considerably since the early experiments but is still based on the original principles as developed by Lassen and Ingvar. The method is currently the standard method for obtaining quantitative data on regional cerebral blood flow in man and animals [40].

The intra-arterial method usually entails dissolving 0.5 to 5.0 millicuries³ of ¹³³Xenon or ⁸⁵Krypton in saline solution and injecting it rapidly into the internal carotid artery. By selecting the internal carotid artery the brain is selectively labelled and contamination of extracerebral tissue such as the scalp and facial areas, is avoided. The gamma emissions of the isotope are detected by means of collimated scintillation crystals mounted externally to the patient's scalp. The degree of localization of radioactivity will depend on the size of the crystals and how narrowly they are collimated.

The inert gases krypton and xenon are quite suitable for this type of study because of their ability to diffuse rapidly across the blood-brain barrier. Also, as the solubility of these gases is much higher in air than in blood or tissue, a high proportion of it will, on reaching the lungs in the venous blood, be excreted into the alveolar air. Therefore, there will be no effective arterial recirculation. Accordingly, if an injection of ¹³³Xenon (or ⁸⁵Krypton), dissolved in saline, is made into the internal

³ The SI (Système International) unit for radiation activity is the becquerel (Bq); 1 curie = $3.7 \cdot 10^{10}$ Bq.

carotid artery, the isotope will equilibrate rapidly between the blood and brain tissue. When the injection is stopped, the arterial blood will wash the gas out of the brain tissue, and the rate of *washout* or clearance will depend on the blood flow. Because of its greater emission of gamma-rays, ^{133}Xe is the isotope more widely used for detection through the skull [40,70].

2.2.4.1 Calculation of Regional Cerebral Blood Flow

Two models are widely used in the computation of rCBF from the clearance curves: the "stochastic" model and the "compartmental" model.

Stochastic analysis

The stochastic model assumes that the transit time of a particle of tracer is a random variable, and thus the clearance curve represents the probability distribution of this variable. Suppose that the bolus of isotope arrives instantaneously in a circumscribed area of the brain and that it does not recirculate into the area. One can then imagine that each small part of the bolus, Δ_i , has a transit time of t_i minutes. The mean value of these transit times, \bar{t} , can therefore be calculated as the weighted average of the individual transit times, ie.,

$$\bar{t} = \frac{\sum(t_i \cdot \Delta_i)}{\sum \Delta_i} \quad (2.4)$$

This equation can be rewritten in terms of the clearance curve as,

$$\bar{t} = A/H \quad (2.5)$$

where A is the area under the curve extrapolated to infinity, and H is its peak value. This simplified derivation of equation (2.5) was first arrived at by Zierler [26,40,90]. This derivation presupposes that A is measured from time zero to infinity without any recirculation of tracer and that H is a measure of the total amount of indicator reaching the counting area. It is also assumed that the tracer is mixed evenly in the arterial blood and that the counting efficiency is uniform.

The relation between \bar{t} and the blood flow through the area is given by the classical equation discussed in detail by Meier and Zierler [51]:

$$\bar{t} = V/F \quad (2.6)$$

where V is the equilibrium volume of distribution (ie. the number of millilitres blood that would, at equilibrium, contain the same amount of indicator as the tissue), and F the total blood flow of that tissue. If this equation is expressed per gram of brain tissue, the Meier-Zierler theorem becomes:

$$\bar{t} = \lambda/f \quad (2.7)$$

where λ is the volume of distribution per gram of brain. Thus, λ is the partition coefficient of Kety, and f is the blood flow per gram of tissue. If we solve for f and express the equation per 100 grams of brain tissue, we obtain

$$rCBF = 100 \cdot \lambda \cdot H/A \quad (2.8)$$

where rCBF is the regional cerebral blood flow for the geometrical volume viewed by the collimated detector. This

is the same fundamental equation first derived by Kety and Schmidt for the saturation of the brain with an inert gas by applying the Fick principle. It is important to note that the basic parameter that is being measured in both cases is the mean transit time of a freely diffusible tracer.

Compartmental analysis

The compartmental model assumes that the cerebral circulation can be regarded as a bicompartamental exponential model in which the faster-clearing compartment, considered to be cerebral grey matter, is in parallel with the slower-clearing compartment, considered to be cerebral white matter. This assumption is supported mainly by the well-documented separation of local blood flow, in general, into two clusters: the fast flows of the different grey matters (cortex, nuclei, etc.), and the slow flows of the white matter [25,26,30,84]. With such a model the equations derived from the Fick principle, described by Kety [36], give for a particular tissue compartment i:

$$C_i(t) = C_i(0) \cdot \exp(-(f_i/\lambda_i) \cdot t) \quad (2.9)$$

where $C_i(t)$ and $C_i(0)$ are the concentrations of the isotope in the tissue at time t and time zero, respectively, f_i the blood flow (millilitres/gram/minute), and λ_i the volume of distribution of the tracer per gram tissue (millilitres/gram).

The average tissue concentration, $C(t)$, in a system

with two compartments in parallel, becomes:

$$C(t) = C(0) \cdot (A_g \cdot \exp(-k_g \cdot t) + A_w \cdot \exp(-k_w \cdot t)) \quad (2.10)$$

$$k_g = f_g / \lambda_g$$

$$k_w = f_w / \lambda_w$$

where f_g , λ_g , f_w , and λ_w are flow and λ values for grey and white matter, respectively, and A_g and A_w are a function of the ordinate value, $C(0)$, belonging to each of the two compartments. The initial distribution of the tracer to the grey and white matter is proportional to the flow within these substances multiplied by their relative weights. Thus, if W_g and W_w represent the relative weight of grey and white matter respectively (ie. $W_g + W_w = 1$), A_g and A_w may be written:

$$A_g = \frac{W_g \cdot f_g}{W_g \cdot f_g + W_w \cdot f_w} \quad (2.11)$$

$$A_w = \frac{W_w \cdot f_w}{W_g \cdot f_g + W_w \cdot f_w}$$

Therefore, if from the clearance curve k_g and k_w can be obtained, the respective flow values can be calculated (since λ_g and λ_w are known values). And if A_g and A_w can be obtained, the respective relative weights can be calculated from equations (2.11). The mean blood flow of the two compartments, \bar{f} , is then given by

$$\bar{f} = f_g \cdot W_g + f_w \cdot W_w \quad (2.12)$$

The four unknowns in equation (2.10) (ie. A_g , k_g , A_w and k_w) can be found using the measured clearance curve with a least-squares method of curve fitting. Alternatively, the blood flow values can be approximated by an exponential

stripping procedure [23,86]. In this procedure the clearance curve is replotted on a semilogarithmic graph. A straight line drawn through the tail of the curve is subtracted from the primary curve to produce a second straight line approximately equal to the slope of the initial portion of the curve (figure 2.2). The half-maximum time ($T_{1/2}$) of the resulting exponential components can then be calculated. The $T_{1/2}$ is the time taken for the radioactivity to decline to half its initial value. This procedure is based on the assumption that the first one or two minutes of the clearance curve represent primarily those regions with relatively high flow values and therefore the initial slope of the curve can be used to estimate the grey matter blood values [60]. Similarly, it is assumed the latter portion of the curve represents primarily the slow compartment (ie.

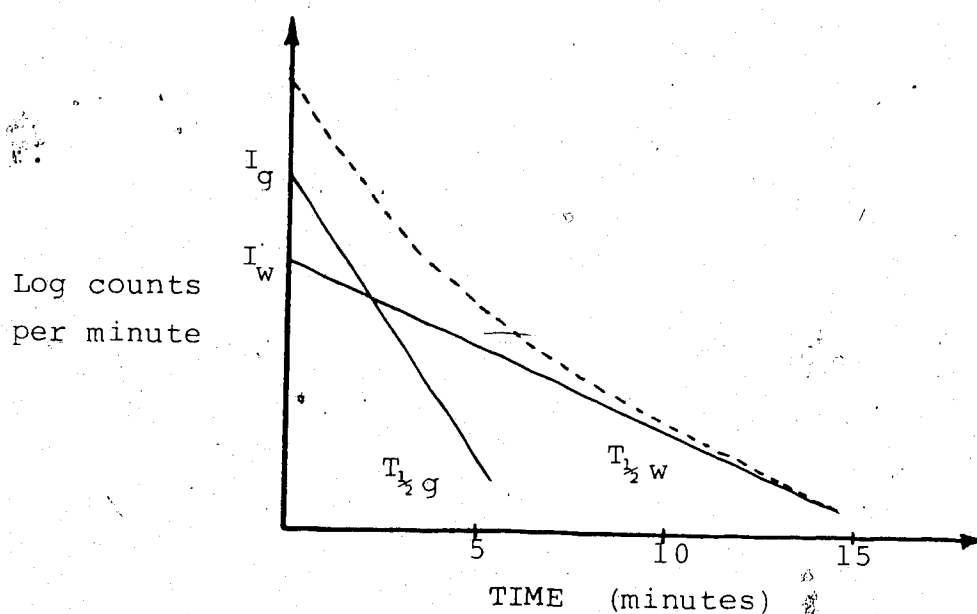


Figure 2.2 Exponential Stripping Procedure

white matter).

If equation (2.10) is rewritten as follows:

$$C(t) = I_g \cdot \exp(-k_g \cdot t) + I_w \cdot \exp(-k_w \cdot t) \quad (2.13)$$

values for the half-maximum times and zero time intercepts of the grey matter and white matter (ie. $T_{1/2g}$, $T_{1/2w}$, I_g , I_w , respectively) can be obtained using conventional graphical analysis. Blood flow and relative weight values can then be evaluated using the following equations:

$$f_g = \lambda_g \cdot k_g \approx \lambda_g \cdot \ln 2 / T_{1/2g} \quad (2.14)$$

$$f_w = \lambda_w \cdot k_w \approx \lambda_w \cdot \ln 2 / T_{1/2w}$$

$$W_g = \frac{I_g / f_g}{I_g / f_g + I_w / f_w} \quad (2.15)$$

$$W_w = 1 - W_g$$

The brain-blood partition coefficients for grey and white cerebral matter have been measured for a range of hemoglobin concentrations in normal tissue by Veall and Mallett [78]. Values that are typically used are (for a hemoglobin concentration of 15 grams/100 millilitres) 0.80, 1.50 and 1.08 (grams/millilitre) for grey matter, white matter, and brain homogenate respectively.

Initial Slope Analysis

A simplification of the exponential stripping procedure, described by Olesen et al. [60], determines an approximate value for the blood flow of grey matter only by using the initial slope of the clearance curves. This initial slope analysis assumes that the blood flow through the grey matter dominates the initial portion of the

clearance curve to such an extent that the slower component may be disregarded. Thus, the initial one to two minutes of the clearance curve can be regarded as monoexponential [60]. For this portion of the curve equation (2.9) may be rearranged and reduced to:

$$d(\ln C(t))/dt = -f/\lambda \quad (2.16)$$

or, in terms of the blood flow, f ,

$$f = -\lambda \cdot d(\ln C(t))/dt \quad (2.17)$$

A blood flow value can then be quickly calculated from that part of the curve, knowing the logarithmic slope. As already mentioned, this calculation provides only an approximate value of the blood flow of grey matter. An advantage of this method is that only a brief portion of the clearance curve is needed thus allowing the possibility of performing repetitive measurements and also rapid analysis.

2.2.4.2 Advantages and Disadvantages

The intra-arterial method has a distinct advantage over the classical Kety-Schmidt technique and its modifications, in that estimates of *regional* cerebral blood flow can be obtained. Also, if the injection of inert gas is made into the internal carotid artery, extracerebral contamination of radioactivity is avoided. The subsequent clearance of the radioisotope from the brain tissue can then be followed using external scintillation detectors.

The principal disadvantage of the method is the necessity for a carotid artery puncture and catheterization. In patients with cerebral vascular disease there is

potential risk in this method [50]. For this reason it is usually used in the operating theatre or in combination with cerebral angiography. Another drawback is that the carotid catheterization should be carried out under fluoroscopic guidance to insure that the catheter has indeed passed into the internal carotid artery rather than into the external carotid artery. Also, unless both carotid arteries are injected with the inert gas, only one cerebral hemisphere can be accurately monitored. Because of these limitations a search for a less traumatic method was made.

2.2.5 Inhalation ^{133}Xe Method

The inhalation method is based on the same principles as the intra-arterial method. However, instead of injecting ^{133}Xe into the carotid artery, the radioisotope is administered to the patient by allowing him/her to breathe ^{133}Xe on a closed-circuit breathing system for a period of one to five minutes. Mallett and Veall pioneered this atraumatic method of measuring regional cerebral blood flow in 1963 [47,48].

The inhalation technique is a very attractive method clinically because of its atraumatic nature. However, it suffers from two major disadvantages. The first is that during the period of inhalation all the body tissues take up the isotope. Consequently, there is an appreciable amount of recirculation with subsequent distortion of the clearance curves. The second disadvantage is the contamination of the

clearance curves by radioactivity in the scalp and extracranial tissues.

2.2.5.1 Sources of Error

Recirculation

Mallett and Veall attempted to correct for recirculation of the radioisotope by measuring the radioactivity of the expired air. They discovered that the concentration of xenon in the end-expired air was closely correlated with the concentration found in the arterial blood [79]. The administration of ^{133}Xe by inhalation can then be considered as a series of intra-arterial injections; each subsequent injection being of a different size depending on the height of the end-expired air curve at that time. In mathematical terms this means that the output response, as measured by the external detectors, is the convolution of the input response, ie. the end-expiratory curve, and the impulse response of the cerebral tissue. The cerebral blood flow can be calculated, therefore, using a deconvolution procedure. That is, one attempts to estimate the impulse response which would have been seen had an intra-arterial injection been made, from which the cerebral blood flow can be determined.

• The equations which describe the measured clearance curves are derived from the Fick principle and have been described in detail, along with their underlying assumptions, by Kety [36,58,59]. The equations, which include a correction for recirculation, can be written for a

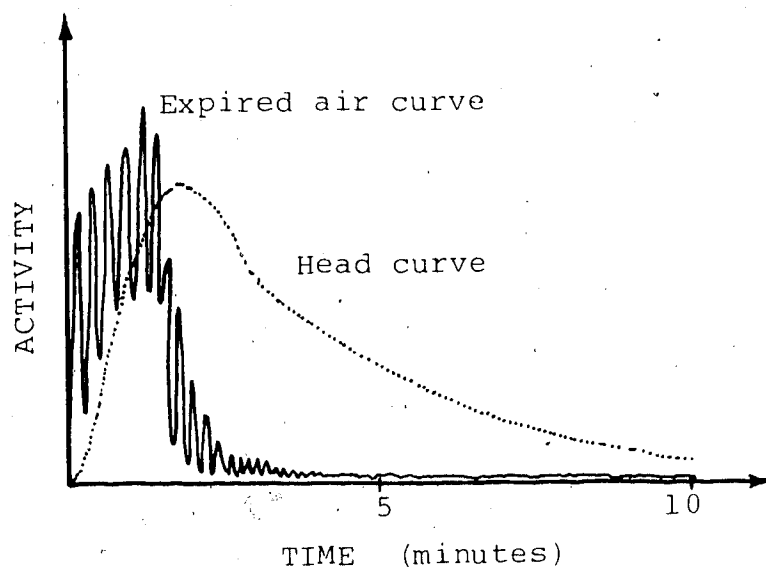


Figure 2.3 Inhalation Method Clearance Curves⁴

particular tissue compartment, i , as:

$$C_i(t) = f_i \int_0^t C_a(u) \cdot \exp(-k_i \cdot (t-u)) du \quad (2.18)$$

where

t = a given time after the beginning of inhalation,

$C_i(t)$ = isotope concentration in the tissue at time t ,

f_i = blood flow per unit volume of tissue,

$k_i = f_i/\lambda_i$, where λ_i is the tissue-blood partition coefficient, and

$C_a(t)$ = isotope concentration of the arterial blood or end-expired air at any time t .

Let $N(t)$ represent the count rate obtained from an external detector at time t . If the isotope is assumed to be

⁴ The activity scale for the expired air curve is of the order of six times that of the head curves. In other words, the activity in the expired air is much greater than the activity recorded from the head.

homogeneously distributed in each tissue compartment and if differences in counting geometry are neglected, $N(t)$ will be proportional to a weighted sum of the isotope concentrations in the several compartments. In a two-compartment system,

$$N(t) = \alpha \cdot \sum_{i=1}^2 (w_i \cdot C_i(t)) \quad (2.19)$$

where α is a proportionality constant relating units of count rate to concentration, and w_i represents the relative tissue weight for each compartment ($\sum w_i = 1$). Substituting equation (2.18) into equation (2.19),

$$N(t) = \alpha \sum_{i=1}^2 w_i f_i \int_0^t C_a(u) \cdot \exp(-k_i \cdot (t-u)) du \quad (2.20)$$

If the parameters before the integral sign are represented by a single coefficient, P_i , an equation in four unknowns can be written:

$$N(t) = \sum_{i=1}^2 P_i \int_0^t C_a(u) \cdot \exp(-k_i \cdot (t-u)) du \quad (2.21)$$

Computer solutions for P_i and k_i are readily obtained from equation (2.21) by means of an unweighted least squares method of curve fitting. Blood flow can then be calculated by multiplying k_i with the appropriate partition coefficient, λ_i . Details of the computer analysis are given in chapter four.

Extracerebral Contamination

The second major disadvantage of the inhalation technique is the contamination of the extracerebral tissues (ie. scalp, facial tissues, etc.) by the radioisotope. Obrist^o et al. [58] originally suggested modelling the extracerebral tissue as a third compartment with flow values

slower than those of the first two compartments. However, both theoretical and practical difficulties arise if this solution is adopted.

In particular, the low flow levels in the extracerebral tissues necessitate long recording times, (about 40 to 45 minutes) for which it is difficult to maintain a stable physiological state [58]. Furthermore, an extra compartment in the model implies integrating three exponentials and thus two more parameters to determine. With six parameters the uncertainty involved in the results increases to such an extent that they can become quite unusable. This has been demonstrated by Glass and De Garreta [19] who found that, taking into account the number of points used, the sampling rate and the baseline noise, the error on k , for a three-exponential analysis was 17 to 100% whereas for a two-exponential analysis under the same conditions it was only 2.5 to 10%. The validity of the model can also be questioned, since the monoexponential nature of the clearance of the extracerebral tissues appears somewhat uncertain. It also seems that in some pathological low flow states the discrimination between the flow values of white matter and extracerebral tissue becomes quite difficult using computer analysis [55,58].

As a result of these difficulties Obrist et al. [59] proposed a two-compartment model in which a faster clearing compartment, considered to be cerebral grey matter, is separated from a slower clearing compartment, considered to

be white matter and extracerebral tissue. Such a model assumes grey matter clearance rates that are high relative to the remaining cerebral and extracerebral components. Although limited to blood flow estimates of grey matter, it is a method better suited for clinical research. It is presently the most commonly used model of the ^{133}Xe inhalation technique.

A second way of minimizing the influence of extracerebral contamination is a spectrum subtraction technique [11,68]. This technique, proposed by Crawley et al., is based on the form of the ^{133}Xe radiation spectrum which comprises two peaks, one at 81 KeV (gamma radiation) and the other at 30 KeV (X-ray radiation). Whereas the radiation of the 81 KeV peak is sufficiently energetic to reach the detector from the deepest part of the brain, the soft radiation of the 30 KeV peak originates primarily from the superficial regions. Thus, by connecting a detector in parallel to two discriminators gating the radiation around 30 KeV and 81 KeV, respectively, it is possible to record two clearance curves, one of which, for the 30 KeV energy level, represents principally the clearance in the extracerebral tissues. Subtracting this curve from the one obtained at the 81 KeV level gives a corrected curve representing primarily the clearance in the brain tissue.

Macey, Filipow, et al. [46], however, have suggested that the spectrum subtraction technique overestimates the contribution of the ^{133}Xe in the scalp for two reasons.

Firstly, Compton scattering of the 81 KeV photons results in a significant proportion of counts in the 30 KeV energy window and secondly, the skull does not act as a perfect filter for the 30 KeV photons emanating from ^{133}Xe in the cerebral tissue. A further disadvantage of the spectrum subtraction method is that it necessitates a significant increase of the dose of the tracer (up to seven times the usual dose [55]) to maintain a sufficiently low ratio of random statistical noise to count rate.⁵

Compton Scatter

Compton scatter refers to the scattering of an x-ray or gamma ray photon upon impact with an electron within an atom. This is accompanied by a transfer of part of the photon's energy to the electron with consequent loss of frequency. Meric and Seylaz [54] state that because of the weak energy levels of the tracers involved, the scattered radiation contributes significantly to the total measured radiation. They, and others [64], have found that, in the absence of any energy discrimination, the intensity of the scattered radiation from outside the collimated zone could attain 55% of the total radiation intensity reaching the detectors. However, the proportion of contaminating radiation in the total detected radiation can be limited by applying an energy discrimination of which the low level is 75 KeV. The relative intensity of the contaminating radiation then falls to 10 to 15% [54,64].

⁵ Most researchers suggest that for accurate data analysis a count rate with a peak value of 1000 cps is necessary.

Airway artefacts

The respiratory passages are highly contaminated during and immediately following ^{133}Xe inhalation. This results in scattered radiation which has a definite effect on curve analysis, particularly for the detectors which are placed proximal to the upper airways. Many attempts have been made, therefore, to minimize this source of error.

The simplest and most commonly used method to compensate for airway artefacts was proposed by Obrist et al. [59]. Obrist and his colleagues concluded that the optimal start fit time is the earliest point on the head curve where scattered radiation from the air passages can be assumed negligible. They determined that such a point is reached after inhalation is over, when the end-expired air curve has decreased to 20% of its maximum. Because of recirculation, the head curve does not peak until several seconds after the end of inhalation, therefore, Obrist's recommended start fit time is usually close to the peak of the head curve.

Risberg [65] found that at the point in time when breathing is switched from ^{133}Xe to air, there is a sharp decline of the air passage concentration of ^{133}Xe . If a head curve shows a rapid decline at the same point, the size of this "drop" is used as an estimate of the size of the contamination by the air passage artefact. A weighted product of the average expired air curve is then subtracted from the head curve. Since this method usually

underestimates the airway artefact it is combined with a late start fit time.

Jablonski et al.[32] use an average $^{133}\text{Xenon}$ concentration in the respiratory air sampled at the mouth as an airway artefact template. They assume that the measured clearance curve is a summation of the airway artefact, the fast and slow blood flow components convolved with the end-expired air curve, and Poisson-distributed noise. The relative sizes of these components are determined by an algorithm that uses a least-squares fit comparison to the recorded isotope curve in the *frequency* domain. While this approach has several advantages over the time domain methods, several researchers [31,57] have noted that this method may give rise to artefacts due to over-correction.

Nilsson et al. [57] recently have developed an improved method for airway artefact compensation based upon Risberg's technique. Instead of determining the influence of the airways by utilizing a single point, as Risberg does, Nilsson et al. uses the first thirty seconds to determine the airway artefact and then subtracts a weighted product of an airway artefact template (respiratory air sampled at the mouth) from the head curve.

2.2.5.2 Initial Slope Index

It has been noticed by several researchers [30,59,66] that attempts to compare fast compartment flow values with the same patient over time have been complicated by the fact that the relative weight of the fast compartment, usually

changes also. Iliff et al. [30] attempted to explain this phenomena by stating that the fast flow compartment is a physiological rather than an anatomical entity. That is, while the fast flow values may increase over time, the relative weight of the fast flow compartment may decrease, signifying that a smaller proportion of the brain is showing fast flow characteristics.

Risberg et al. [66] created the initial slope index (ISI) which is unaffected by the so-called compartmental "slippage" and is minimally influenced by recirculation. Risberg et al. reconstructed a curve from the biexponential solution according to the formula

$$N_1(t) = N_1(x) \cdot \exp(-k_1 \cdot (t-x)) + N_2(x) \cdot \exp(-k_2 \cdot (t-x)) \quad (2.22)$$

where

$N_1(t)$ = total counting rate corrected for recirculation at any time t (minutes),

$N_1(x)$ = counting rate of the first compartment at the start fit time, x , and

$N_2(x)$ = counting rate of the second compartment at the start fit time, x .

k_1 , k_2 , $N_1(x)$ and $N_2(x)$ are solutions of Obrist's biexponential analysis (ie. equation(2.21)). The ISI is defined as the slope constant of a monoexponential function connecting the points at two-minutes and three-minutes of this curve, and is calculated according to the formula

$$ISI = (\ln N_1(2) - \ln N_1(3)) \cdot 100 \quad (2.23)$$

The ISI is an index of the blood flow of all tissues

recorded, but is highly dominated by the grey matter blood flow and influenced very little by extracerebral components. While it does not provide a quantitative value of blood flow, it is used regularly for comparing serial measurements of the same patient.

2.2.5.3 Advantages and Disadvantages

The ^{133}Xe inhalation method is widely used primarily due to its atraumatic nature and also because it is technically simple to administer. However, it has several sources of contamination and as a result requires relatively complex analysis algorithms. In addition to the disadvantages previously mentioned, the inhalation technique has two further limitations. Firstly, because of the manner of administration of the isotope the success of this method is dependent upon satisfactory pulmonary function of the patient. Should the patient have a pathologic pulmonary condition, some other means of determining the arterial isotope concentration is required or the method must be discarded. The second limitation is one that the inhalation method shares with other two-dimensional methods, and that is, contributions from very slowly clearing or ischemic brain tissue are inadequately measured. The extreme case of low flow is that of a brain infarct with no circulation. ^{133}Xe does not enter such an area as there is no arterial inflow. Hence such an infarct is completely overlooked. The development of atraumatic tomographic three-dimensional regional cerebral blood flow methods hopefully will

circumvent these problems.

2.2.6 Intravenous ^{133}Xe Xenon Method

The intravenous ^{133}Xe Xenon method shares the same principles and complicating factors as the inhalation method. The only major difference is that in this method an injection of approximately ten millicuries of ^{133}Xe is given as a bolus into a vein in the arm [69]. The algorithm used to calculate cerebral blood flow for the inhalation method can also be used for the intravenous method.

The intravenous method suffers from the disadvantage that, since a relatively large amount of xenon is excreted via the lungs before it reaches the brain, the count rates at the head are significantly reduced. On the other hand, this method of ^{133}Xe administration is much simpler than inhalation, making the technique useful during neurosurgical procedures where administration of xenon gas by way of the anaesthetic machine may result in problems due to anaesthetic gas dilution. This technique is also useful in the intensive care unit where lack of patient co-operation may make the inhalation method difficult. Due to count rate limitations, use of this technique is often limited to the measurement of total blood flow or to inter-hemispheric comparisons [69].

2.3 Three-Dimensional Methods

The two-dimensional methods previously described are widely used, and a certain regionality of cerebral blood flow can be obtained particularly with regard to blood flow in the cortex. However, flow in a focal area cannot be adequately recorded with such methods. This is particularly true for low flow or ischemic areas where the small amount of isotope entering the area is "hidden" behind radiation from other parts within the field of vision. It is as if one "looks through" the practically unlabelled infarct. Only a three-dimensional tomographic approach can effectively avoid the so-called "look-through phenomenon" [41]. Three-dimensional methods of measuring blood flow are still in the early development stages. Atraumatic tomographic methods that are currently being developed are briefly mentioned herein.

The *clearance method* is based on using a rapidly rotating four-gamma camera system and single-photon emission tomography [31,41]. This method often uses ^{133}Xe or ^{133}Xe administered by inhalation or intravenous injection. Due to the necessity for making repeated scans with a short interval, the counting rate obtained is low. This fact, along with Compton scattering effects, limits the spatial resolution. An adaptation of this method utilizes positron emission tomography. The indicators used in this technique are diffusible positron-emitting tracers such as ^{81}Kr , ^{15}O -labelled water, ^{18}F -antipyrine,

CH_3^{18}F , and ^{14}C -labelled alcohols [62].

The *continuous inhalation method* has used continuous delivery of C^{18}O_2 gas which is converted to H_2^{18}O in the lungs by carbonic anhydrase [62]. The technique relies upon a continuous concentration gradient of H_2^{18}O from blood to tissue to maintain a steady-state tissue concentration of H_2^{18}O that is directly related to cerebral blood flow. This is maintained because new H_2^{18}O is being continuously delivered to the blood while radioactive decay of ^{18}O (with a half-life of 2.1 minutes) and biological clearance is continually reducing tissue concentration of H_2^{18}O . This technique also utilizes positron emission technology.

At equilibrium, the amount of tracer entering the tissue per unit of time equals the loss per unit of time due to decay plus the amount of tracer exiting from the tissue by blood flow. Thus,

$$F \cdot C_i = X \cdot \lambda_d + F \cdot X/V \quad (2.24)$$

where X is the recorded steady-state content of tracer in a tissue with volume V , F is the blood flow to that tissue in ml/min, C_i is the arterial concentration of tracer and λ_d the isotope's radioactive decay constant (min^{-1}).⁴ Rearranging,

$$X/V = \frac{F/V \cdot C_i}{F/V + \lambda_d} = C_t \quad (2.25)$$

where C_t is the tissue concentration of the tracer.

⁴ Note that λ_d is not a partition coefficient.

Therefore,

$$F/V = \frac{\lambda_d}{C_i/C_t - 1} \quad (2.26)$$

Thus, provided the steady state levels of C_i and C_t can be measured, we can solve for the blood flow per unit volume of tissue since λ_d is a known constant [35].

The *tissue trapping model* is difficult to implement because of the requirements placed on the tracer [62]. The model assumes that the tracer delivered to the brain after intravenous injection is extracted and retained by the tissue during the course of the experiment. While labelled microspheres are sometimes used to approximate this model, a more realistic (ie. non-occlusive) tracer is preferred. That is, the tracer must be trapped in the tissue by some process such as metabolic incorporation, selective tissue binding, or a chemical change of the compound while in the tissue that does not allow clearance of the tracer back into the blood. The only non-occlusive tracer that has been successfully used is ^{15}N Nitrogen ammonia ($^{15}\text{NH}_3$). The equation for this model is given by

$$\text{CBF} = (F \cdot C_i) / C_t \quad (2.27)$$

where F is the flow rate in millilitres/minute of a pump used to withdraw blood at a fixed rate from a peripheral artery, C_i is the tissue concentration in $\mu\text{Ci/g}$ in region i as measured with positron emission tomography, and C_t is the total activity in μCi in the blood sample withdrawn with the pump.

Various methods to measure blood flow are also being developed using *nuclear magnetic resonance techniques* [13]. These include (1) measuring the change in the effective relaxation time T_2 and relating it to flow, (2) using a field gradient along the direction of flow and measuring the relative changes in phase of the precessing proton employed, and (3) using a two-coil system, measuring the transit time of the magnetized protons flowing between the transmitter and receiver coils.

3. System Hardware

The microprocessor controlled cerebral blood flow measuring system consists of two separate units. That is, the Medimatic Inhamatic system and the microprocessor system. Since most of the hardware components of these systems are commercially available, the subsequent descriptions in this chapter will be relatively brief. Emphasis will be placed on the components which were modified and on areas which help the reader understand the software development.

3.1 Inhamatic System

The Inhamatic system is a multidetector system for measurement of regional cerebral blood flow using $^{133}\text{Xenon}$ clearance. This system includes thirty-two possible hemispheric detectors and associated electronics, and a xenon administration system with an air curve detector for inhalation studies. The Inhamatic system is also applicable to intravenous and intra-arterial studies.

The Medimatic inhalation system is housed in a moveable "main frame" which contains the complete system, inclusive of the xenon administration system and electronics (figure 3.1). The detector suspension and the patient mask are mounted on an adjustable lift at the front of the main frame. This makes it possible to examine patients lying down as well as sitting, and, if necessary, the detectors and mask can be positioned down over the patient's own bed. The

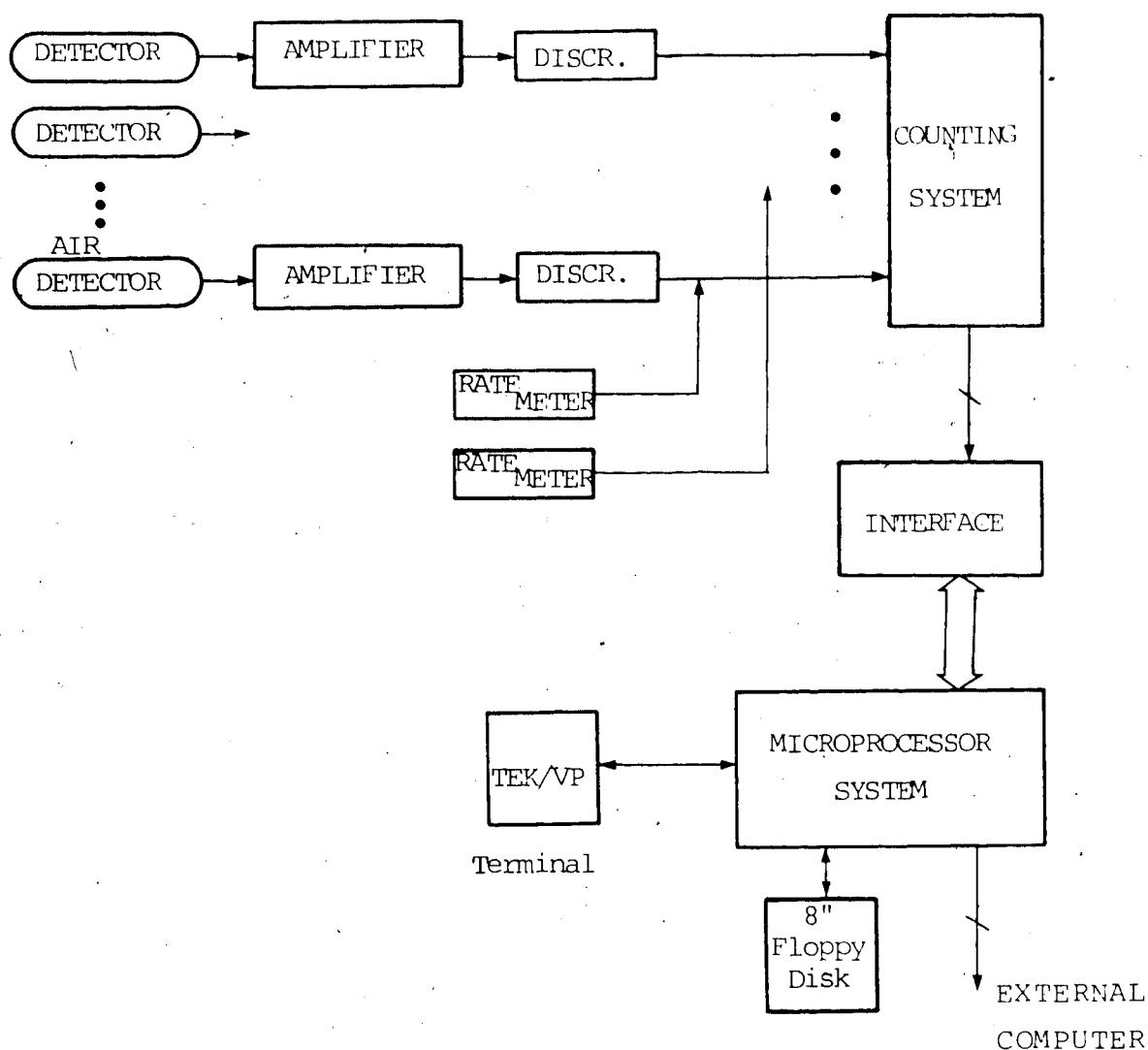


Figure 3.1 System Block Diagram

mechanical dimensions of the main frame are 1.5 by 0.5 meters and 1.6 meters high. The system requires a line supply of 110 volts AC.

The measured data can be recorded directly on paper tape or, alternatively, on floppy disk via the developed microprocessor system. Medimatic does supply an on-line version of the Inhamatic, which includes a Varian mini-computer and a colour display, but the cost was considered

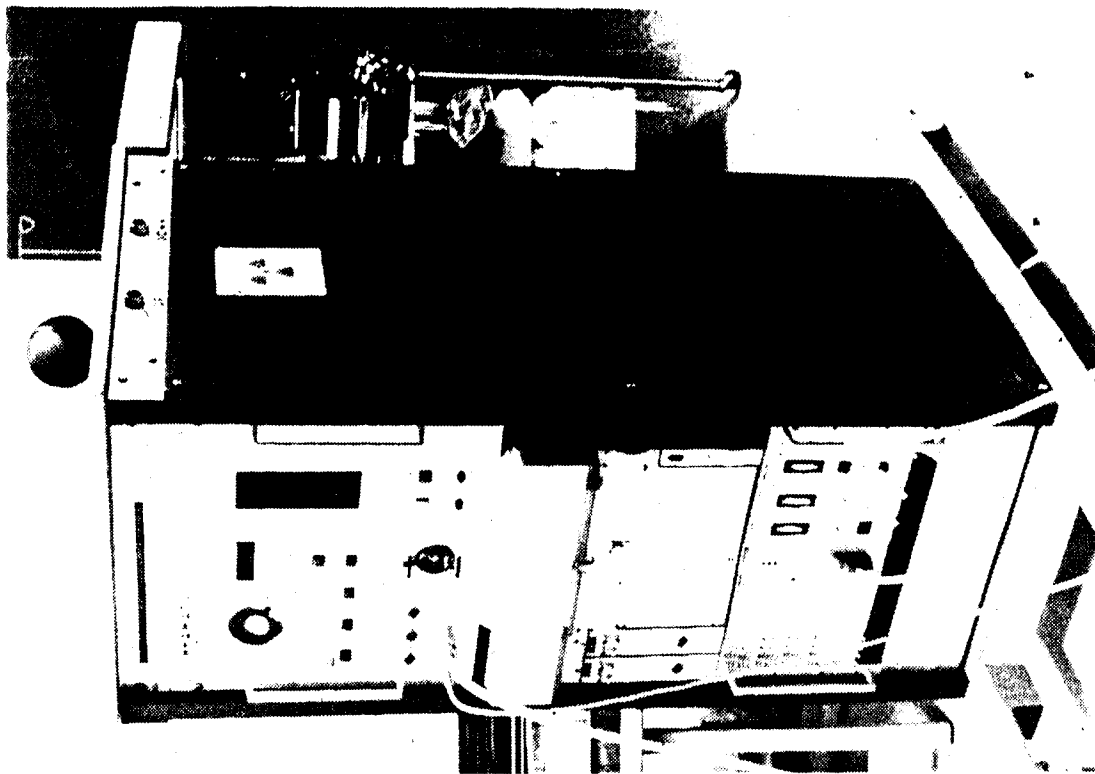


Plate 3.1 Front Panel of Inhamatic System

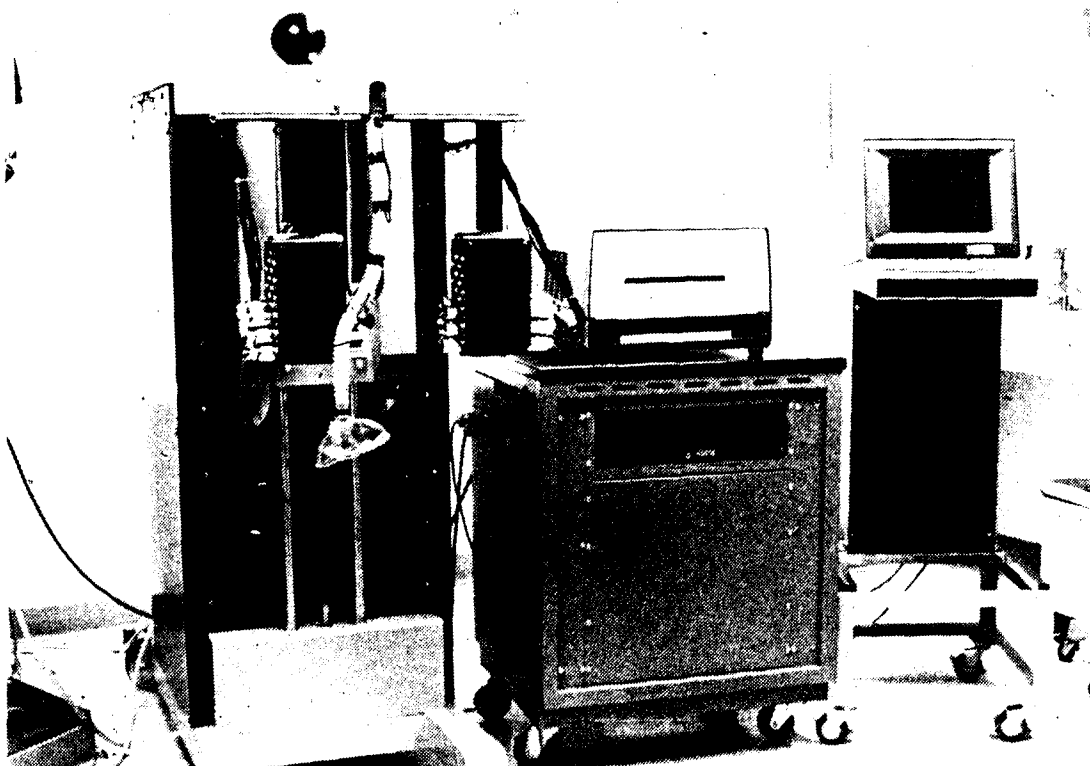


Plate 3.2 Microprocessor-based Cerebral Blood Flow System
(l-r) Inhamatic System, Microprocessor System with Tektronix
Hard Copy unit, Tektronix 4010 terminal.

prohibitive. The hardware components of the microprocessor system can be purchased for under \$7,000 [39].⁷

The measurement procedure initially involves filling the administration system with ^{133}Xe at two to five millicuries/litre. Using the adjustable lift, the detectors are positioned correctly relative to the patient's scalp and the mask is securely held over the patient's face. At the outset the patient breathes room air until a satisfactory respiratory pattern is obtained and while the system measures the background level of radioactivity. The patient is then switched to the re-breathing system, containing ^{133}Xe , for a period of one minute. Immediately after the inhalation period, the system automatically switches the patient back to room air and continues to collect data for an additional nine minutes. There is also a manual mode in which the operator may collect data for any length of time. (Refer to Appendix B for a detailed measuring procedure*.)

3.1.1 Detectors

Primary considerations in regards to selection of a detector include: resolution, efficiency, energy of radiation, counting rates, and size. Energy resolution of a detector is its ability to distinguish between different energy photons. Detector efficiency refers to the percentage

⁷ A price quotation from Medimatic dated May 11, 1978 estimated the cost of the on-line expansion to be in excess of \$50,000.

* The Inhamatic system was originally purchased in November, 1977, for a total cost of approximately \$46,800.

of radioactive particles at a specified energy that will interact with the detector rather than simply passing through it. Most current cerebral blood flow systems utilize scintillation detectors, although some are using solid state detectors, in particular cadmium telluride (CdTe) detectors [10,29,87].

A scintillation detector consists of a crystal, usually sodium iodide, connected to a photomultiplier. X or gamma photons traversing the crystal interact with the crystal to produce Compton electrons, photoelectrons or electron-positron pairs. The energy of these charged particles is absorbed by the crystal which produces small flashes of ultraviolet light. These photons strike a photocathode optically coupled to one side of the crystal, which ejects low energy photoelectrons. The number of electrons ejected from the photocathode is proportional to the energy of the incident photon absorbed in the crystal. Use of a Thallium impurity (0.1%) in the sodium iodide crystal acts as a wavelength shifter causing the crystal to emit two or more low energy photons (visible light) instead of a single ultraviolet photon. Ultraviolet photons are not suitable since they are absorbed by most materials, even those transparent to visible light.

The essential parts of the photomultiplier are the photocathode, ten dynodes, and an anode. The electrons which are ejected from the photocathode are attracted to the first dynode, which is over 100 volts positive with respect to the

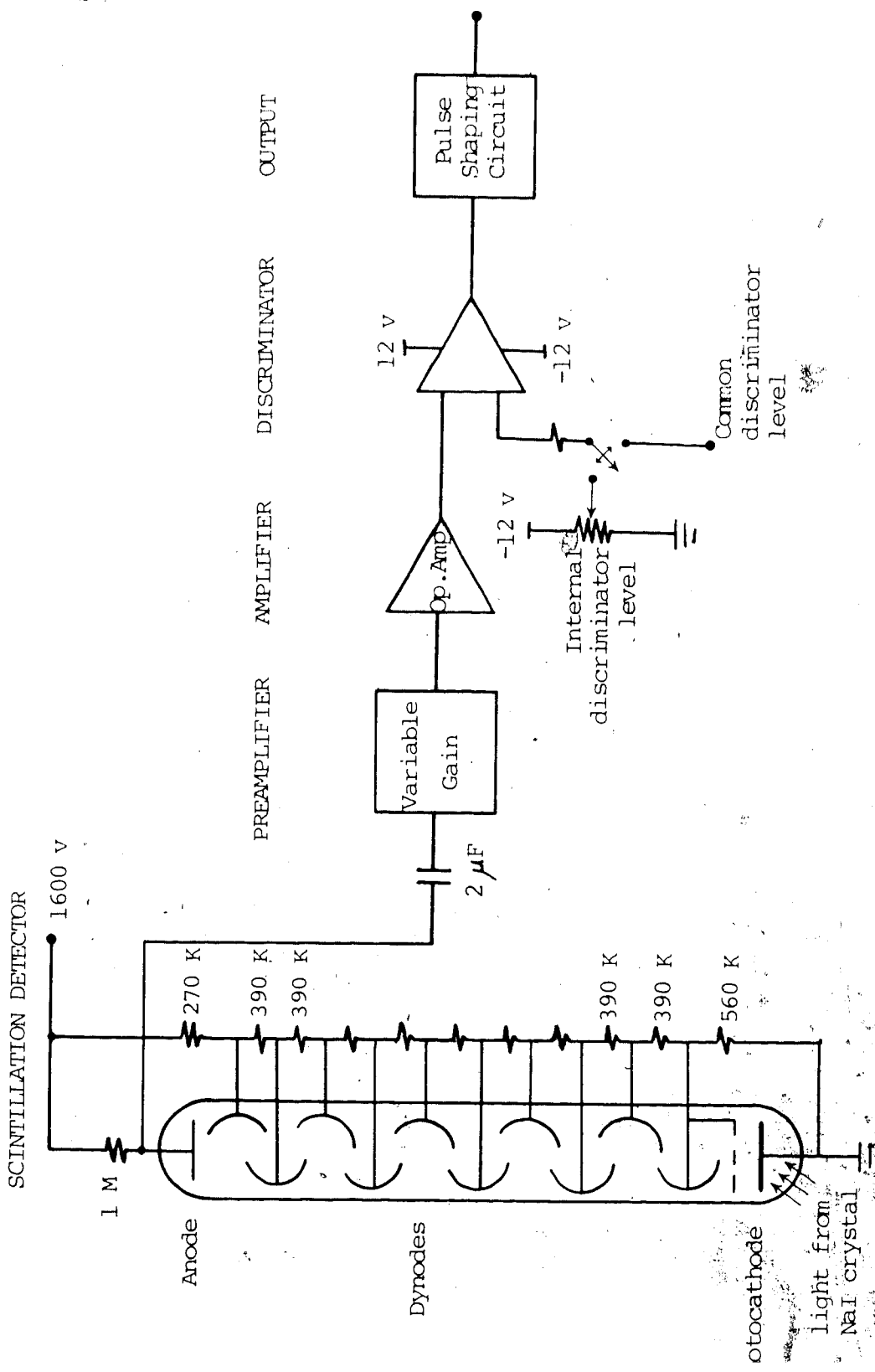


Figure 3.2 Scintillation Detector and Amplifier Module

photocathode. These primary electrons strike the first dynode with sufficient velocity to eject two or more secondary electrons from the surface. These secondary electrons in turn are accelerated to the second dynode, which is over 100 volts positive with respect to the first. This procedure is continued throughout the arrangement of dynodes until a multiplication factor of about one million is attained by the time the final anode is reached. The negative output pulse is the input to the subsequent amplifier circuitry.

The Inhamatic system has the capability of using thirty-two hemispheric detectors, although only sixteen are presently in use. The detectors use $3/4$ inch diameter by $3/4$ inch thallium-activated sodium iodide (NaI(Tl)) crystals, and $3/4$ inch by 1 inch collimators. The air detector uses a $3/4$ inch diameter by 1 inch crystal with a built-in copper spiral through which a sample of expired air is drawn. Thicker crystals provide more efficient light collection and increase crystal efficiency. The air detector is completely surrounded by a lead shield to minimize background radiation.

The radioisotope used is the inert gas ^{133}Xe . It was selected primarily due to its suitability, availability, and reasonable cost. ^{133}Xe emits a rather soft, electromagnetic radiation in the form of an 81 KeV primary gamma ray and a 31 KeV X-ray, and has a half-life of 5.5 days.

3.1.2 Electronics

The Inhamatic system contains a standard CAMAC crate for mounting of the electronic modules. These modules include four quadruple amplifiers with built-in discriminators, a high voltage supply for the detectors, two SCA ratemeters (one for the air curve and one for a selected head curve), a data acquisition and counting system with a common discriminator level generator, and an interface module for a paper tape punch or the microprocessor system.

3.1.2.1 Amplifier Modules

The amplifier modules contain four channels, each of which consists of a charge sensitive preamplifier with variable gain, a pulse shaping circuit, and a lower level discriminator. The discriminator uses a standard comparator, referencing the input pulse to either an internal discriminator level, which can be varied individually for each channel, or to a common discriminator level. The discriminator allows only those pulses to be counted which are equal to or greater than the reference discriminator level (ie. internal or common). In order to calibrate the channels, so that for a given test source of ^{133}Xe each individual energy spectrum was the same, a common discriminator level was used. Each individual gain was then adjusted so that the same number of counts with the same energy levels were recorded for each detector.

The common discriminator was set at a level which allowed only those radioactive particles with energy levels

of above approximately 50 KeV to be counted. This level was chosen for two reasons. Firstly, the copper spiral through which the respired air is drawn effectively attenuates all the X-radiation in the lower energy peak of 31 KeV. In order for the head detectors to measure radiation over the same spectrum as the air detector, the common discriminator was set at a level above the lower energy peak (ie. 50 KeV). Secondly, by setting the discriminator level so that the lower energy peak is ignored, the effect of Compton scatter and extracerebral contamination is minimized. As mentioned in the previous chapter, a greater portion of the 31 KeV energy peak originates from the scalp and facial tissues than that of the 81 KeV peak. Also, the particles which result from Compton scatter are of lower energy levels. The prime disadvantage of setting the discriminator level to eliminate the lower peak is the significant reduction in count rate. As a result, the amount of ^{133}Xe administered to the patient must be correspondingly increased.

3.1.2.2 High Voltage Module

The high voltage module is designed to supply thirty-three detectors with a dc regulated voltage from 0 to 2000 volts. It also limits the current to 20 milliamperes. The high voltage was adjusted to supply each detector with 1600 volts.

3.1.2.3 Ratemeter Modules

The SCA ratemeters provide an analog output of the air curve and one head curve. The air curve ratemeter also contains an amplifier circuit which is identical to the head curve amplifiers. The head curve ratemeter is able to display any channel by means of a front panel selector.

3.1.2.4 Counting System Module

The function of the data acquisition and counting system is to accumulate count numbers for each of the thirty-three channels. At set intervals of time the count numbers are read out to the CAMAC bus. The read-out of data is controlled by the interface module, via the bus.

The pulses from the detectors and amplifier circuits are fed into the input of the asynchronous buffer (see figure 3.3), which consists of thirty-three RS flip-flops. Normally all thirty-three flip-flops are set, but if a pulse arrives to one of the inputs, the corresponding flip-flop will be reset. When the synchronous buffer, consisting of thirty-three D flip-flops, is clocked next, the information of an arriving pulse will be transferred to the input of the encoder. The address of the input in question will appear at the output of the encoder as a binary coded number.

This address is transferred to the set decoder, and via the address selector to the random access memory (RAM). In the set decoder the address is used to set the flip-flop which had been reset by the arriving pulse. If two flip-flops are reset simultaneously the address at the

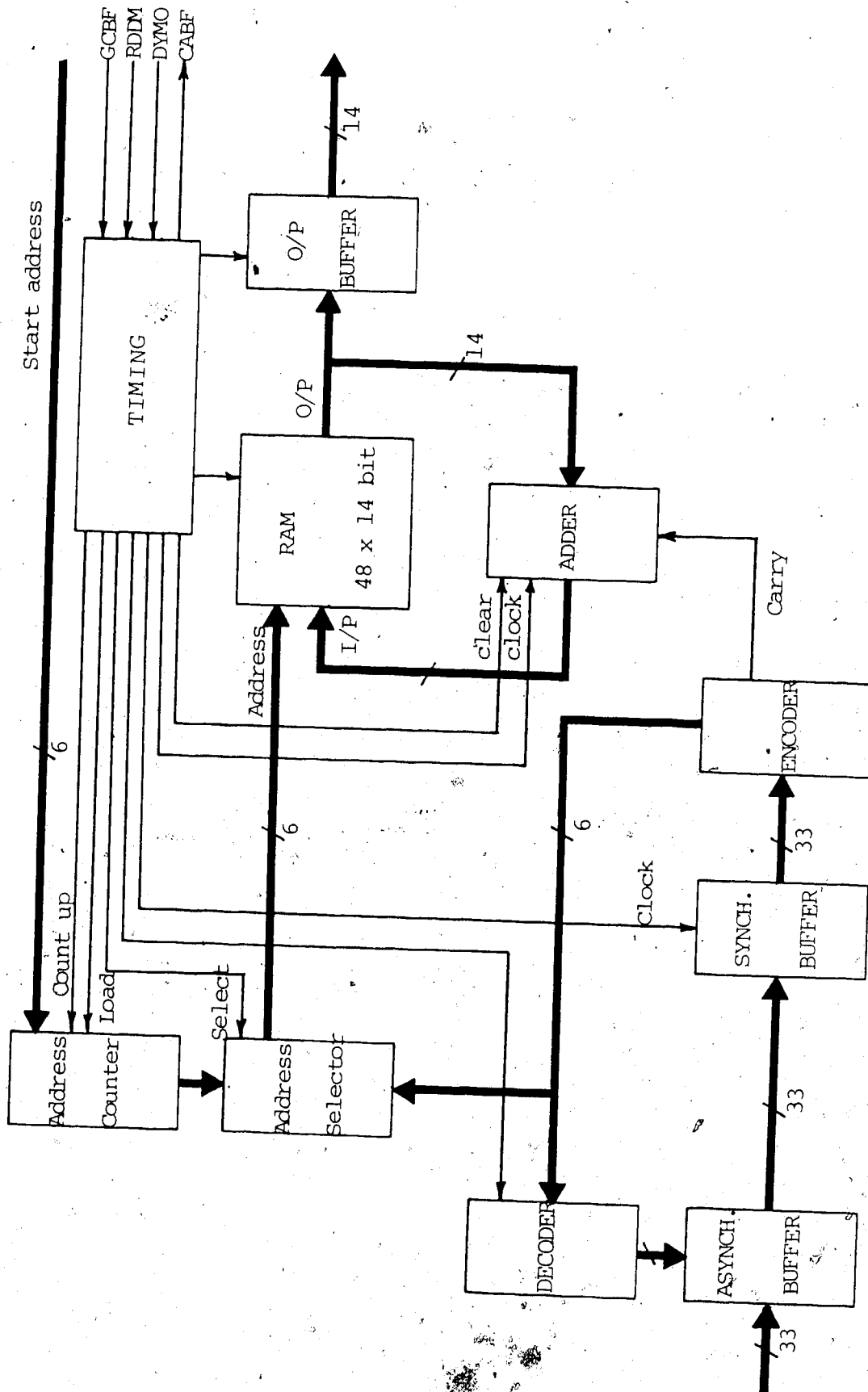


Figure 3.3 Block Diagram of Counting System

output of the encoder will be that with the highest channel number. The corresponding RS flip-flop is then set and next time the synchronous buffer is clocked, the address of the other channel will arrive at the encoder output.

The information of the count numbers for each channel are stored in RAM. If a pulse arrives at a channel the current count number for that channel will appear at the output of the RAM. This count number will then be incremented by the adder and the contents of the RAM are updated with the new count number. The counting system can be inhibited by lowering the signal DYMO from the interface module.

The interface module initiates the read-out procedure by raising the signal RDDM. This has the following effect in the counting system:

1. The address of the first channel which is to be read out is loaded into the address counter.
2. The address selector is switched from the encoder output to the address counter, so the address of the first channel to be read out will appear at the address input of the RAM. Therefore the count number of this channel will appear at the output of the RAM.
3. The count number is clocked into the output buffer and onto the bus.
4. The adder buffer is cleared and the null which thereby appears at the output is written into the RAM (ie. clearing the memory).

5. The address counter is incremented to give the address of the next channel to be read out.
6. The signal CABF goes high to signify that the data is ready.
7. When the data has been successfully transmitted, the receiving unit can raise the signal GCBF. This has the effect of repeating points two through five for each subsequent channel. All channels except the first can then be read out by letting the signal GCBF go up and down while RDDM remains high.
8. When the data transmission is complete, the signal RDDM goes low again.

It should be noted that before a measurement can be started, the RAM must be cleared by reading out all the channels. Also, the RAM uses 14-bit words which means the maximum counts per channel per sampling interval is 16,383. The clock in the timing circuit runs at 7.14 MHz, and after dividing this by eight, it provides timing pulses at a frequency of 893 KHz. The maximum count rate per channel is therefore approximately 10,000 counts per second.

3.1.2.5 Interface Module

The interface module is the link between the data acquisition and counting system and the microprocessor system. Its function is to collect the data from the bus and transmit it at set intervals of time to the microprocessor in sequential 8-bit bytes. The sample interval length is selected by means of a switch on the front panel and can be

of two, three, four, five, ten, twenty, or thirty second duration.'

The sequence of data transfer begins with the sample interval length being read out. This is followed by the first air curve point and then data from channels 1 and 2. After $1/16$ sample interval, the next air curve point is read out, followed by data from channels 3 and 4. In this manner, at the end of one sample period, each of the thirty-two head curve channels and sixteen air curve data points have been transmitted. Thus, the effective sample interval for the air curve is sixteen times faster than the selected sample interval for the head curves. Each of the above data points is transmitted in the form of two bytes with odd parity, the first of which is the most significant byte followed by the least significant byte.

The procedure by which the interface module receives and transmits data is described as follows (see figure 3.4):

1. The data collection routine is initiated when the RUN switch on the 'Xenon administration system is pressed. This raises the signal PUNCH ON which initiates the timing circuitry in the interface module and raises the signal DYMO.
2. The head address counter is cleared and the address for the first channel is transferred to the bus via the address selector.
3. The signal RDDM is raised to request a data transfer.

' The normal sample interval length is five seconds.

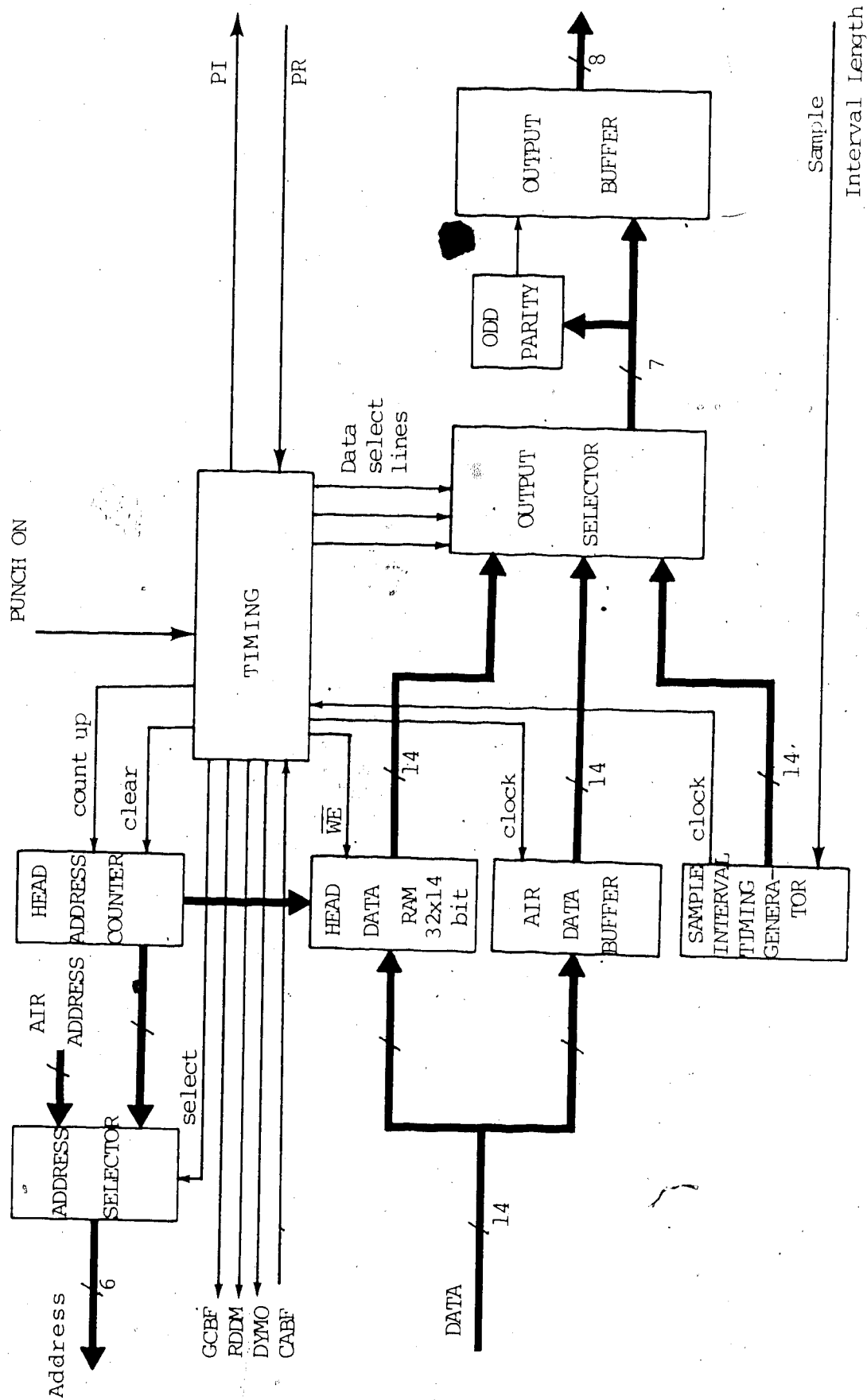


Figure 3.4 Block Diagram of Interface Module

4. When the signal CABF goes high to signify that the counting system has the data ready for transfer, the data is stored into RAM. The signal RDDM then goes low, followed by the signal CABF. The interface module does not use the GCBF line.
5. The head address is then incremented to give the address of the next channel to be transferred.
6. Steps 3 through 5 are repeated until all of the head data for one sample interval is transferred to the RAM.
7. Meanwhile, if the punch ready (PR) line is high, signifying the microprocessor is ready for data transfer, the output selector places the first byte of the sample interval length (the most significant byte) in the output buffer.
8. The punch instruction (PI) line goes high indicating to the microprocessor that data is available (see figure 3.5).
9. Once the microprocessor has read the data, it lowers the signal PR, followed by the signal PI going low.
10. The output selector then places the least significant byte in the output buffer. When the microprocessor raises the signal PR again, steps 8 and 9 are repeated. Subsequent data is transferred to the microprocessor in the same handshaking manner.
11. The address selector transfers the air channel address to the bus, and the corresponding data is requested. The air curve data is then clocked into the output buffer,

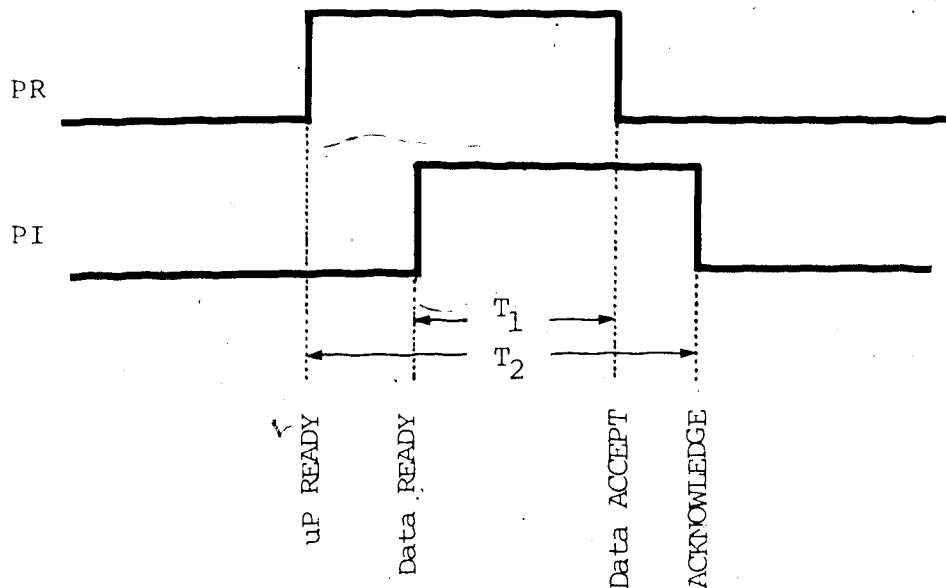


Figure 3.5 Handshaking Protocol

via the air data buffer and output selector, one byte at a time (as described in steps 7 through 10).

12. This is followed by a transfer of channels 1 and 2 data from the RAM to the output buffer.
13. After 1/16 sample interval, the next air curve data point is transferred, followed by channels 3 and 4, and so on.
14. At the end of one sample period, the procedure is repeated from step 2.

The output port of the interface module is a standard 25-pin connector (see figure 3.6).

3.1.3 ¹³³Xenon Administration System

The ¹³³Xenon administration system consists of a ¹³³Xenon filling system, a rebreathing system, and a

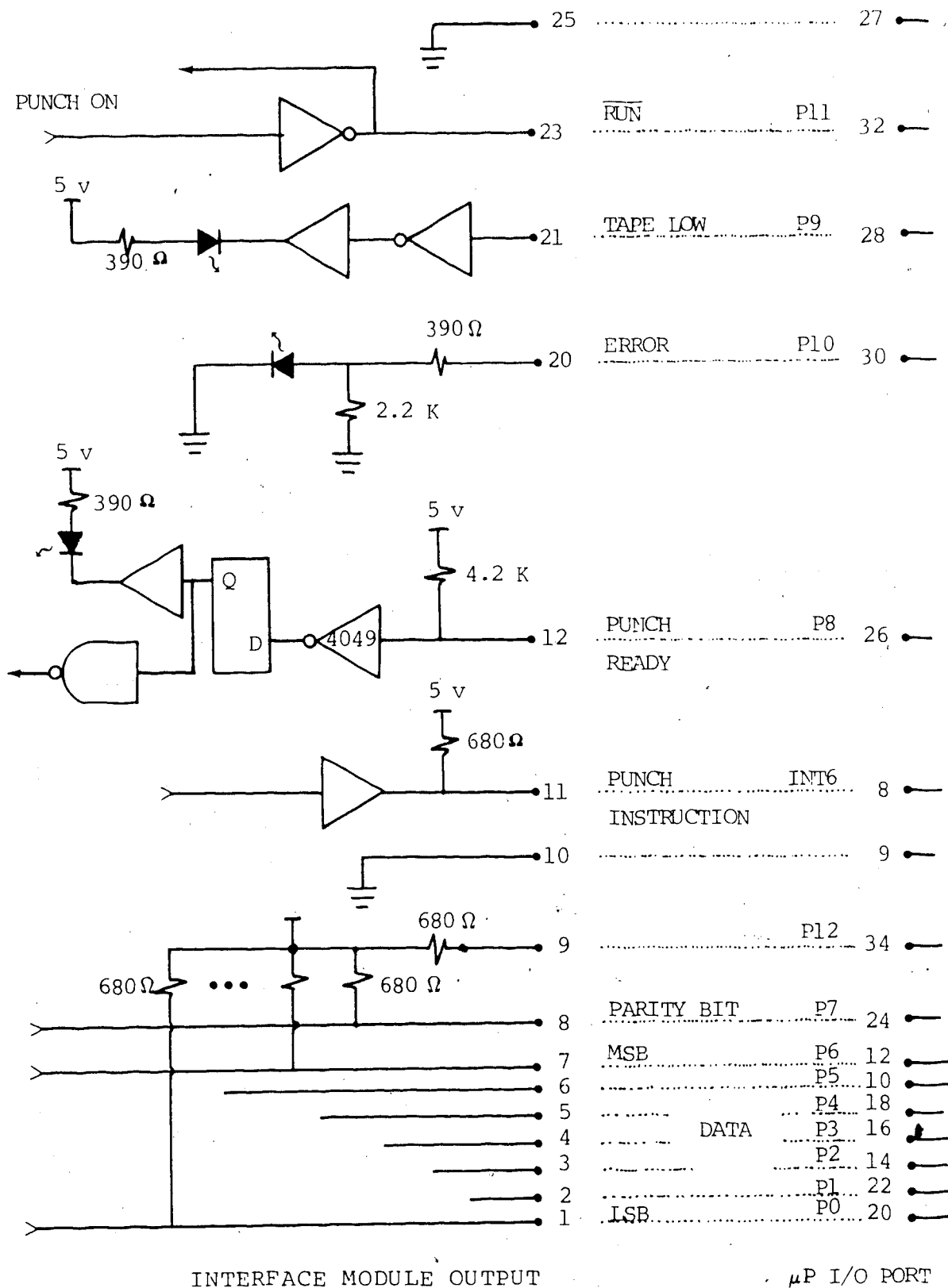


Figure 3.6 Inhamatic/Microprocessor Interface

Xenon charcoal trap. The rebreathing system is a closed circuit, consisting of a carbon dioxide absorbing filter, a breathing bag, and a circulation fan (see figure 3.7). The patient mask is connected to this system via two three-way valves which are controlled by a timer. Air samples are drawn either from the mask or the air bag to the air detector via another three-way valve which is controlled by a switch on the front panel. The entire system is shielded with lead. (Refer to appendix B for a description of the filling procedure.)

3.2 Microprocessor System

The microprocessor system consists of four Texas Instruments TM990 series microcomputer modules, two Qume floppy disk drives, and either an ADDS Viewpoint terminal or a Tektronix 4010 terminal. The TM990 single-board modules include a 101MA microcomputer module, a 201 memory expansion module, a 310 input/output expansion module, and a 303B floppy disk controller module. The 310 I/O expansion module is used for the communications port to an external computer.

3.2.1 Microcomputer

The microcomputer module uses as its central processing unit (CPU) a Texas Instrument TMS 9900 microprocessor. It is a single-chip 16-bit microprocessor produced using NMOS technology. The TMS 9900 was chosen for this project primarily because of its availability and also for its

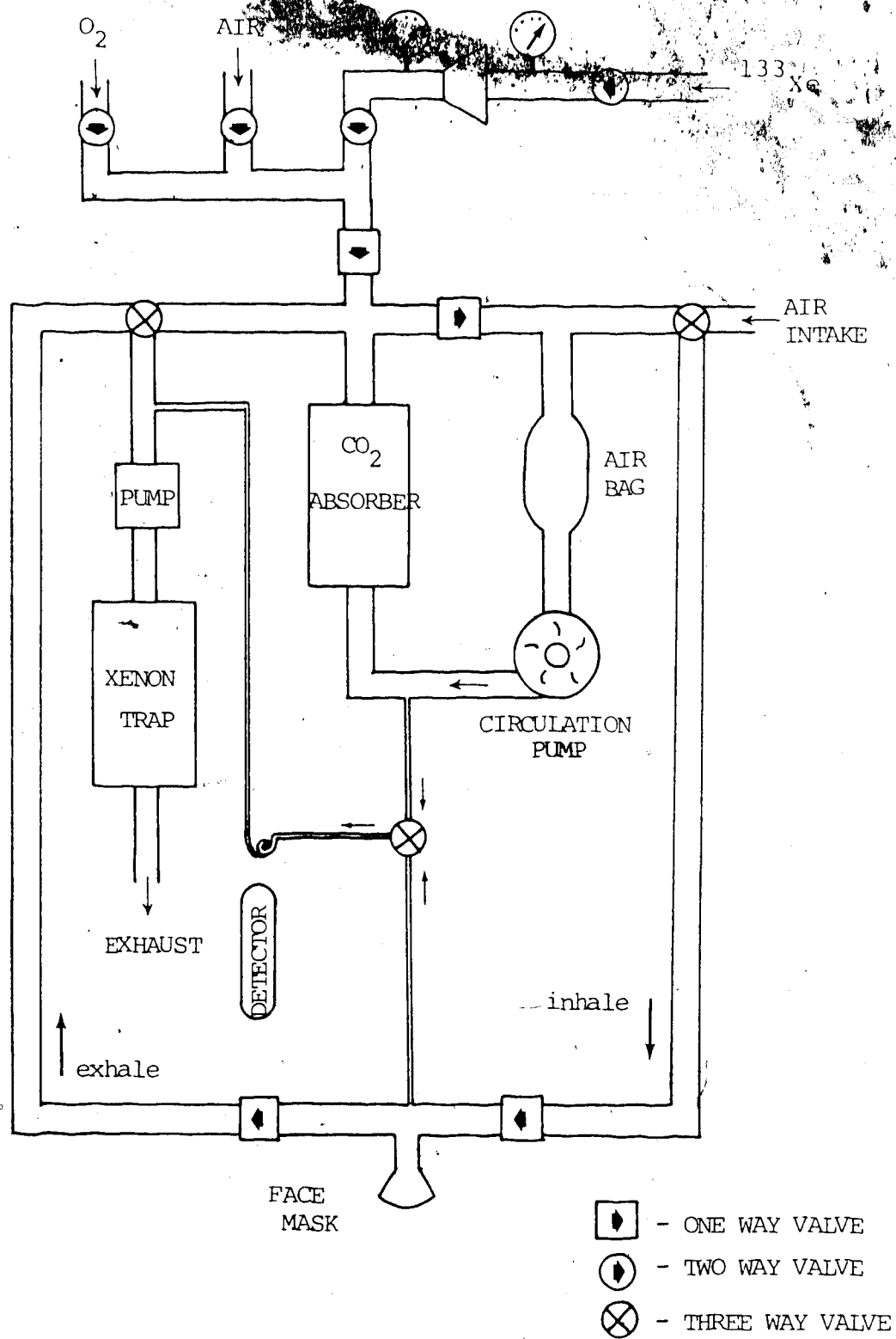


Figure 3.7 ^{133}Xe Administration System

16-bit word and context switching capabilities.

3.2.1.1 System Structure

The major blocks of the microcomputer system design are the microprocessor, the miscellaneous control signals, address decoding, on-board memory, the clock driver, one 16-bit parallel I/O port, two serial I/O ports, and the miscellaneous communications register unit (CRU) devices (figure 3.8). Functionally, these major blocks represent the processing, memory, and I/O portions of the microcomputer.

The system clock is provided by the TIM 9904 clock driver which produces four non-overlapping clock pulse signals at a frequency of 3.0 MHz. Two clock cycles, however, are required for each machine state. Therefore, the effective clock frequency for comparing with other microcomputers is actually only 1.5 MHz [61].

The microcomputer centers around five buses: power, control, address, data, and CRU. The address bus consists of 16 lines, A0 through A15. The least significant bit of this bus, A0, is normally grounded since memory access deals with 16-bit words. Therefore, since A0 appears as zero, words are fetched on even boundaries. Byte operations are handled by fetching a 16-bit word, modifying the addressed byte, and rewriting the 16-bit word back to memory if necessary. The data bus consists of 16 bidirectional lines which are routed from the microprocessor to memory and to the bidirectional buffers for off-board use.

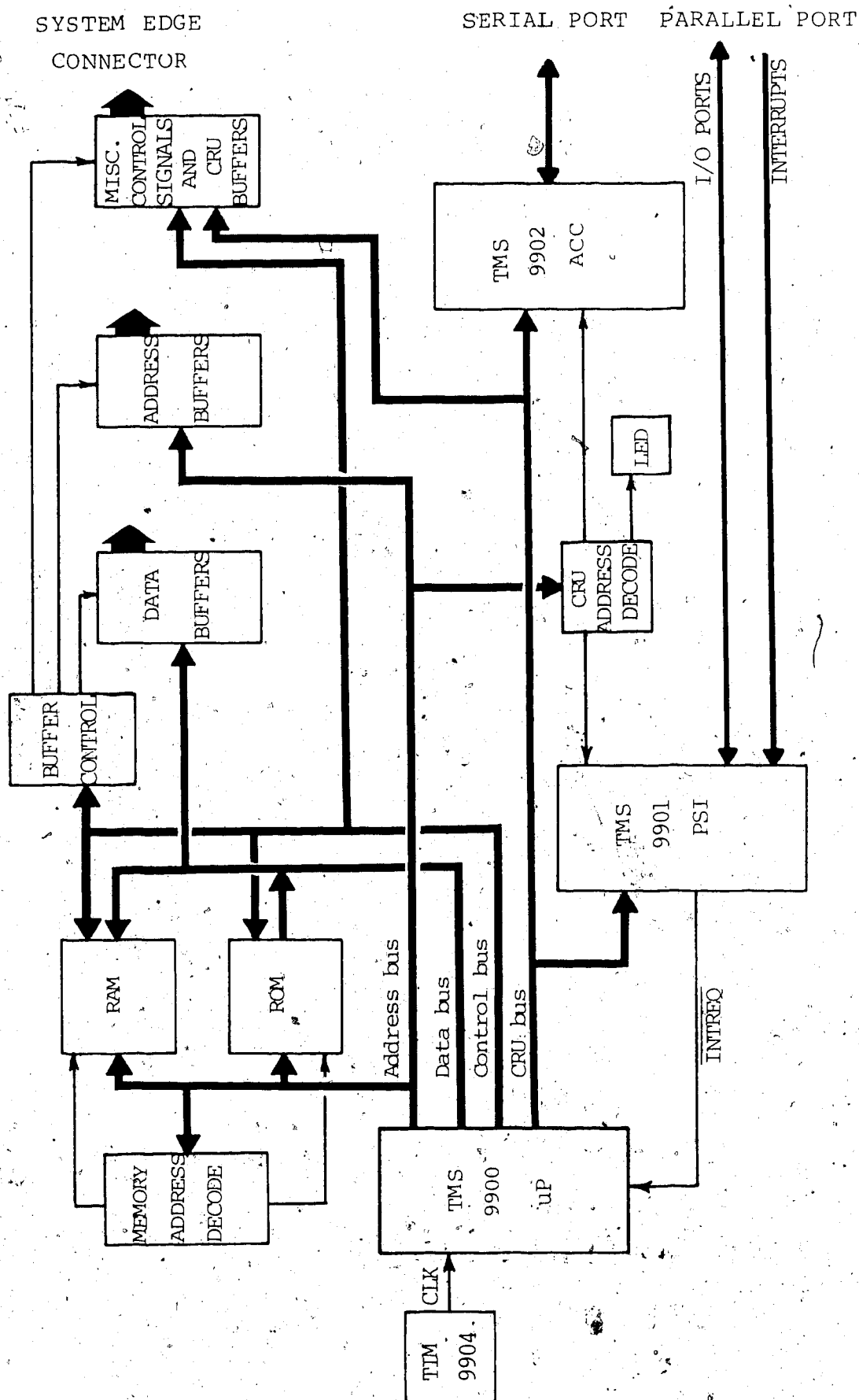


Figure 3.8. Microcomputer Block Diagram

3.2.1.2 Microprocessor Architecture

The TMS 9900 microprocessor is responsible for memory, CRU and general bus control; instruction acquisition and interpretation; timing of most control signals and data; and general system initialization. The operation of the microprocessor is fairly straightforward. There is no instruction prefetch or pipelining.

The microprocessor contains three primary internal hardware registers: the program counter (PC), the status register (ST), and the workspace pointer (WP). The program counter contains the address of the instruction following the current instruction being executed. The status register contains a 4-bit interrupt mask and seven processor status bits. The workspace pointer contains the address of the first word in the currently active set of workspace registers.

A workspace occupies sixteen contiguous 16-bit memory words or registers in any general RAM area. Each workspace register may hold data or addresses, and function as operand registers, accumulators, address registers or index registers. During instruction execution, the processor addresses any register in the workspace by adding the register number to the contents of the workspace pointer and initiating a memory request for the word.

The workspace concept is also valuable during operations that require a context switch, such as in interrupt service routines, extended operations, or

subroutine calls. A context switch defines a new set of workspace registers in main memory. If a context switch is requested, the processor fetches the new context WP and PC from vector locations, in the case of interrupts or extended operations, or from specified memory locations, in the case of subroutines. Then, the previous context WP, PC, and ST are stored in workspace registers 13, 14, and 15, respectively, of the new workspace. Thus the 9900 can accomplish a complete context switch with only three store cycles and three fetch cycles, and without requiring the contents of the workspace registers to be stored or stacked. This is particularly suited to this specific application since there is extensive use of subroutines requiring context switches and interrupts.

The TMS 9900 employs 16 interrupt levels with the highest priority level 0 and the lowest level 15. When the microprocessor receives an interrupt request (INTREQ) it compares the interrupt code (IC0 through IC3) with the interrupt mask contained in the status register. When the priority of the interrupt is higher than or equal to the mask level, the microprocessor recognizes the interrupt, sets the mask level to one less than the current interrupt number, and initiates a context switch. Thus, only interrupts of higher priority are allowed to interrupt a service routine. The microprocessor fetches the new context PC and WP from the interrupt vector locations.

The TMS 9900 utilizes a command-driven I/O interface designated as the communications register unit (CRU). The CRU provides up to 4096 addressable input and output bits. The I/O bits can be addressed individually or in fields of 1 to 16 bits. The microprocessor uses the three CRU bus lines (CRUIN, CRUOUT, CRUCLK) and 12 bits (A3 through A14) of the address bus to interface with the CRU system. The microprocessor instructions that affect the CRU can set, reset, or test any bit in the CRU array, or move data between memory and the CRU.

A CRU bit address is developed from the CRU base address, contained in bits 3 through 14 in workspace register 12, and the signed displacement count, contained in bits 8 through 15 of the instruction. The base address from register 12 is added to the signed displacement and the result is loaded onto the address bus. Data transfers to and from I/O devices and memory are handled serially through the CRUIN and CRUOUT lines using CRUCLK as a strobe. Aside from I/O purposes, CRU operations also program the operation of such devices as TMS 9901 and 9902.

3.2.1.3 Programmable Systems Interface

The TMS 9901 programmable systems interface (PSI) provides interrupt and I/O ports, and an interval timer. Up to 16 individually controlled, parallel I/O ports are available (seven dedicated, P0 through P6, and nine programmable, that is, they can be used as I/O ports or interrupt inputs). Power-up resets all I/O ports to the

input mode. Writing data to a port will switch it to the output mode. A reset bit on the TMS 9901 can execute a software reset of the I/O pins.

The TMS 9901 is used as the communication port with the Inhamatic system. I/O ports (P0 through P12) are connected directly to the external parallel I/O port on the 101MA microcomputer module which, in turn, is connected to the interface module port on the Inhamatic system via an 8-meter long cable (see figure 3.6). It is by means of the TMS 9901, then, that the microprocessor can collect data from the Inhamatic system and transmit control signals.

The TMS 9901 PSI also acts as an interrupt interface for the microprocessor. The interrupt inputs (six dedicated, INT1 through INT6, and nine programmable) are sampled, inverted, and ANDed with their respective mask bits. The TMS 9901 prioritizes and encodes the masked interrupts and transmits a four-bit encoding of the highest priority interrupt present (IC0 through IC3) to the microprocessor. The INTREQ line is then held low to indicate to the microprocessor that an interrupt is present. Each interrupt input has a mask bit individually set or reset under software control. Writing a one to an interrupt mask bit will enable that interrupt; writing a zero will disable that interrupt. When an interrupt occurs, the interrupt service routine needs to reset the interrupt mask to avoid further interrupts of that particular priority from occurring until the service routine is completed, at which time the mask bit

can be set again.

There are, therefore, two levels of interrupt masks (one in the TMS 9901 and one in the microprocessor). Both masks must be enabled for an interrupt to be honoured. Note that the condition of the microprocessor's status register priority mask is irrelevant if the TMS 9901's interrupt mask is zero for a particular interrupt.

The microprocessor system uses seven of the sixteen interrupt levels. Interrupt input level 6 is connected to the Inhamatic punch instruction line through an inverter. When the Inhamatic system raises the punch instruction signal signifying that data is ready to be transmitted, an interrupt occurs in the microprocessor system. The microprocessor initiates the interrupt service routine which proceeds to collect the waiting data, using TMS 9901 ports P0 through P7. The microprocessor then lowers the punch ready line (P8) to signify that the data has been collected, and sets the appropriate mask bit in preparation for the next interrupt. Originally, the interrupt 6 input was connected to a edge-triggered logic circuit which would send an interrupt to the TMS 9901 upon making a LOW-to-HIGH transition. However, problems with glitches producing false interrupts obliged the author to by-pass the edge-triggering circuit, thus making interrupt 6 level-sensitive (as the other interrupt inputs are). When an interrupt, on level 6 occurs, the microprocessor, under software control, can subsequently test the interrupt input to ensure that a valid

interrupt has indeed occurred.

The TMS 9901 also provides an internal clock which can be used as either an interval timer or an event timer. The clock is enabled to cause interrupts by writing non-zero value to it, and is then disabled by writing zero to it. When the clock decrements down to zero, it issues a level 3 interrupt. The decrements, when it becomes zero, will be reloaded from the clock register and decrementing will start again. The clock decrements at a frequency equal to the system clock frequency divided by 64 ($3.0 \text{ MHz}/64 = 46875 \text{ Hz}$). The mask for level 3 in the TMS 9901 must be set so that the microprocessor will see the clock interrupt.

The microprocessor communicates with the TMS 9901 via the communications register unit (CRU). The TMS 9901 occupies 32 bits of CRU input and output space. Bit zero is the control bit which determines if the TMS 9901 is in the interrupt mode (0) or the clock mode (1). The TMS 9901 must be in the clock mode in order for a value to be loaded into the clock register, and it must be in the interrupt mode for the mask bits to be set or reset and to allow interrupts to occur. Writing a zero to bit 15 while in the clock mode executes a software reset of the I/O pins.

Several TMS 9901 devices may be cascaded to expand I/O and interrupt capability simply by connecting all CRU and address select lines in parallel and providing each device with a unique chip enable signal. The 310 I/O expansion module does just that by cascading three TMS 9901's

together. This module thus provides 48 parallel I/O ports. Thirty-two of these ports are used in communicating with the VAX 11-750 computer.

3.2.1.4 Asynchronous Communications Controller

The TMS 9902 asynchronous communications controller (ACC) provides an interface between the microprocessor and a serial, asynchronous communications channel. The ACC performs the timing and data serialization and deserialization functions, facilitating microprocessor control of the asynchronous channel. The TMS 9902 is utilized in this case to communicate with the terminal.

The TMS 9902 has five main subsections: CRU interface, transmitter section, receiver section, interval timer, and interrupt section. The CRU is the means by which the microprocessor communicates with the TMS 9902. The TMS 9902 occupies 32 bits of output CRU space, 23 of which are used by the microprocessor to communicate command and control information to the ACC. It also occupies 32 bits of input CRU space, which the microprocessor reads to sense the status of the device.

The TMS 9902 accepts the EIA Standard RS-232-C protocol. It interfaces to the asynchronous communications channel on five lines: request to send (RTS), data set ready (DSR), clear to send (CTS), serial transmit out (XOUT), and serial receive data (RIN).

The TMS 9902 also generates an interrupt to level 4 when any of the following conditions occurs:

1. DSR or CTS changes levels;
2. a character has been received and stored in the Receive Buffer Register;
3. the Transmit Buffer Register is empty; or
4. the selected time interval has elapsed.

It is by means of these conditions and the interrupts that result, that the TMS 9902, and thus the microprocessor, can communicate asynchronously with the terminal.

3.2.1.5 Memory

The TMS 9900 microprocessor can access up to 65,536 (or 64K) bytes of memory space. This microprocessor system actually uses 20 kilobytes of random access memory (RAM) and 32 kilobytes of instruction code spread over 36 kilobytes of read-only memory (ROM). The 101MA microcomputer module has on-board 8 kilobytes of ROM, using four TMS 2716 erasable programmable ROM's (EPROM), and 4 kilobytes of static RAM, using eight TMS 2114 memories. The remainder of the memory is provided by the 201 memory expansion module.

The first thirty-two words of memory are used for interrupt trap vectors, with the first word of each interrupt vector being the new workspace pointer, and the second word being the program counter. The next contiguous block of thirty-two memory words is used by the extended operation (XOP) instruction for trap vectors. The last two remaining memory words, $FFFC_{16}$ and $FFFE_{16}$, are used for the trap vector of the LOAD signal. The LOAD signal is actuated by the RESET switch on the 101MA microcomputer board. The

remaining memory is then available for program instruction code, data, and workspace registers.

3.2.2 Floppy Disk Drive

The microprocessor system utilizes two Shugart SA800 floppy disk drives that use standard eight-inch floppy disks. A TM 990/303B disk controller module is used as the interface between the microcomputer system and the disk drives.

The disks are formatted in an IBM single-sided, single-density track format. There are seventy-seven tracks per disk with twenty-six soft sectors per track. Each sector has 128 bytes of data and therefore the capacity of the disk is over 250 kilobytes. Each set, or sequence, of collected data requires four tracks. This allows nineteen data sequences to be stored on a disk.

The 303B disk controller consists of a local microprocessor system which utilizes a TMS 9900 microprocessor, a disk drive interface containing a TMS 9901 programmable systems interface, a host system interface, and a read/write controller. The host system interface consists of a communications register unit (CRU) and a direct memory access (DMA) interface. The disc controller communicates with the microcomputer system using the CRU for initialization and DMA for command, status, and data transfer.

Using the CRU, a 20-bit address is passed to the disk controller describing the location in the host memory of a

ten-word block called the command list. This command list defines a command for the controller to execute. It is used to transfer command data to the controller, and return status and error data to the host microcomputer. The controller accesses the command list via direct memory access. It executes the command in the command list and reports back completion status. The disk controller indicates a command completion by generating an interrupt to level 7.

3.2.3 Terminals

The microprocessor system has been designed to be able to use one of two video display terminals: either an ADDS Viewpoint or a Tektronix 4010 terminal. The terminal serves as the interface between the user and the microprocessor system. It is used as the entry port for system commands and as a display medium for the acquired and calculated data.

The ADDS Viewpoint is an inexpensive terminal capable of displaying alphanumeric characters. The display consists of twenty-four lines of eighty characters each. The characters can be displayed with a visual attribute such as reverse video, blinking, half intensity, underlined, or various configurations of these. The Viewpoint does not have any graphics capabilities, although by using the reverse video attribute, data can be displayed in a horizontal bar graph format.

The Tektronix 4010 terminal is capable of displaying alphanumeric characters and graphically displaying data. It has three modes of operation: an alphanumeric mode, a graphic plot mode and a graphic input mode. The operating modes are changed from one to another by issuing control characters. In the alphanumeric mode, the display screen allows up to thirty-five lines with seventy-four characters each. In the graphic plot mode, the 4010 uses 1024 addressable points in each axis. However, only 780 of these points are visible in the vertical axis. Graphic plotting information is sent from the microprocessor in a four byte sequence, containing high and low order y-axis coordinates and high and low order x-axis coordinates. In the graphic input mode the microprocessor can request information concerning a cross-hair cursor coordinate location or the alphanumeric cursor coordinate location. The latter is used in this system to determine when the display is full since the 4010 has no scrolling feature as the Viewpoint terminal does.

There are several operational differences between the terminals which have required software solutions (ie. scrolling, graphics capability, etc.). These will be described, along with the solutions utilized, in chapter four.

System Software

The organizational structure of the software of this microprocessor system is based upon a data acquisition system developed by Dr. Z. Koles of the Department of Applied Sciences in Medicine. The intent of this chapter is to provide a brief overview of the software organization and to describe the major modifications that were made in the design and development of a cerebral blood flow measuring system.

All of the software was written in assembler language with the aid of a Tektronix 8002A development system. The Texas Instrument TM990 assembler language has available sixty-nine software instructions. These commands support most of the common addressing modes, include some byte instructions, and access bit-addressable input/output space. The memory-to-memory architecture of the TMS 9900 microprocessor permits operations to be performed on any word in memory by any other word in memory.

4.1 Software Organization

The essential operation of this microprocessor system is menu-driven. That is, a list, or menu of commands is available to the user from which he/she can control the number and order of tasks that the system performs. In order for the system to be "user-friendly", many of the commands respond with descriptive error messages if prerequisite tasks have not been performed.

At power-up, the microprocessor loads the workspace pointer and program counter from the first two words of memory, and vectors to the beginning of the main CONTROL program. The initialization procedure clears several data memory buffers, loads a block of program constants from ROM to RAM, initializes the programmable systems interface (TMS 9901) and the asynchronous communications controller (TMS 9902), and waits for a two second warm-up period. The system then issues a prompt character and enters a READY state waiting for incoming commands from the terminal. The block of program constants (PCON) contains various system constants, flags, and variables as well as the disk command lists. Many of the words in this memory block are used as a common communication link, or "message board", between the command subroutines.

When a command is received, it is compared with the list of possible commands and control is then given to the appropriate subroutine. If the received command is not in the available command list, the system responds with a question mark. When control is returned from the subroutine, the system re-enters the READY state and awaits further commands (see figure 4.1).

There are two modes of operation which divide the commands into functional groups: the data acquisition mode and the analysis mode. This functional division was done to emphasize the separate roles each mode performs and to ensure that the collected raw data has been stored on disk

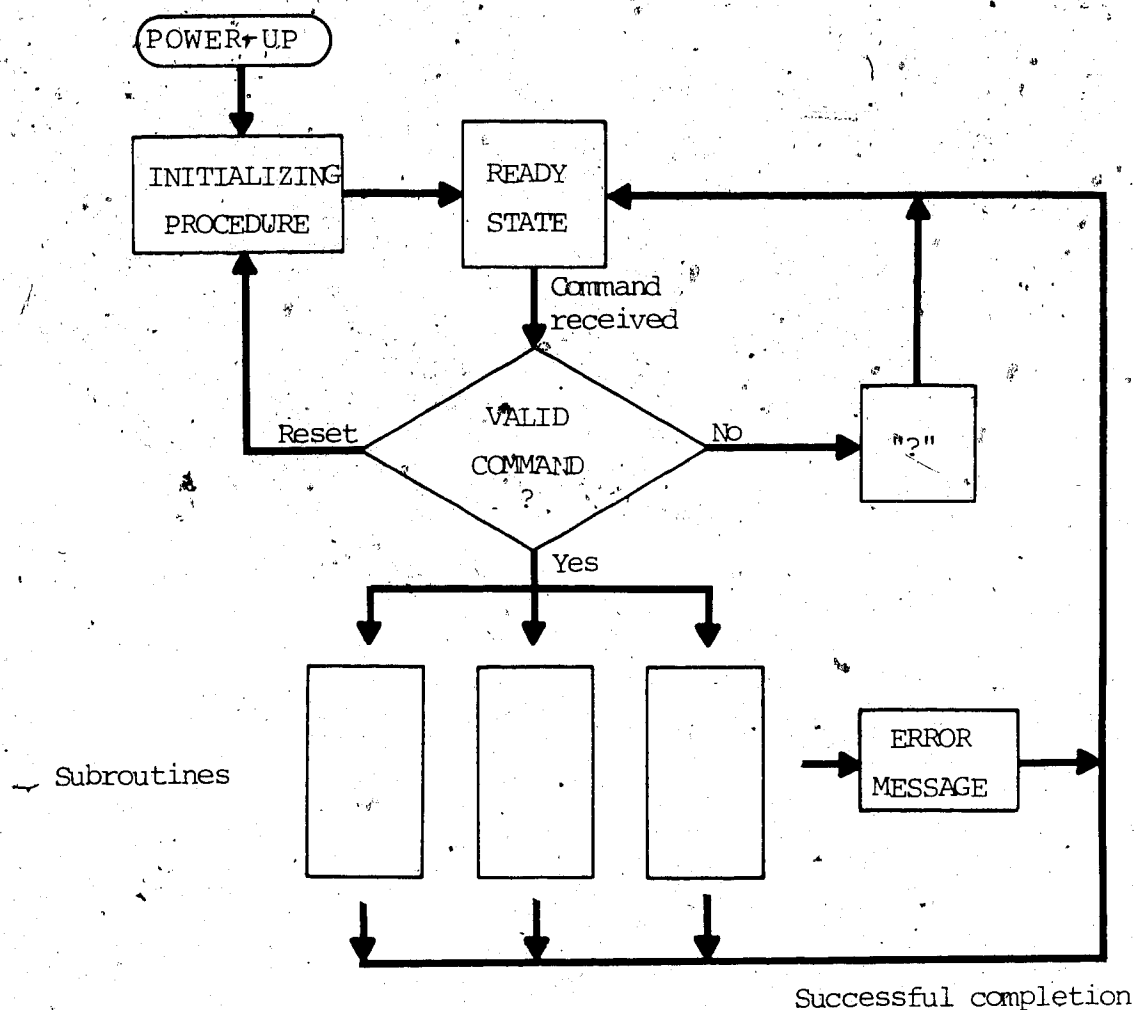


Figure 4.1 Basic System Task Flowchart

prior to any analysis. Before entering the analysis mode, the user must STORE the data on disk or RECALL it from disk to the main memory. Also, the command menu overflowed the screen of the Viewpoint terminal, and splitting the operation into two modes conveniently provided two separate menus, one for each mode. The data acquisition mode is the normal operating mode.

The command menus are listed in tables 4.1 and 4.2. These commands can be categorized into functional groups of

Table 4.1 Data Acquisition Mode Command Menu

COMMAND	DESCRIPTION	FUNCTION
DA n BKGD	-initiates data acquisition (n=disk unit) -initiates background measurement	Data Acquisition
DBKG DISPL f l	-displays background activity data -displays data collected from channels f to l	Data Display
FORMAT n FRESH STORE RCALL n s LABEL n HEADER n RLABEL n	-formats disk on unit n -clears data field on disk unit n -stores collected data on disk on unit n -retrieves data sequence s from disk on unit n -labels disk on unit n (termination //) -labels disk on unit n (fill in the blanks) -reads label from disk on unit n	Disk Management
CLEAR DUMP xxxx EXAMINE CHANGE	-clears data buffer memory -dumps a section of memory beginning at xxxx -displays a specified memory location -allows a specified memory location to be changed	Memory Management
ANALYSIS DSTAT UPLOAD OFF	-enters analysis mode -displays system status information -initiates uploading -terminates uploading	System Management

Table 4.2 Analysis Mode Command Menu

COMMAND	DESCRIPTION	FUNCTION
AIR HEAD	-calculates the air curve -performs a two-compartment CBF analysis	Analysis
CBF DBKG	-displays CBF analysis results -displays background activity data	Data Display
DISPL f 1	-displays data collected from channels f to 1	
STORE	-stores CBF results on disk on unit n	Disk Management
END	-returns system to data acquisition mode	System Management

system management, data acquisition, data display, disk management, memory management, and analysis. Through the use of these commands the user can acquire and display data, store this data on a disk, retrieve it later from the disk back to the memory, analyze the data, and display the results. While the use of several of the commands have prerequisite tasks, the sequence of tasks performed is largely up to the discretion of the user. The user may write a label on the disk in either an open, or fill-in-the-blank type format (ie. LABEL and HEADER commands, respectively), and, subsequently, read the label from the disk (ie. RLABEL

command). Memory management commands allow the user to CLEAR data buffers in preparation for new data, and to display any location of memory. The user can also CHANGE any memory location in RAM, including the program constant area. The UPLOAD command allows the system to initiate an uploading procedure which transfers data from a disk to an external computer (eg. VAX 11-750).

The software programs and subroutines which support these commands can also be divided into functional groups similar to that of the command menus. Some of these programs will be described in more detail later in this chapter.

4.1.1 Terminal Software Support

In order for the microprocessor system to be able to support two terminals with different characteristics, several additions to the existing software were required. While the Viewpoint terminal is a relatively simple terminal to communicate with, the Tektronix 4010 terminal, because of its graphics capabilities, requires additional software support.

The means by which the microprocessor communicates with either terminal are four communication driver routines. These driver routines incorporate extended operations (XOP) and an interrupt service routine to provide an asynchronous communications channel. The first XOP is used to clear and initialize the asynchronous communications controller. A status XOP provides information concerning the current

operation (ie. read, write), the previous operation, and the number of characters transmitted. The read and write XOP's initiate their respective operations while the interrupt service routine (interrupt level 4) facilitates subsequent asynchronous transmission of characters. These driver routines are used by the microprocessor to transmit and receive characters with both terminal types.

The Tektronix terminal also has several subroutines which provide dedicated software support. These subroutines are named: CURSOR, ERASE, IPLOT and SYMB. The CURSOR subroutine returns the x and y screen coordinates of either the alphanumerics cursor or the cross-hair cursor, depending on which ASCII control characters it transmits to the terminal. Unlike the Viewpoint terminal, the Tektronix terminal has no "scrolling" ability. Therefore, whenever a message is written to the Tektronix screen, an integer value is first placed in a *minimum row count* memory word in the program constant area (PCON + 204)¹⁰, equal to the height of the message in screen points (twenty-two points per line). Before writing the message, the system uses the subroutine CURSOR to determine the present position of the alphanumeric cursor. If there is sufficient room for the message, it is transmitted; if there is not, the screen is first erased using the subroutine ERASE, and then the message is transmitted. The ERASE subroutine erases the Tektronix

¹⁰ PCON is a label equal to the memory address of the first word in the program constant area, and therefore PCON + 204 is equal to the memory address of the word starting at the 204th byte.

screen by sending the ASCII control characters ESC and FF. A time delay of .75 seconds is then required before transmitting further data,

The subroutine IPLOT is used to plot points on the Tektronix 4010 screen. IPLOT puts the terminal into the graphics plot mode, plots the points, and then leaves the terminal in the alphanumerics mode. The input buffer data must be x and y screen point coordinates. IPLOT converts this data into a format accepted by the Tektronix terminal (ie. high and low order bytes), and places it into an output buffer before transmitting it. The input data can be of the form $x_1, y_1, x_2, y_2, \dots$, or of the form y_1, y_2, y_3, \dots , with a constant-incrementing increase in the value of the x coordinate (ie. X-STEP).

The subroutine SYMB draws ASCII characters on the Tektronix 4010 terminal. When this subroutine is called, Workspace register 12 must contain the address of where the particular ASCII character array begins. The first three words of this array must contain the following information:

1. the number of ASCII characters,
2. their size (in integer multiples of normal character size), and
3. their orientation (in integer multiples of 45 degrees).

The x and y coordinates of the lower left corner of the first character must also be given in workspace registers 14 and 15, respectively. If the number of characters is a negative quantity, then the characters are centered at the x

and y coordinates.

SYMB uses two look-up tables to describe and plot each character. The first table, TAB1, is used to access TABLE which contains the x,y points that define the ASCII characters. Each word in TAB1 specifies the offset into TABLE and the number of x,y coordinate parts for that particular ASCII character. Access into TAB1 is made by using the hexadecimal ASCII value of the character. SYMB then acts upon these coordinate pairs, according to the size and orientation information given, and assembles the final x,y coordinate pairs in an output buffer. The subroutine IPLOT is then called to transmit and plot these character points to the terminal.

The microprocessor system determines which terminal type is connected by means of a *terminal type flag* (PCON + 202). This flag is cleared at power-up or can be changed by a TTYPE command. Whenever the microprocessor has a task to perform which is dependent upon the terminal type, it checks the terminal type flag. The flag will be zero for the Viewpoint terminal and nonzero for the Tektronix 4010 terminal.

For example, the HEADER command requests pertinent patient information by writing a fill-in-the-blank type message to the screen, whereupon the user responds by inserting data in the proper blank. With the Viewpoint terminal the cursor can be moved to each new answer location by issuing appropriate control characters. However, when in

the Tektronix mode, the microprocessor uses the subroutine IPLOT and transmits a single x,y coordinate pair corresponding to each location.

4.2 Data Acquisition

The data acquisition software consists of two primary tasks: to ensure that the entire system is prepared to collect data, and, to acquire data and display it in real-time. Both the BKGD and DATA commands utilize much of the same software. However, they differ in two aspects: Firstly, unlike the DATA command, the BKGD command does not access the disk controller. And secondly, at the termination of data acquisition, the BKGD command sums and averages the data for each channel and stores the number of counts per second in a background data buffer (see figure 4.2).

Both data acquisition commands (ie. BKGD and DATA) begin by initiating a system readiness check (subroutine SRDY). This involves initially ensuring that the Inhamatic system is connected to the microprocessor system, and secondly, that the Inhamatic system is powered on. The software accomplishes this by testing I/O port 10, via the TMS 9901 and the CRU, which is connected to the ERROR line on the interface module (see figure 3.6). Since the I/O ports on the TMS 9901 are normally held high by 10K resistors, connecting a port to ground through a resistance of 2.6K, as the ERROR line does, will change the state of that port. Thus, testing the state of port 10 will indicate

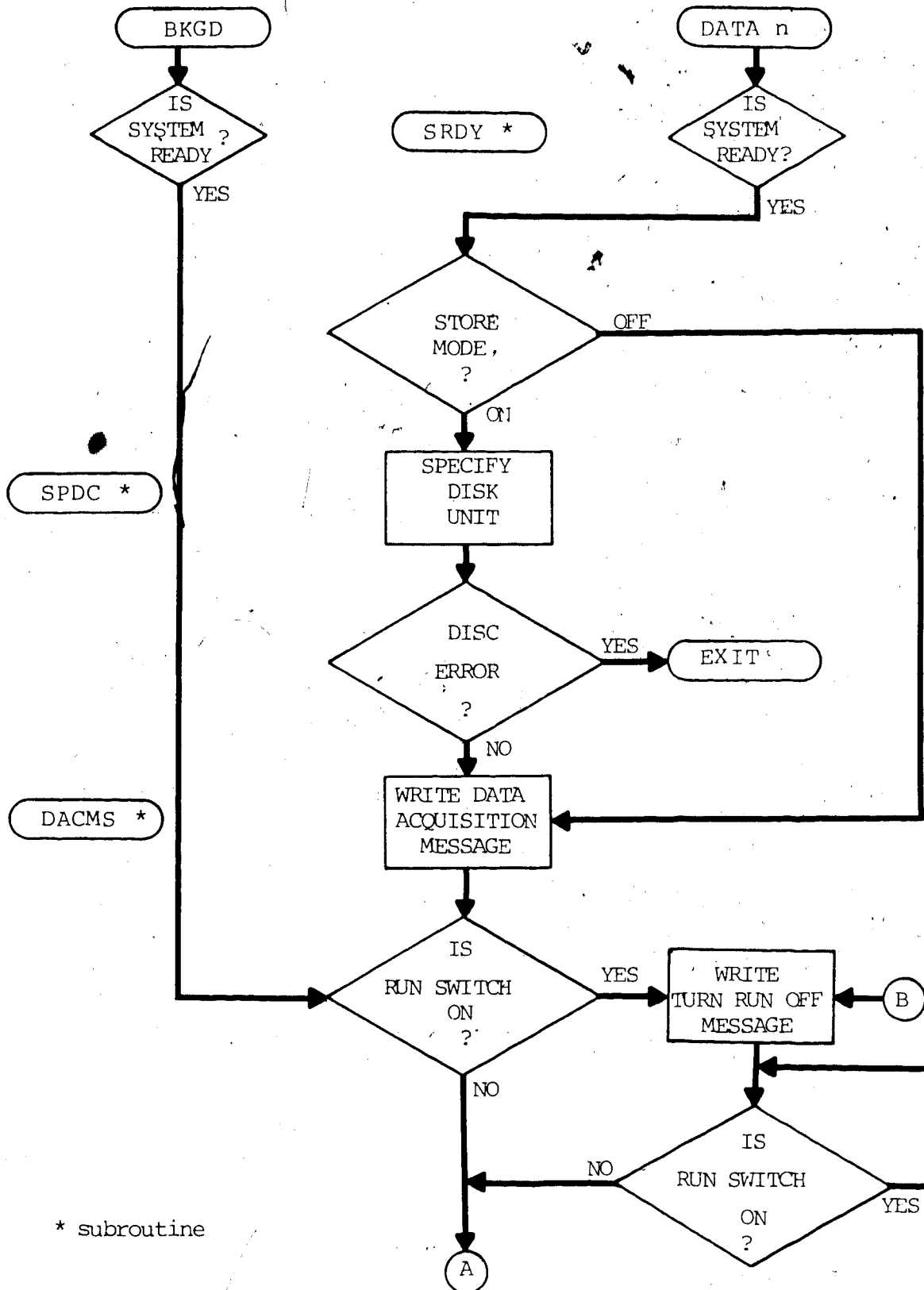


Figure 4.2 Data Acquisition Flowchart

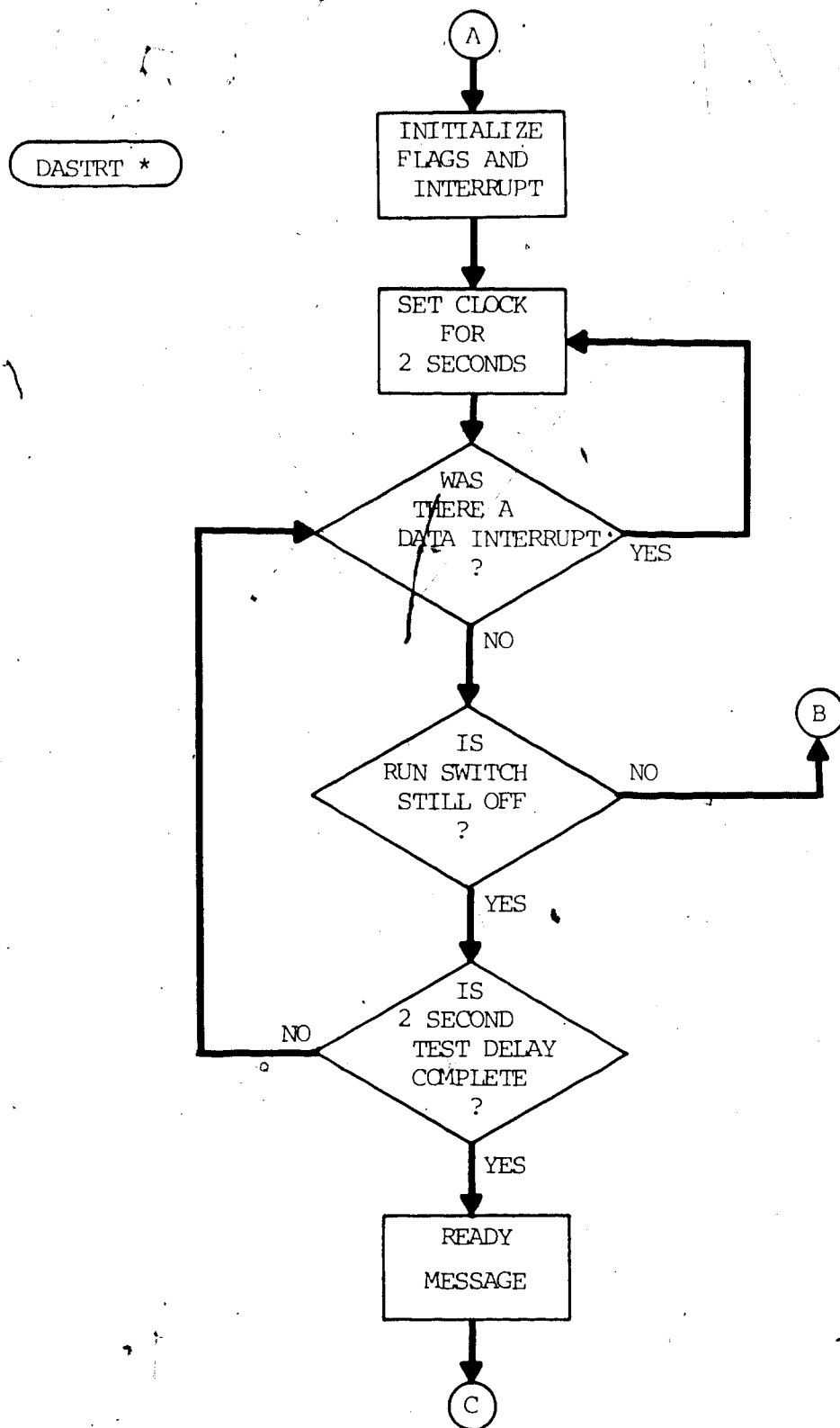


Figure 4.2 (cont'd.)

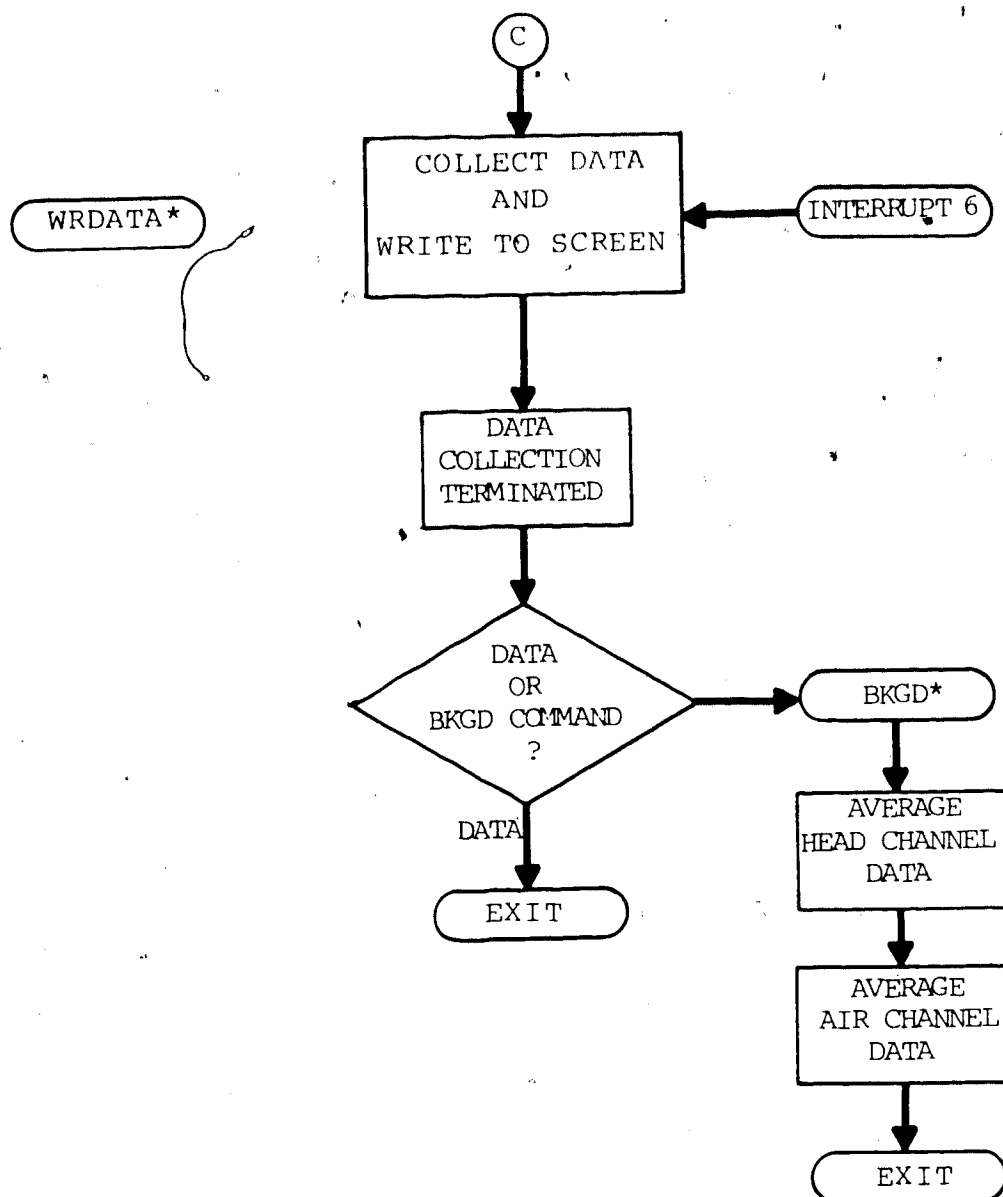


Figure 4.2 (cont'd.)

whether the Inhamatic system has been connected. Once that has been established, the software tests I/O port 12 to check if the Inhamatic system has been powered on. Port 12 is connected to the five volt power supply in the interface module. If the Inhamatic system is turned off, this line will be grounded through the supply and other circuitry. If it is on, the line will be held high. The software also verifies that previous data has been either cleared from memory or stored on disk.

The DATA command may or may not specify a disk unit number. If it does not, data is still able to be collected, but it cannot be stored on disk subsequent to data acquisition. Normally, the user should specify a disk unit number unless there is no need to store the data. If a disk unit is indicated (ie. store mode is ON), the microprocessor accesses the disk controller and verifies the disk drive's operational status. Regardless of the store mode status, the microprocessor system will then write a message to the terminal screen, prompting the user for patient's pertinent physiological parameters (eg. hemoglobin, hematocrit, PaCO_2 , blood pressure, etc.). These parameters are stored in the program constant area.

The next task that the data acquisition commands perform is to establish the status of the RUN switch, which is on the front panel of the Inhamatic system. The RUN button is connected to the interface module (PUNCH ON line) and then, via an inverter, to its output port (figure 3.6).

The microprocessor can check this inverted RUN line by testing its I/O port 11. If the RUN button is determined to be on, the microprocessor issues a message directing the user to turn the RUN button off, and then resides in a testing loop until he/she does so. Knowing that the RUN button is off, the microprocessor can then clear several flags and load parameters that are utilized by the data interrupt service routine, and also enable the data interrupt (level 6).

The importance of this aforementioned, and apparently elaborate, procedure is to ensure the integrity and validity of the collected data. The main impediment to simple and successful data transfer is that the sequence of data that the Inhamatic system transmits contains no flags or markers signifying the beginning or end of valid data. Thus, if the microprocessor system was prepared to accept data before, for example, the Inhamatic system was connected or powered on, such action could produce glitches or false interrupts which the microprocessor would accept as valid data. When valid data was transmitted, the data sequence would be offset such that the microprocessor would have no way of determining what data type it was collecting (ie. head channel data or air channel data).

A further problem is that when data transmission is terminated before a complete sample interval is transmitted, the data from the remaining partial interval continues to reside in the interface module memory. When the

microprocessor system initiates a subsequent data acquisition sequence, the Inhamatic system transmits the data from the partial sample interval before transmitting a new data sequence. Thus, the proper sequential order of data transmission is once again disrupted. To avoid this difficulty, the software initiates a two second delay. During this delay, should any data interrupts occur, the clock is reset for a further two second delay and, as long as the RUN button remains off, the data is ignored. If the RUN button is turned on during this period, a message instructing the user to turn the RUN button off is transmitted to the terminal screen, and program control is returned to the RUN button test delay loop described previously. Therefore, a two second period with no data interrupts must occur before the microprocessor system is ready for the transmission of valid data. The time length of two seconds was chosen because, since the Inhamatic system transmits data every $1/16$ of a sample period, the longest possible time period between data transmissions would be with the 30 second sample interval length, or $30/16$ seconds.

The acquisition of data is accomplished using a WRDATA subroutine and the data interrupt service routine. When the Inhamatic system raises the punch instruction line signifying that data is ready to be transmitted, an interrupt on level 6 occurs. The interrupt service routine first of all verifies that the interrupt is valid. If the interrupt line remains high (ie. valid interrupt), the data is read on I/O

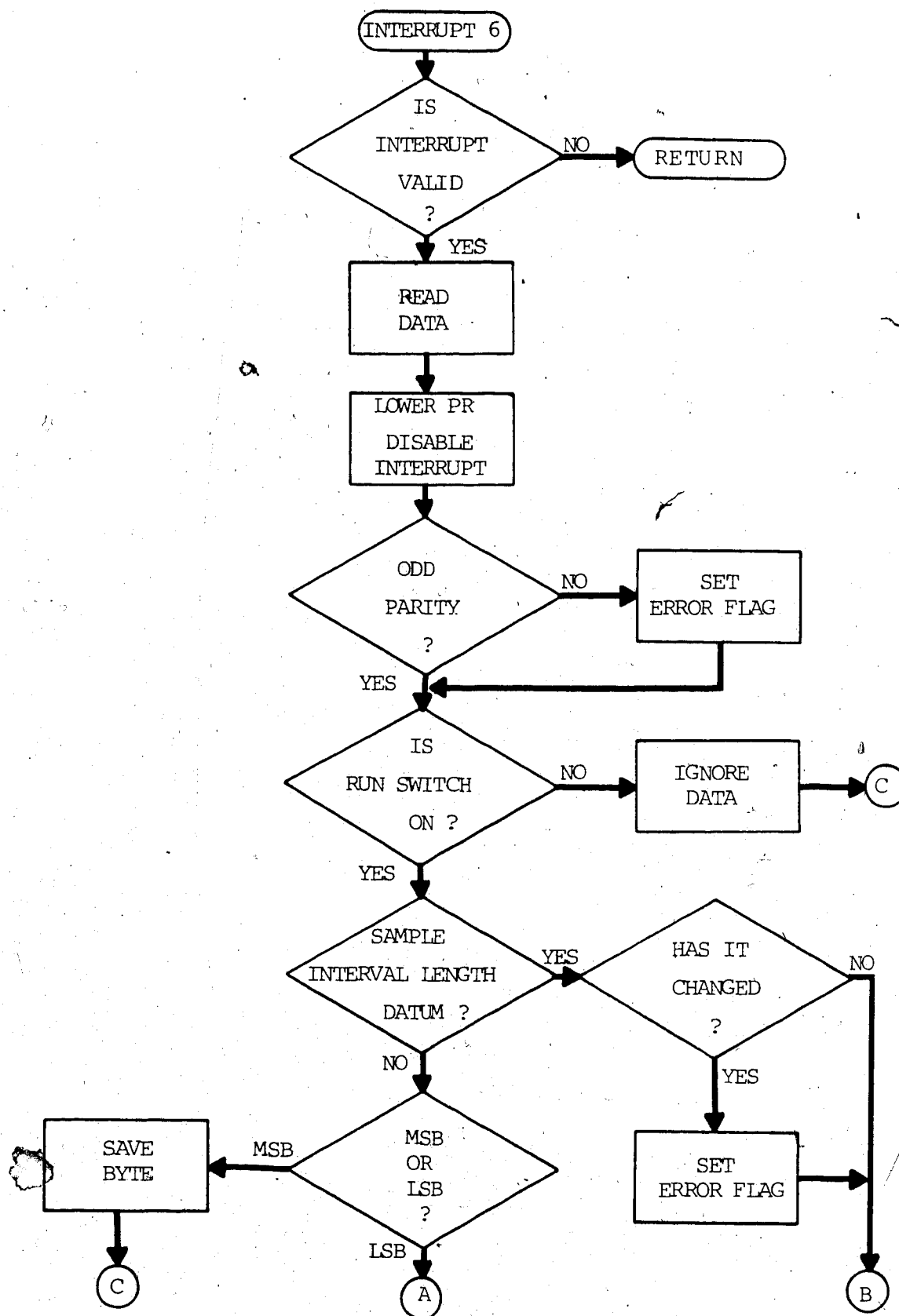


Figure 4.3 Data Interrupt Service Routine Flowchart

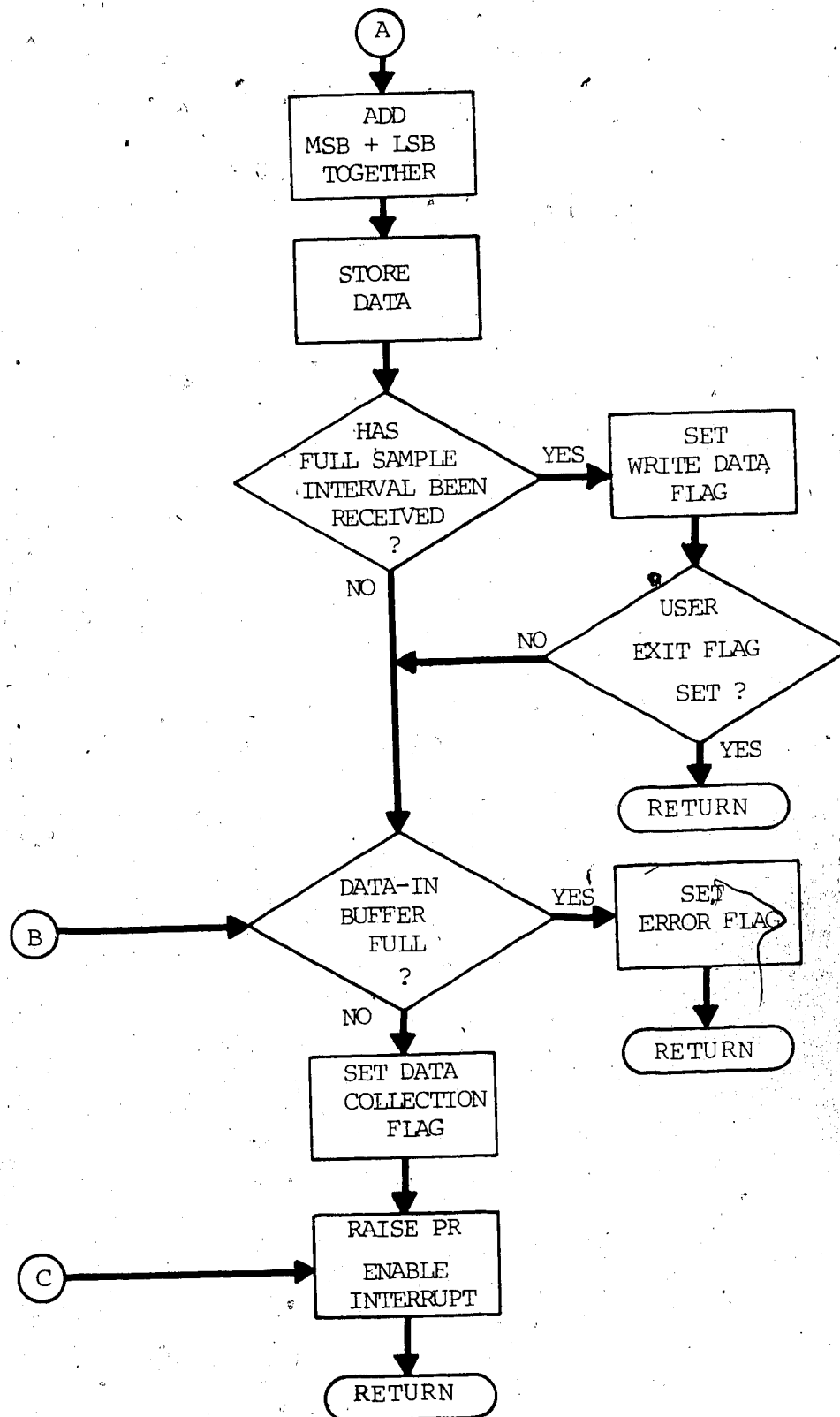


Figure 4.3 (cont'd.)

ports 0 through 7. The software then disables the level 6 interrupt mask bit at the TMS 9901 and lowers the punch ready line (I/O port 8) informing the Inhamatic system that it has received the data. The data is checked for odd parity and an error flag is set if it is even. The error flag is a word in the program constant area into which a value of one is placed for a parity error, a value of two if the sample interval length changes from one interval to the next, and a value of three if the data buffer memory is filled. The WRDATA subroutine subsequently acts according to the value present in this error flag.

Before the interrupt service routine stores or acts upon the data that has been read, it verifies that the RUN button is on. If it is off, the data is ignored, the punch ready line is raised, and the interrupt enabled in preparation for the next data transmission. In this manner, any data that is transmitted during the two second delay can be ignored, while still allowing any remaining data in the interface module memory to be read out.

The first two bytes of each sample interval describe the sample interval length. This is compared with the previous sample interval length to ensure that it has not changed in the interim. If it has, a value of two is placed in the error flag. The following byte of information will be the most significant byte of the air channel data. This byte is temporarily stored until the least significant byte (ie. the next byte in the data sequence) is acquired. These two

bytes are combined to form a data word which is then stored in the appropriate memory buffer. This procedure continues similarly for all of the air and head channel data in one sample interval.

The raw data memory buffers for the air and head channel data are labelled DATIN and HEDAT, respectively. DATIN begins at memory location B000₁₆ but starts storing air data, after a short header buffer, at B020₁₆. Head channel data is stored in HEDAT beginning at D310₁₆, in a sequential manner (ie. channel 1, channel 2, etc.). Both data buffers are sufficiently large to store data for 279 sample intervals. With each data word that is stored, the interrupt service routine compares the total number of data words stored with the length of the data buffer, to ensure that there is sufficient space for subsequent data. If there is insufficient space left, the service routine sets the error flag and returns without enabling the interrupt mask bit, thereby preventing further interrupts from occurring.

When the interrupt service routine has received data for a full sample interval (ie. 98 bytes), it sets the *write data flag*. It also checks if the *user exit flag* is set. If it is, the service routine returns to the subroutine WRDATA without enabling the interrupt mask bit.

Before a normal return, the interrupt service routine raises the punch ready line, signifying to the Inhamatic system that the microprocessor system is ready to accept new data, and enables the interrupt mask bit. When the first

byte of data is successfully received, the *data collection flag* is set and remains so throughout the data acquisition sequence.

The subroutine WRDATA is where the microprocessor system resides during the acquisition and real-time display of data. The core of this program is a monitoring loop in which three conditions are continuously tested: user stop request, the error flag, and the write data flag (figure 4.4). The interrupt service routine will set the error flag and the write data flag when appropriate, as previously described. If the error flag is set, WRDATA determines which error has occurred, writes the corresponding error message on the terminal screen, and then resumes normal operation. The exception is the memory full error, in which case the subroutine WRDATA returns control back to the main program. This is the only condition which will terminate the data acquisition procedure, other than a user request.

If the write data flag is set, WRDATA transmits the air and head channel data for the immediately preceding sample interval, to the terminal screen. Before every tenth interval, it also writes a data header. Prior to returning to the monitoring loop, WRDATA tests the user exit flag. If it is set, control is returned to the main program and data acquisition is terminated.

In the interim time between when data is being written on the screen, the terminal is in a read mode. That is, it is waiting for input from the user. The software recognizes

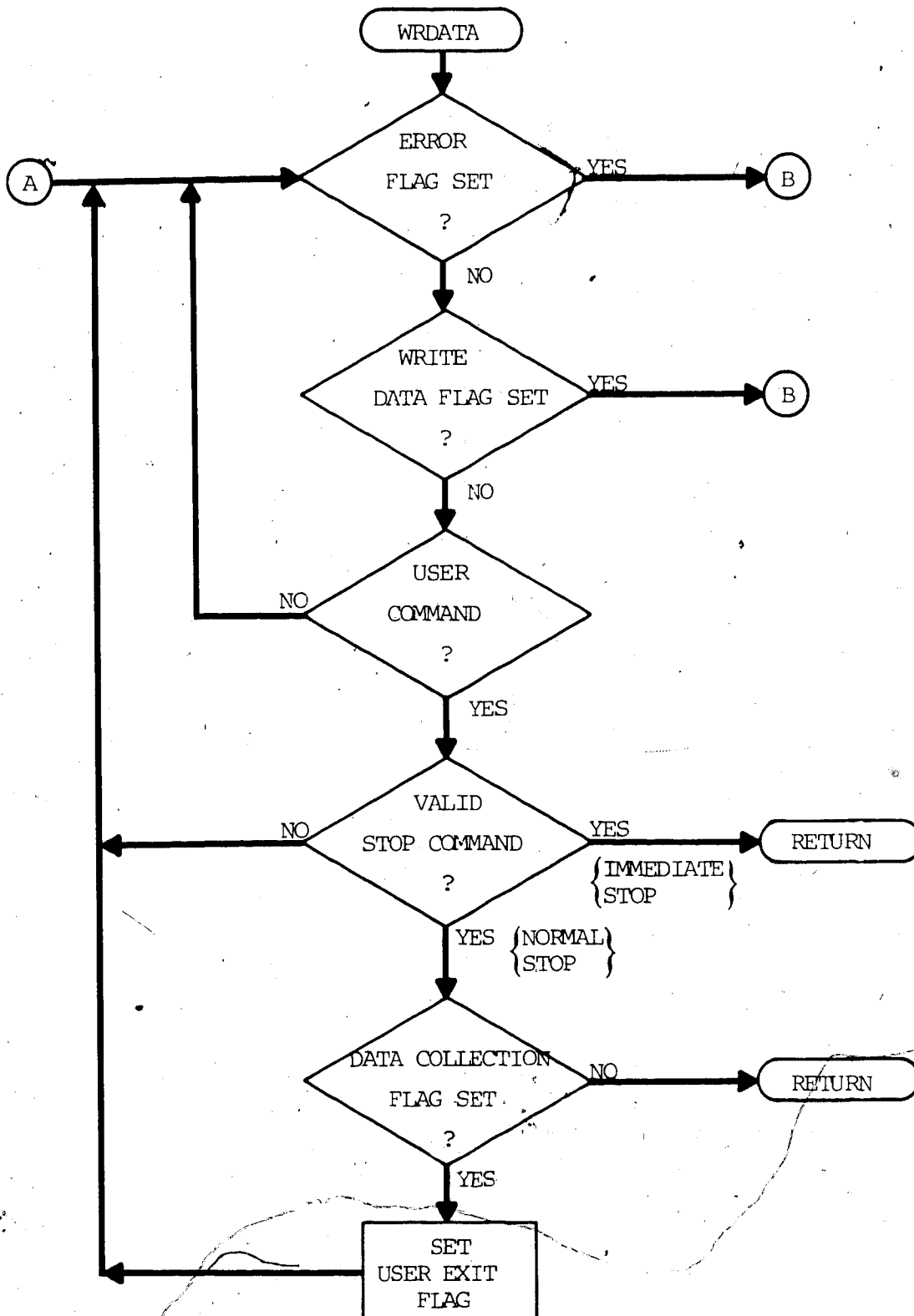


Figure 4.4 Real-Time Data Display Subroutine Flowchart

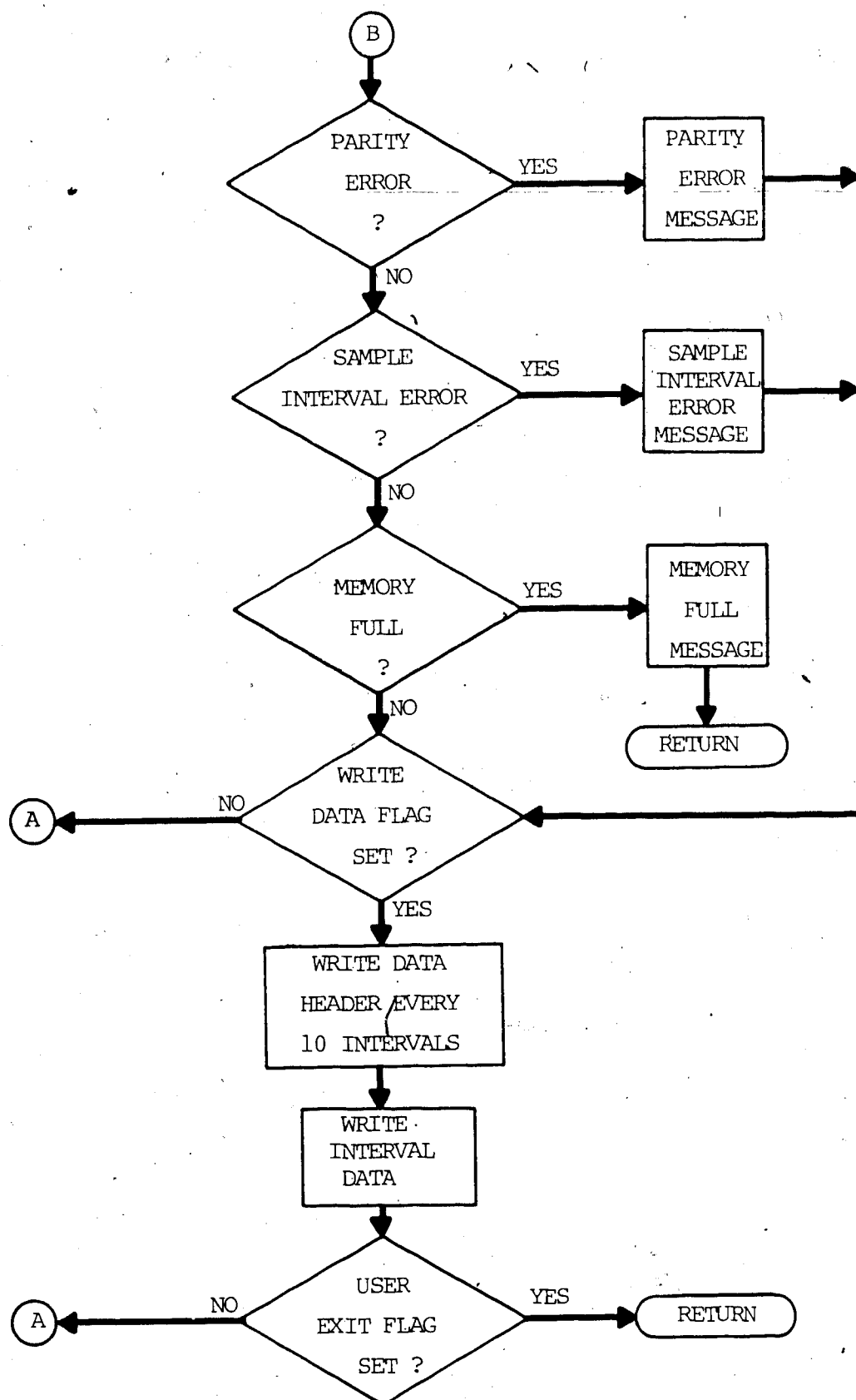


Figure 4.4 (cont'd.)

two stop commands, representing a normal stop or an immediate stop. If the user requests a normal stop (ie. space bar), WRDATA tests the data collection flag. If it has not been set (ie. no data has been collected), software control returns immediately to the main program. If the data collection flag has been set, WRDATA sets the user exit flag. By this method, data can continue to be acquired for the duration of the current sample interval, after which WRDATA writes the interval data on the terminal screen and returns control to the main program. In other words, the normal stop command terminates data acquisition at the end of the current sample interval. If the user requests an immediate stop (ie. control S), WRDATA returns control to the main program abruptly, regardless of the data acquisition state. This immediate stop command is required when the Inhamatic system ceases to transmit data, and the microprocessor system continues to wait for data to be transmitted. In this case, a normal stop command would require a further sample interval of data to be received before data acquisition is terminated.

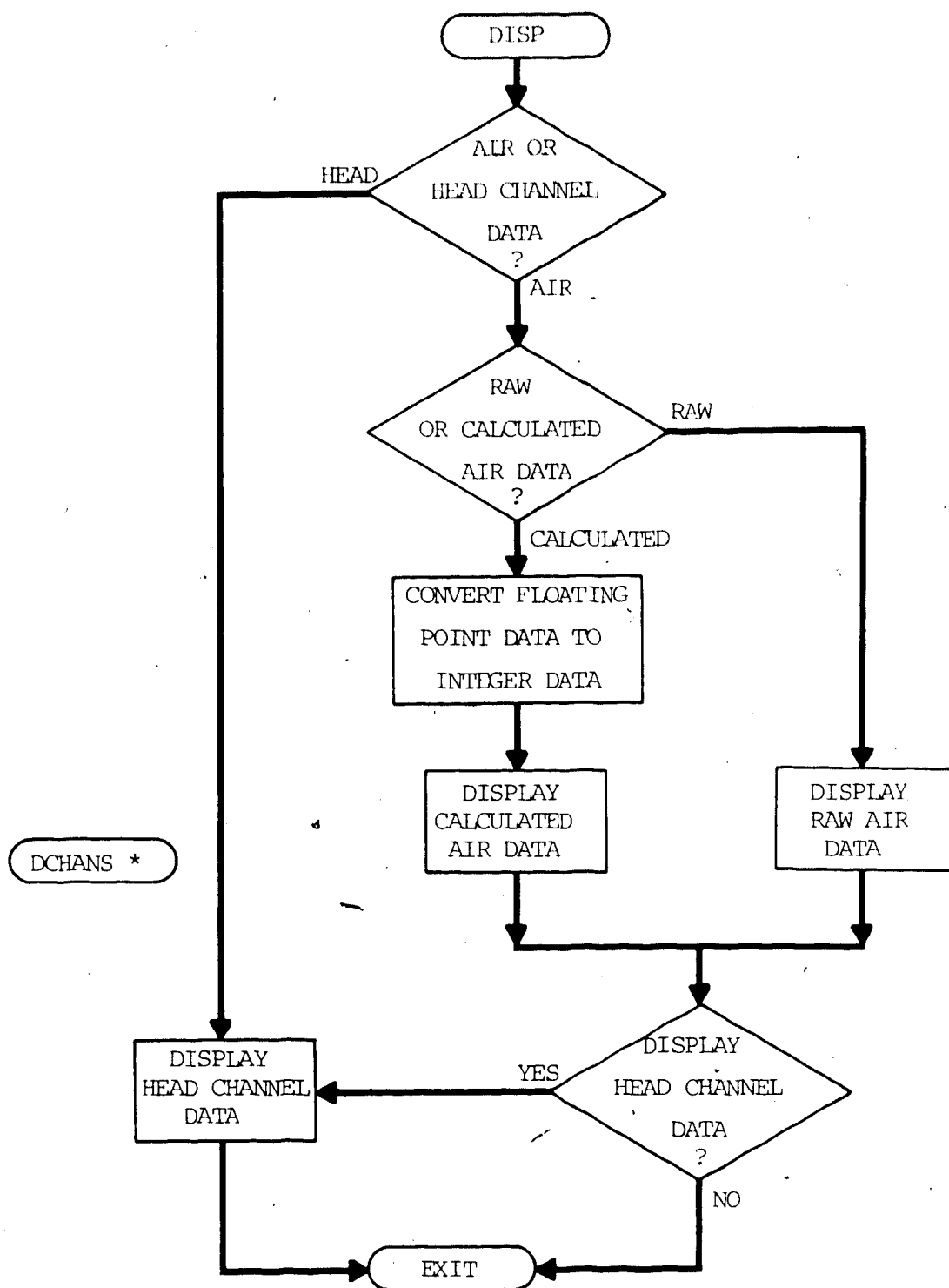
When control is returned to the main program, the data interrupt mask bit is immediately disabled, all the data acquisition flags are cleared, and the punch ready line is lowered. The microprocessor system then returns to the ready state in preparation for subsequent user commands.

4.3 Data Display

The data display software was designed in order to display three possible data types on two different terminals, using the same DISPL command. The data that can be displayed are raw and calculated air data, and head channel data. The subroutine DISP (figure 4.5) determines what data type the user is requesting to be displayed by the channel number specified in the DISPL command (ie. air channel is number zero), and by the air curve calculation flag. The air curve analysis program locates the maxima and minima of the raw air data curve, and interpolates between these values to provide a final, or calculated, air data curve. When this air curve analysis is performed, the air curve calculation flag is set.

The calculated air data is stored in a memory buffer in floating point notation. Therefore, before displaying this data, it must be converted to integer values. The subroutine DISP also specifies which channels are to be displayed, according to the user's request, and where in memory that specific data is stored. It then calls the subroutine DCHANS which contains the data display routines.

The subroutine DCHANS has two data display modes which correspond to the two terminal types. Which specific mode is chosen, is dependent on the terminal type flag. The main difference is the ability of the Tektronix terminal to graphically plot data.



* subroutine

Figure 4.5 Display Subroutine Flowchart

4.3.1 Viewpoint Terminal Display

The Viewpoint terminal is strictly an alphanumeric terminal. In order for it to graphically display data, therefore, a reverse video attribute is used in a horizontal bar graph format. By finding the maximum value of the data to be displayed, this value can be used to scale the data, such that each data value is represented by a relative number of horizontal spaces with respect to the total width of the screen. These spaces are then displayed on the screen using a reverse video attribute (ie. light spaces on a dark screen). Each horizontal line represents one sample interval data value. Data is displayed until the screen is full, at which time the microprocessor system waits for the user to strike any key before displaying further data.

After each channel is displayed, a subtitle is written on the screen describing the maximum data value, and in which interval and channel number it may be found. The subtitle also includes the sample interval length and the number of intervals collected.

4.3.2 Tektronix 4010 Graphical Display

The objectives in using the graphic capabilities of the Tektronix 4010 terminal were to plot any number of sample intervals, utilizing the full length of the horizontal axis of the graph, and to be able to use two graph sizes. The small graph size would permit four graphs to be drawn on the terminal screen at a time, while the large graph would allow

only one. These objectives presented several difficulties.

The main challenge was the development of an algorithm that could map any integer number of intervals onto a fixed number of available screen points. When the number of intervals is less than the number of screen points, the mapping solution can be fairly simple. However, in some situations only half of the available screen points would be used (for example, a one-to-one mapping of 201 intervals onto 400 screen points). When the number of intervals is greater than the number of screen points, the mapping solution becomes more complex. The problem is compounded further if the algorithm is to work with different graph sizes.

The algorithm that was developed has two essential elements. Firstly, rather than having a horizontal axis of fixed length, a *nominal* number of available screen points on the horizontal axis was specified. Then, depending on the number of sample intervals to be plotted, the length of the horizontal axis is allowed to vary within certain boundaries. This allows maximal use of the full scale of the horizontal axis. Secondly, in the situation where there are more intervals to plot than available screen points, one solution would be to divide the available number of screen points into the number of intervals to determine how many intervals can be plotted (for example, 800 sample intervals mapped onto 400 screen points means that every second interval can be plotted). However, it was found that if a

smaller divisor than the number of available screen points was used, the limits of variation of the horizontal axis could be made narrower. Using a given nominal number of screen points (ie. 390 for the small graph, and 838 for the large graph), optimal values of the divisor were found for the two graph sizes, which provided maximum horizontal axial lengths which were also within relatively narrow limits of variation. The values that were chosen were 125 for the small graph and 250 for the large graph.

This horizontal axis scaling algorithm can be described, then, as follows. It is important to note that the arithmetic operations that the microprocessor uses are integer operations. Therefore, any division that occurs requires a decision as to whether the answer will be rounded up or down to the nearest integer.

1. Plot every $(I/125)^{\uparrow}$ th interval collected¹¹, where I is the total number of sample intervals collected.¹² Or, in other words, plot the following number of intervals:

$$I' = (I/(I/125)^{\uparrow})^{\downarrow} \quad (4.1)$$

2. The next largest integer value greater than I' that is divisible by four can be found as follows:

$$I_m = 4 \cdot (I'/4)^{\uparrow} \quad (4.2)$$

This value is used to determine four integer values that label the horizontal axis. The largest of these label values will be equal to $(I_m) \cdot (I/125)^{\uparrow}$, while the

¹¹ Plot every $(I/250)^{\uparrow}$ th interval on the large graph.

¹² The arrows indicate a round-up, round-down, or round-to-the-nearest integer operation.

remaining three values will be equal to one-quarter, one-half, and three-quarters of this value, respectively.

3. The number of screen points between each consecutive sample interval datum that is plotted can be calculated as:

$$X\text{-STEP} = (H/I_m) + 1 \quad (4.3)$$

where H is the nominal number of available screen points on the horizontal axis. $X\text{-STEP}$ is used by the subroutine IPLOT to plot a sample interval datum on every $(X\text{-STEP})$ th screen point on the horizontal axis.

4. To find the actual length of the horizontal axis in screen points, H_m , we must multiply the maximum number of interval values that are plotted by the number of screen points between each datum, or

$$H_m = I_m \cdot (X\text{-STEP}). \quad (4.4)$$

Since there are eight ticks on the horizontal axis (four of which are labelled), the number of points between each tick is simply H_m divided by eight.

Thus, using the above calculated values, the horizontal axis can be adequately described, and the data can be scaled over most of the available horizontal length.

The software chooses a particular size of graph depending on the type and number of channels requested in the DISPL command. If the air channel and/or a single head channel are requested, the subroutine DCHANS draws a large graph on the screen. If more than one head channel is

requested, the subroutine DCHANS draws the small graphs on the screen. Rather than storing the coordinate pairs for four separate small graphs, the software contains the dimensions of one generic graph. Before drawing each graph, the appropriate x,y origin values are added to the coordinate pairs of this generic graph. The graph axis' and labels are then drawn on the screen along with the corresponding data. The data is scaled both horizontally, as previously described, and vertically, and then added to the appropriate x,y origin values before being plotted on the terminal screen.

The vertical scaling of the data compared with the horizontal scaling, is quite simple. The largest value of the data to be displayed determines the scaling factor. This scaling factor can be one or any multiple of ten (ie. one, ten, one hundred, etc.), and it is displayed on the vertical axis. The number of available screen points on the vertical axis is 250 for the small graph, and 600 for the large graph. The data display algorithm can accomodate any number and values of data, up to a maximum of $FFFF_{16}$ (ie. 65535_{10}).

When all of the requested channels have been displayed, or the screen is full, the program writes a subtitle message to the terminal, similar to the one on the Viewpoint terminal. The microprocessor will then wait for the user to strike any terminal key before erasing the screen. It will then display additional data, if it has been requested, or return to the READY state in preparation for the next

command.

4.4 Data Analysis

The technique of cerebral blood flow measurement used in this system is that of ^{133}Xe inhalation. The algorithm, which analyzes the collected data, utilizes a two-compartment exponential model in which a faster clearing compartment, considered to be cerebral grey matter, is separated from a slower clearing compartment, considered to be white matter and extracerebral tissue. This algorithm incorporates the method proposed by Obrist et al.[59], along with the Initial Slope Index (ISI) that was defined by Risberg et al.[66]. The technique was chosen for reasons that have been described previously. The algorithm used to calculate the cerebral blood flow parameters was chosen on the basis of its availability, and its well-established and common usage.

The data analysis consists of two separate operations, represented by the AIR and HEAD commands. These commands reside only in the analysis mode (table 4.2). The analysis mode also contains data display commands, and a STORE command. The data display commands, DBKG and DISPL, are the same commands as found in the data acquisition mode. The CBF command displays cerebral blood flow analysis results in a tabular form, on the terminal screen.

The STORE command differs slightly from the STORE command in the data acquisition mode menu. The STORE command

in the data acquisition mode transfers each sequence of data from memory to four consecutive and contiguous tracks on the disk. The STORE command in the analysis mode, however, transfers data from memory to the *same* four disk tracks that were last referenced. Since the data must be stored (or recalled) before the system permits the user to enter the analysis mode, this second STORE command allows the user to transfer cerebral blood flow analysis results and/or calculated air data to the same four tracks on the disk as the original data. A cautionary note that the user should be aware of is that should the data be restored on the disk in this manner, subsequent to an air data calculation, the original raw air data will be lost, since the new calculated air data will be written over it. The original head and background data, however, are preserved.

The two main subroutines involved in data analysis are AIRCRV and HEAD. These computer programs, which were developed by Obrist et al.[59] and Risberg et al.[66], are available in FORTRAN from the Department of Applied Sciences in Medicine. They were transcribed into Texas Instrument assembler language for use in this microprocessor-based system.

4.4.1 Air Curve Analysis

As previously mentioned, the inhalation method requires, as an approximation of the arterial input function, an end-expired air curve. The subroutine AIRCRV

calculates this curve from the expired air data. The procedure by which this is accomplished can be described in four basic steps:

1. find the maximum and minimum data values,
2. edit and smooth the resulting curve,
3. find the maximum value, and the subsequent start point of fitting, and
4. interpolate between the data values to find points which correspond with the head data points.

During the period of time in which ^{133}Xe is being inhaled, the minimum values of the expired air curve represent the *end*-expired air. When the patient begins to breath room air, the maximum values represent the *end*-expired air. The subroutine AIRCRV finds the minimum values by using a moving "window" of five data points. Within this window, whenever the *middle* data point is determined to be less than any of the remaining four points, a decision to choose that data point as a minimum is made. Similarly, this same technique is used in determining the subsequent maximum data values. That is, whenever the middle data point of a moving five point window is greater than the remaining four points, that point is considered a maximum.

Some editing of the end-expired air curve is also performed in which any data values which are outside specified limits are removed. The subroutine AIRCRV also determines the start fit time, which occurs when the end-expired air curve is less than 20% of its maximum value

(as proposed by Obrist et al.[59]). And finally, the subroutine linearly interpolates between the data points to find values which correspond in time with the head data points. These final air data values constitute the calculated air curve.

Since a time delay exists between the end-expired air curve and the arterial concentration curve, a time shift Δ_1 , is added to the time values of the calculated air curve. The value of this delay is estimated to be -6.0 seconds.

4.4.2 Head Curve Analysis

Head curve analysis is carried out in accordance with the two-compartment model as described by equation (2.19). Let $0 = t_0 < t_1 < t_2 \dots$ be equally spaced time points and let $N(t_j)$, $j = 1, 2, \dots$, be the count rate in the interval (t_{j-1}, t_j) . Expressed using equation (2.19),

$$N(t_j) = \sum_{i=1}^2 P_i \cdot \int_0^{t_j} Ca(u) \cdot \exp(-k_i \cdot (t_j - u)) du \quad (4.5)$$

Computer solutions for P_1 , P_2 , k_1 , and k_2 are obtained by means of an unweighted least squares method of curve fitting. The desired solution is the set of these parameters which minimizes

$$\sum_{j=m}^n [N(t_j) - \sum_{i=1}^2 P_i \cdot \int_0^{t_j} Ca(u) \cdot \exp(-k_i \cdot (t_j - u)) du]^2 \quad (4.6)$$

where t_m is the start fit time, and t_n is the end fit time.

Since P_1 and P_2 are linear parameters, minimization of

the above function can be reduced to a two-variable problem.

Let

$$f(k_1, k_2) = \sum_{j=m}^n [N(t_j) - \sum_{i=1}^2 P_i(k_1, k_2) \int_0^{t_j} Ca(u) \cdot \exp(-k_i \cdot (t_j - u)) du]^2 \quad (4.7)$$

where $P_1(k_1, k_2)$ and $P_2(k_1, k_2)$ are the least square solutions for P_1 and P_2 in equation (4.6), given arbitrary but fixed values of k_1 and k_2 . The least squares curve fit is obtained by minimizing the function f of the two non-linear variables, k_1 and k_2 . This is accomplished by using a variable metric algorithm for function minimization developed by Fletcher [18]. The algorithm requires the computation of the gradient vector $(\partial f / \partial k_1, \partial f / \partial k_2)$, as well as the value of the function f at each iteration. This information, accumulated from all previous iterations, determines both the direction and magnitude of the change in k_1 and k_2 at each stage of the iterative process.

Thus, by estimating the initial values of k_1 and k_2 (ie. 0.8 and 0.1 respectively), the values of P_1 and P_2 can be found by minimizing the sum of the squared deviations of equation (4.6). Subsequent values of k_1 and k_2 are estimated using the value of the function f and its gradient vector, with respect to k_1 and k_2 , at each iteration. Convergence typically occurs within ten to fifteen iterations, depending on the final values of the decay constants, k_1 and k_2 .

The software program HEAD performs the above analysis by calling the subroutines VMM and FUNCT. Before calling VMM, it subtracts the background activity value from each

channel of head data. VMM then calculates each subsequent estimation of k_1 and k_2 , using FUNCT to calculate the value of the function f and its gradient vector.

The program HEAD writes several parameters to the terminal screen after each channel is analyzed, indicating the degree of curve fit. These parameters include the variance (SSQ), standard deviation (SSD), the calculated count rate at the start fit time (PMAX), the number of iterations that were required (CALLS), the number of resets that occurred (RESET), and an error code (ERROR). The error code will be zero for a normal completion, one if too many iterations occurred (more than thirty), and two if too many resets occurred (more than five). A reset occurs whenever the iteration process does not converge.

The cerebral blood flow parameters (including the above) are stored in a results buffer. These parameters include k_1 , k_2 , P_1 , and P_2 . The grey matter blood flow, f_1 , is calculated by multiplying the grey matter clearance rate, k_1 , with the partition coefficient, λ_g . Because the partition coefficient for the combined white matter and extracerebral compartment is unknown, a similar estimate of blood flow based on k_2 is not possible. In the above calculation, λ_g is corrected according to the patients' hemoglobin levels using the following equation,

$$\lambda_g = 0.77 \cdot \frac{0.744}{\text{HGB}/34 + 0.487(1 - \text{HGB}/34)} \quad (4.8)$$

where HGB is the hemoglobin level in grams per 100

millilitres of blood. This correction was determined by Veall and Mallett [26,78]. If the hemoglobin level is not given, a partition coefficient of 0.8 is assumed.

The relative weight, w_1 , is estimated using the following equation,

$$w_1 = \frac{P_1 / (k_1 \cdot \lambda_g)}{P_1 / (k_1 \cdot \lambda_g) + P_2 / (k_2 \cdot \lambda_w)} \quad (4.9)$$

where λ_g and λ_w is assumed to be 0.8 and 1.5, respectively.

Another parameter that provides information about the relative contribution of the first compartment is the fractional flow (FF) [59]. It is expressed as a percentage of the total cerebral blood flow and can be calculated as follows,

$$FF = \frac{f_1}{f_1 + f_2} = \frac{P_1}{P_1 + P_2} \quad (4.10)$$

This index is not equivalent to tissue weight since it is influenced by both the weight of the grey matter and its blood flow. The last remaining parameter calculated is the initial slope index (ISI). It is determined using the equations (2.22) and (2.23).

5. System Evaluation

The microprocessor system was evaluated in terms of the original objectives, and its functional roles of data acquisition, data display, and data analysis. This chapter discusses, as objectively as possible, its performance with regards to these roles, and also suggests several improvements that would aid in the design of any future systems or modifications of the existing system.

5.1 Performance

The microprocessor-based cerebral blood flow system has, at the time of writing, successfully collected over fifty sequences of patient data. While not all of these sets of data have provided valid results, the problems seem to be physiological or procedural in origin. For example, several of the patients have had poor respiratory function, which makes the end-expired air curve an unsatisfactory approximation of the arterial input concentration. Also, insufficient ^{133}Xe is occasionally administered, resulting in a low peak count rate. This does not facilitate good data analysis results. Another difficulty is that radiation contamination from the airway passages seems to severely affect the head curves obtained from the detectors positioned proximal to the airway passages. Artefacts in the end-expired air curves due to abnormal breathing patterns often appear in these head curves. This problem, however, is inherent with the inhalation method of administering

Xenon.

The technical performance of the data acquisition portion of the microprocessor system has been quite satisfactory. Since the last bugs have been eliminated and the system put into use, no problems have been encountered. While the ease of operation may be hampered somewhat because the user is required to coordinate the operation of two systems (ie. the Inhamatic and the microprocessor system), the error messages provided by the microprocessor system are hopefully succinct and clear enough to provide the user with the necessary corrective action.

The data display software has, for the most part, also performed well (figures 5.1 to 5.4). The ability to display data on either one of two terminals is a useful feature. The horizontal axis scaling algorithm, on the Tektronix terminal, succeeds in plotting data over most of the available horizontal space for a wide range of data. The vertical scaling, however, does not fare quite as well. By using only five vertical scaling factors, the data occasionally uses as little as 10% of the vertical full scale. Some suggested improvements and additions to the display software are mentioned later in this chapter. Nevertheless, the general appearance of the graphic display, and the flexibility of two graph sizes, offers an aesthetically pleasing display.

Subsequent to the acquisition and storage of data, the microprocessor system provides the option of analyzing the

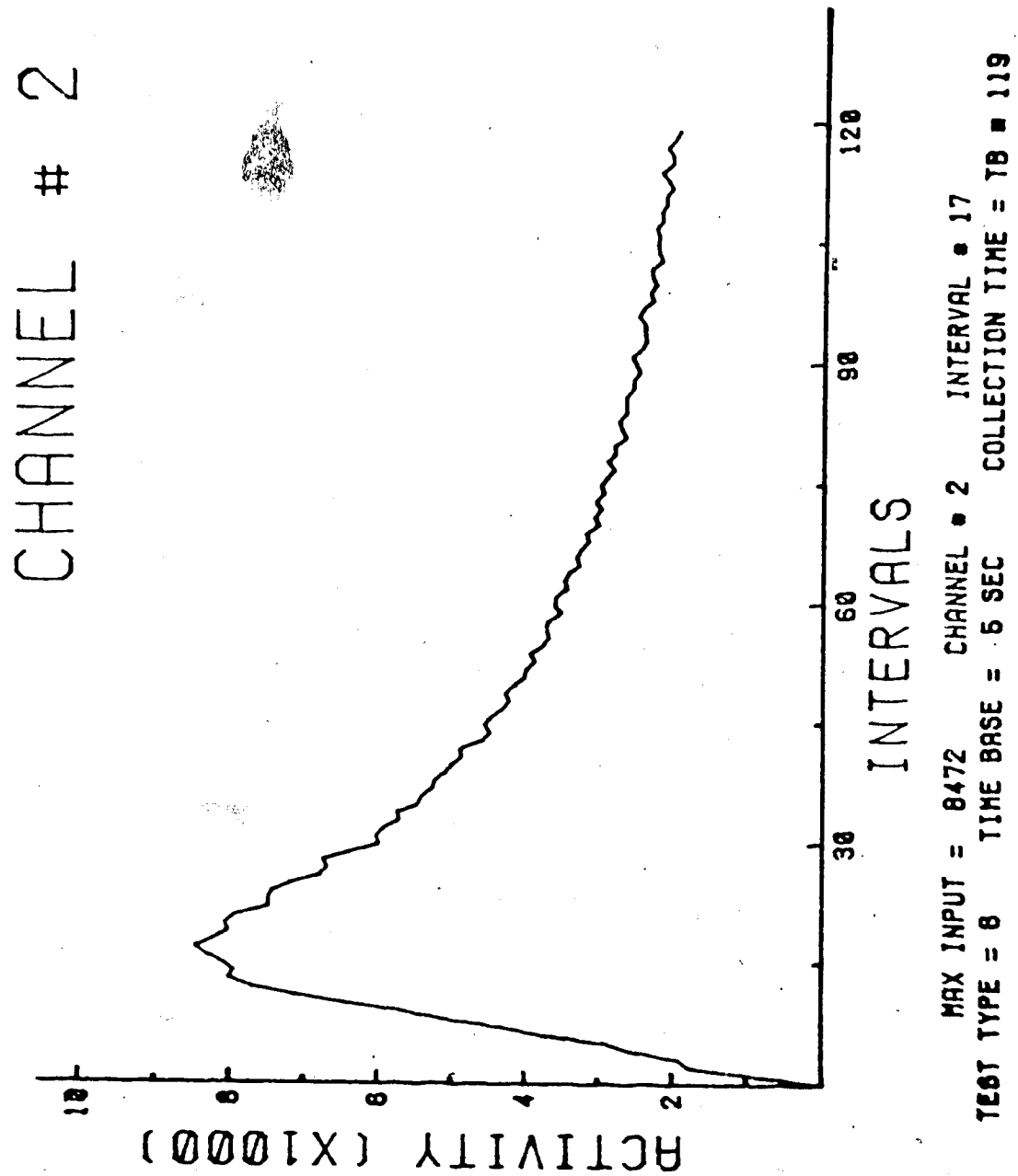
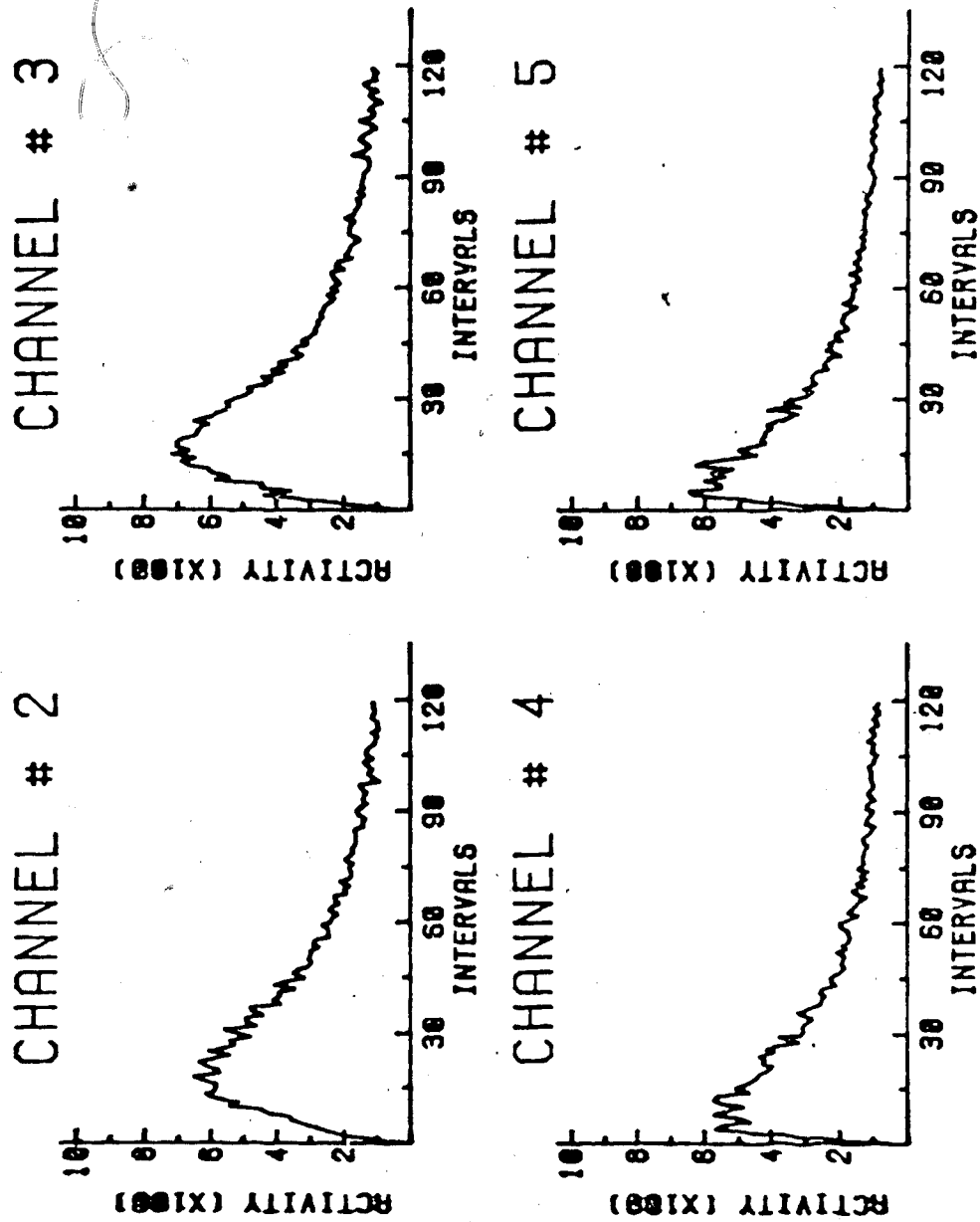


Figure 5.1 Large Graphic Display of Head Data



MAX INPUT = 716 CHANNEL # 3 INTERVAL # 16
 TEST TYPE = 6 TIME BASE = 5 SEC COLLECTION TIME = TB = 119

Figure 5.2 Small Graphic Display of Head Data

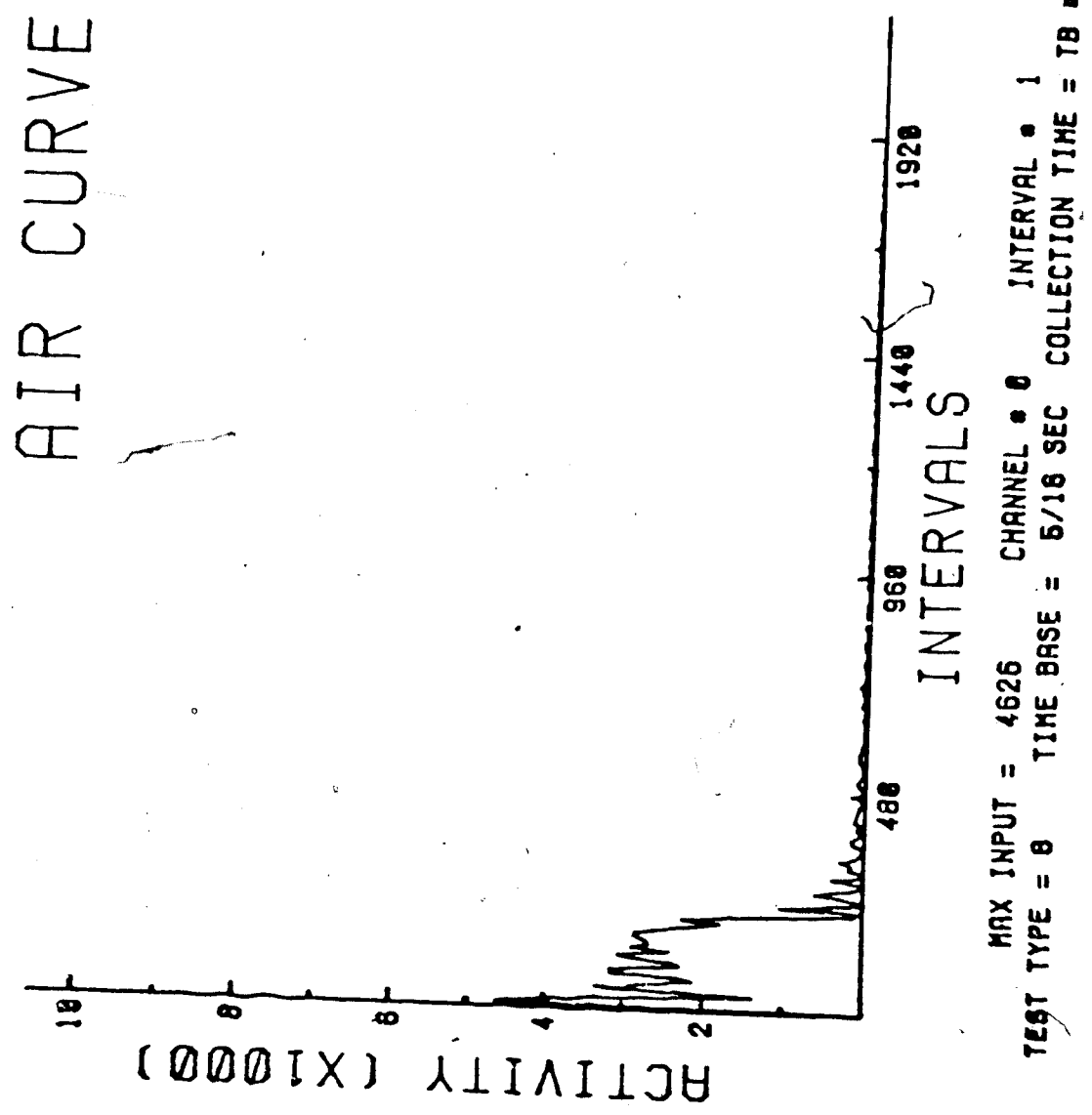


Figure 5.3 Raw Air Curve Data

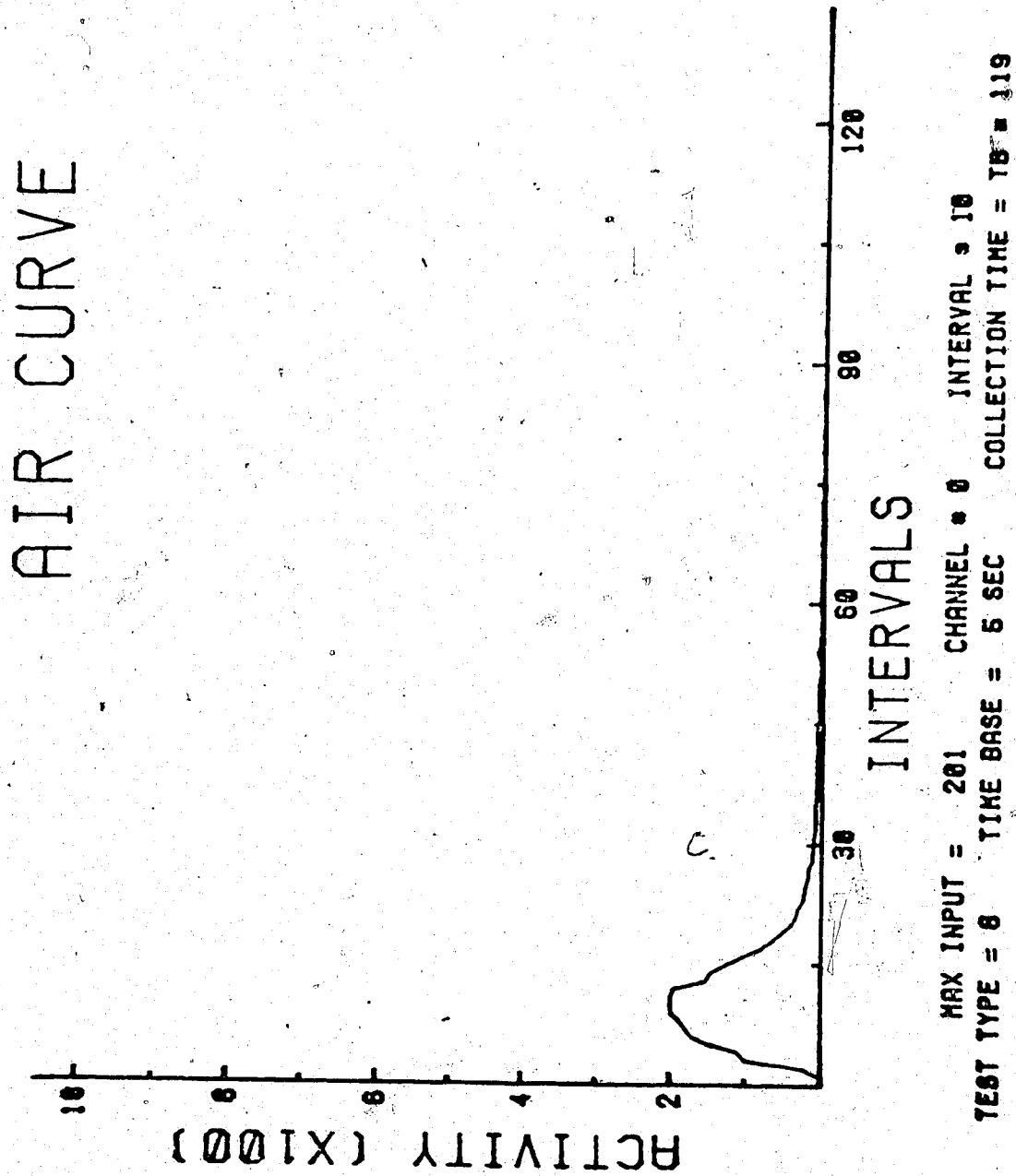


Figure 5.4 Calculated Air Curve Data

data or uploading it to an external computer for more extensive analysis. The major disadvantage of the analysis program is the length of time it needs to complete the calculations. Depending on the number of iterations each channel requires, convergence is typically achieved in 1.5 minutes per channel. Therefore, the length of time required for the complete analysis of sixteen channels is almost one half hour. In many situations this may not be a problem. However, in a setting such as an operating theatre, in which the course of surgery is dependent upon the cerebral blood flow values, a shorter time period would be desirable. The display of analysis results is shown in figures 5.5 and 5.6.

The accuracy of the analysis program and the calculated results are good. The accuracy was checked by comparing the calculated results obtained using a VAX 11-750 computer and the original FORTRAN program, with the results of the microprocessor system. With reasonably good data, the two results are typically within 1.5% of each other. Even with poor data and many iterations, the difference never is greater than approximately 2%. These discrepancies can easily be accounted for by round-off error. According to Fletcher, the effect of round-off error can become serious for large numbers of iterations [18]. Also, the VAX computer uses a floating point format which allows an additional bit of accuracy than for the microprocessor software. In both cases, the floating point arithmetic is single precision (ie. 12 bit mantissa, 4 bit exponent). Repeated analysis of

START FIT TIME = 91 SEC INTERVAL NO. = 18
 MAX AIR COUNT = 2441

>HE

DETECTOR NO.	SSD-N	SSD	MAX COUNT	CALLS	RESETS	ERROR
1	7550	1.19	2604.8	11	0	0
2	5022	1.12	2034.2	9	0	0
3	5264	1.21	1742.9	12	0	0
4	5189	1.20	1670.4	11	0	0
5	6332	1.27	2129.7	10	0	0
6	6069	1.16	2259.5	11	0	0
7	5712	1.10	2525.3	14	0	0
8	6266	1.13	2657.7	14	0	0
9	3823	.97	2194.8	12	0	0
10	3735	1.03	2040.9	11	0	0
11	4938	1.05	2538.2	14	0	0
12	6310	1.22	2177.7	13	0	0
13	10012	1.35	3009.1	12	0	0
14	4970	1.07	1892.1	10	0	0
15	21038	1.60	3276.7	13	0	0
16	5206	1.03	2458.7	10	0	0

***ANALYSIS COMPLETED**

Figure 5.5 Air Curve Calculation Results and Curve Fit Parameters

CEEF ANALYSIS RESULTS									
DET	F1 ML/100GM/MIN	ISI	W1 %	FF %	F1	P2	K1	K2	
1	56.14	39.95	40.96	72.63	4.424	1.666	791	0.097	
2	67.64	38.37	32.12	65.62	3.194	1.673	845	111	
3	68.79	35.64	27.54	62.69	2.582	1.536	859	103	
4	81.24	38.16	26.61	64.64	2.704	1.479	1	107	
5	79.97	41.11	30.71	67.16	3.627	1.773	999	115	
6	56.25	37.11	35.85	69.14	3.598	1.605	703	0.093	
7	53.11	38.11	40.66	71.71	4.155	1.638	663	0.095	
8	54.47	38.78	40.89	71.60	4.397	1.743	680	0.099	
9	65.87	39.81	35.03	67.77	3.571	1.697	823	112	
10	63.41	37.80	32.20	67.54	3.256	1.564	792	0.096	
11	66.09	39.82	35.57	66.73	4.060	2.023	826	121	
12	77.60	42.29	33.75	67.37	3.705	1.793	970	127	
13	77.04	41.09	31.53	67.63	5.112	2.446	963	113	
14	69.43	38.29	30.50	66.17	3.018	1.543	867	103	
15	104.55	42.69	29.53	57.47	6.731	3.245	1	134	
16	61.21	39.19	36.04	69.42	4.033	1.776	765	101	

Figure 5.6 Cerebral Blood Flow Analysis Results

the same data, but with different initial values of k_1 and k_2 , provides almost identical results, which is evidence that the algorithm is stable.

5.2 Possible Improvements

While the existing system is quite satisfactory in most respects, several improvements could be made. Its main disadvantage is the length of time required for data analysis. The solution to this problem, though, would likely require a new system based upon some other microprocessor or microcomputer. Two aspects of the TMS 9900 microprocessor provide for slow analysis: (1) no floating point arithmetic instructions, and (2) a clock speed of only 3 MHz. The more recently designed 16-bit microprocessors, such as Motorola's 68000, Intel's 8086, and Texas Instrument's 99000, have effective clock speeds up to three and four times faster than that of the TMS 9900 [77]. Also, most of them have access to hardware floating point instructions which are much faster than the software subroutines used in this system.

Another disadvantage with this system is the amount of effort required for any modifications to the analysis algorithm. Since this large program is written in assembler language and burnt into the EPROM's, even minor modifications can be a nontrivial task. The advantage of using a microprocessor such as the Motorola 68000 is the availability of a FORTRAN compiler. This would allow the

analysis program to be written in FORTRAN, thus permitting subsequent modifications to be made relatively easily.¹³

In conclusion, if any major improvements are to be made to the analysis software, the author suggests that an entirely new system be considered. As a further suggestion, many personal computers (eg. IBM, Apple, etc.) have become powerful and inexpensive enough, such that they should also be considered for such an application. Not only can many personal computers provide rapid data analysis, but available software packages can assist in graphically displaying data. Data acquisition, however, would likely still require software written in assembler language, and a personal computer with good I/O capabilities.

An ideal CBF system would be one that could be housed entirely within one cabinet. The difficulty in achieving this is primarily the administration system, which is bulky and heavy. However, if the intra-arterial method of ¹³³Xenon administration was used, an air pump and a xenon trap to contain the expired radioisotope, would be all that was necessary. This could conceivably be housed within one cabinet of a manageable size. If fewer detectors were used (or miniature cadmium¹⁰⁹telluride detectors), a portable stand could be used to position them. Such a system would be more easily transported to areas like the operating theatre.

Modifications and additions to the data display software are limited only by the imagination. Some possible

¹³ While FORTRAN compilers undoubtedly exist for the TMS 9900, none could be located for the existing system.

improvements suggested by the author (most of which would require minimal effort to implement), are the following:

1. visually identify, by an arrow or some other means, the location of the start fit time,
2. improve the vertical scaling by using a greater selection of scaling factors,
3. better identification of whether the air data being displayed is raw or calculated,
4. display the fitted data curve, and
5. draw a diagram of the brain with blood flow values appropriately placed on it.

Other improvements to the software might include:

1. an option which would allow the user to change the start fit time interactively using the cross-hairs on the Tektronix terminal,
2. the display of the calculated partition coefficient, λ ,
3. providing average hemispheric blood flow values, and
4. permitting the user to exit the analysis program before it is completed.

5.3 Conclusion

The microprocessor-based cerebral blood flow system, described in this thesis, was developed in order that the acquisition of cerebral blood flow data could be monitored in real-time, stored on floppy disk, and subsequently graphically displayed and analyzed. It is used in conjunction with the Inhamatic rCBF System, which contains

the scintillation detectors, the amplifier and counting circuits, and the ^{133}Xe administration system. The microprocessor system communicates with the Inhamatic system using two main control lines (PUNCH READY and PUNCH INSTRUCTION) in a handshaking protocol.

The method of administering the ^{133}Xe was chosen to be inhalation primarily because of its atraumatic nature. However, this method suffers from two major disadvantages: contamination of extracerebral tissue, and extensive recirculation of the radioisotope. The algorithm that is used to calculate the blood flow parameters is one that is commonly in use, and is based upon the algorithm employed by Obrist et al. [59], with modifications by Risberg et al. [66]. The data analysis utilizes a two-compartment exponential model in which a faster clearing compartment, considered to be cerebral grey matter, is separated from a slower clearing compartment, considered to be white matter and extracerebral tissue. By deconvolving the end-expired air curve data with the head curve data, the problem of recirculation is taken into account.

The software that was developed for this system was primarily in the areas of data acquisition, data display, and data analysis. There was also additional software written in order that the microprocessor system could support two different terminals (ie. ADDS Viewpoint terminal or a Tektronix 4010 terminal). The advantage of the Tektronix terminal is its graphics capabilities. It also has

an optional hard copy unit.

The performance of the microprocessor system has been, to this date, quite satisfactory. While some improvements to the system may be made, in general, the system has achieved the original objectives. This mobile system is relatively simple to operate, and provides accurate and onsite analysis of data and results. The application of this cerebral blood flow system will potentially benefit studies of a variety of cerebral circulatory conditions, and assist the clinician in developing accurate prognoses to improve the condition of the patient.

References

1. ADDS, Inc. Viewpoint Terminal Users Manual, 1981.
2. Allen G.S., Ahn, H.S., Preziosi, T.J., Battye, R., Weir, B., et al. "Cerebral Arterial Spasm - A Controlled Trial of Nimodipine in Patients with Subarachnoid Hemorrhage." *New England Journal of Medicine* 1983, 308: 619-624.
3. Anderson, R. and Sundt, Jr., T. "An Automated Cerebral Blood Flow Analyzer: Concise Communication." *Journal of Nuclear Medicine* 1977, 18(7): 728-731.
4. Angevine, J.B. and Cotman, C.W. *Principles of Neuroanatomy* New York: Oxford University Press, 1981.
5. Atkins, H.L., et al. "Estimates of Radiation Absorbed Doses from Radioxenons in Lung Imaging." *Journal of Nuclear Medicine* 1980, 21: 459-465.
6. Austin, G., Horn, N., Rouhe, S., and Hayward, W. "Description and Early Results of an Intravenous Radioisotope Technique for Measuring Regional Cerebral Blood Flow in Man." *Cerebral Blood Flow and Intracranial Pressure; Proceedings 5th International Symposium, Part II. Europa Neurology* 1972, 8: 43-51.
7. Austin, G., Laffin, D., Rouhe, S., et al. "Intravenous

Isotope Injection Method of Cerebral Blood Flow
Measurement: Accuracy and Reproducibility."
*Proceedings of 6th International Symposium on
Cerebral Blood Flow and Metabolism* 1973, 391-393.

8. Carpenter, M.B. *Core Text of Neuroanatomy* Baltimore:
Williams and Wilkins Company, 1978.
9. Cerretelli, P., Blau, M., Pendergast, D., et al.
"Cadmium Telluride ^{133}Xe Clearance Detector for
Muscle Blood Flow Studies." *IEEE Transactions on
Nuclear Science* 1978, 25(1): 620-623.
10. Correia, J., Ackerman, R., Buonanno, F., et al. "A
Portable Device for the Measurement of Regional
Cerebral Blood Flow in the ICU and or Using CdTe
Detectors and a Fourier Transform Based Data
Analysis." *IEEE Transactions on Nuclear Science*
1981, 28(1): 50-54.
11. Crawley, J.C.W., O'Brien, M.D. and Veall, N. "The Gamma
Spectrum Subtraction Technique Applied to Cerebral
Blood Flow Measurement by the Inhalation of
 ^{133}Xe ." *Proceedings of 4th International
Symposium on Regulation of Cerebral Blood Flow. In:
Brain and Blood Flow* Russell, R.W.R. (ed.), 1970,
54-56.
12. Cronquist, S., Ingvar, D.H. and Lassen, N.A.
"Quantitative Measurements of Cerebral Blood Flow,

Related to Neuroradiological Findings." *British Journal of Anaesthesiology* 1965, 37: 222.

13. Devine, R.A.B., Clarke, L.P. and Vaughan, S.

"Theoretical Analysis of the Two-Coil Method for Measuring Fluid Flow Using Nuclear Magnetic Resonance." *Medical Physics* 1982, 9(5): 668-672.

14. van Duyl, W.A., Mechelse, K., Sparreboom, D., et al.

"Interpretation of Differences Between 81 KeV and 31 KeV Decay Curves Recorded During Clearance of ¹³³Xenon in Cerebral Tissue of the Pig." *Proceedings of 6th International Symposium on Cerebral Blood Flow and Metabolism* 1973, 409-412.

15. Entine, G. and Serreze, H.B. "High Spacial Resolution CdTe Medical Probes." *IEEE Transactions on Nuclear Science* 1974, 21: 726-730.

16. Farrar, J.K., Gamache, F.W., Ferguson, G.G., Barker, J.,

Varkey, G., and Drake, C. "Effects of Profound Hypotension on Cerebral Blood Flow During Surgery for Intracranial Aneurysms." *Journal of Neurosurgery* 1981, 55: 857.

17. Fieschi, C., Agnoli, A., Battistini, N. and Bazzao, L.

"Relationships Between Cerebral Transit Time of Non-Diffusible Indicators and Cerebral Blood Flow." *Experientia* 1966, 22: 189.

18. Fletcher, R. "A New Approach to Variable Metric Algorithms." *Computer Journal* 1970, 13(3): 317-322.

19. Glass, H.I. and De Garreta, A.C. "Quantative Analysis of Exponential Curve Fitting for Biological Applications." *Physical Medicine and Biology* 1967, 2: 379-388.

20. Goddard, B.A. and Ackevy, D.M. "¹³³Xenon, ¹²⁷Xenon, and ¹²⁵Xenon for Lung Function Investigations: A Dosimetric Comparison." *Journal of Nuclear Medicine* 1975, 16: 780-786.

21. Guyton, A.C. *Textbook of Medical Physiology* Toronto: W.B. Saunders Company, 1981.

22. Harper, A.M. "General Physiology of Cerebral Circulation." *International Anaesthesiology Clinics* 1969, 7(3): 473-506.

23. Harper, A.M. "Measurement of Cerebral Blood Flow." *International Anaesthesiology Clinics* 1969, 7(3): 447-472.

24. Hazelrig, J., Katholi, C., Blauenstein, U., Halsey, Jr., J., Wilson, E. and Wills, E. "Total Curve Analysis of Regional Cerebral Blood Flow with ¹³³Xenon Inhalation: Description of Method and Values Obtained with Normal Volunteers." *IEEE Transactions*

on *Biomedical Engineering* 1981, 28(9): 609-615.

25. Hoedt-Rasmussen, K. and Skinhoj, E. "In Vivo Measurement of the Relative Weights of the Grey and White Matter in the Human Brain." *Neurology* 1966, 16: 515-520.
26. Hoedt-Rasmussen, K., Sveinsdottir, E. and Lassen, N.A. "Regional Cerebral Blood Flow in Man Determined by Intra-arterial Injection of Radioactive Inert Gas." *Circulation Research* 1966, 18: 237-247.
27. Hoedt-Rasmussen, K. and Veall, N. "Studies of Cerebral Blood Flow." Source Unknown.
28. Hoffer, P.B., Berger, H.J., Steidley, J., et al. "A Miniature Cadmium Telluride Detector Module for Continuous Monitoring of Left Ventricular Function." *Radiology* 1981, 138: 471-481.
29. Howard, G., Griffith, D.W., [redacted], D. and Hinschelwood, L. "A Mobile Device for Measuring Regional Cerebral Circulation." *Proceedings of 4th Annual Symposium on Computer Applications in Medical Care* Washington, D.C., November 2-5, 1980, 159-164.
30. Iliff, L., Zilkha, E., Bull, J.W.D., et al. "Effect of Changes in Cerebral Blood Flow on Proportion of High and Low Flow Tissue in the Brain." *Journal of Neurology, Neurosurgery and Psychiatry* 1974, 37:

631-635.

31. Ingvar, D.H. and Lassen, N.A. "Atraumatic Two-Dimensional rCBF Measurements Using Stationary Detectors and Inhalation or Intravenous Administration of ^{133}Xe ." (Editorial) *Journal of Cerebral Blood Flow and Metabolism* 1982, 2: 271-274.
32. Jablonski, T., Prohovnik, I., Risberg, J., et al. "Fourier Analysis of ^{133}Xe Inhalation Curves: Accuracy and Sensitivity." In: *Cerebral Blood Flow and Metabolism Acta Neurologica Scandinavica* 1979, 60(Supplement 72): 216-217.
33. Jennett, W.B. "Cerebral Blood Flow Measurement in Clinical Practise." *International Anaesthesiology Clinics* 1969, 7(3): 579-596.
34. Johns, H.E. and Cunningham, J.R. *The Physics of Radiology* Springfield: Charles C. Thomas, 1983.
35. Jones, T. "The Steady State Radioisotopic Measurement of Regional Tissue Blood Flow." In: *Blood Flow Measurement in Man* Mathie, R.T.(ed.), 1982, 28-36.
36. Kety, S.S. "The Theory and Applications of the Exchange of Inert Gas at the Lungs and Tissues." *Pharmacological Review* 1951, 3: 1-41.
37. Kety, S.S. and Schmidt, C.F. "The Determination of

Cerebral Blood Flow in Man by the Use of Nitrous Oxide in Low Concentrations." *American Journal of Physiology* 1945, 143: 53-66.

38. Keyser, R.M. "Cerebral Blood Flow System." *IEEE Transactions on Nuclear Science* 1975, 22: 425-427.
39. Koles, Z.J. and Menon, D. "A Data-Acquisition System for Nuclear Medicine Research." *Proceedings of the 10th Canadian Medical and Biological Engineering Conference* (Ottawa), 1984.
40. Lassen, N.A. "Methods for Measurement of Cerebral Blood Flow in Man." *Medical Progress through Technology* 1976, 3: 149-160.
41. Lassen, N.A. "Regional Cerebral Blood Flow Measurements in Stroke: The Necessity of a Tomographic Approach." (Editorial) *Journal of Cerebral Blood Flow and Metabolism* 1981, 1: 141-142.
42. Lassen, N.A., Hoedt-Rasmussen, K., Ingvar, D.H., et al. "Regional Cerebral Blood Flow in Man Determined by a Radioactive Inert Gas (Krypton 85)." *Neurology* 1963, 13: 719.
43. Lassen, N., Ingvar, D. and Skinhoj, E. "Brain Function and Blood Flow." *Scientific American* 1978, 239(4): 62-71.
44. Lofthus, A. and Ogden, D. "16-Bit Processor Performs

Like Minicomputer." *Electronics* May 1976, 99-105.

45. Loken, M.K. and Kush, G.S. "Handling, Uses and Radiation Dosimetry of ^{133}Xe ." *Medical Radionuclides: Radiation Dose and Effects* Cloutier, R.J., Edwards, C.L. and Snyder, W.S. (eds) June 1970, 253-270.
46. Macey, D.J., Filipow, L.J., McCarthy, S.T. and Pitkanen, M. "Analysis of the Gamma Ray Spectra Recorded in the Use of ^{133}Xe for Cerebral Blood Flow Studies." *Stroke* 1982, 13(4): 519-521.
47. Mallett, B.L. and Veall, N. "Investigation of Cerebral Blood Flow in Hypertension, Using ^{133}Xe Inhalation and Extracranial Recording." *Lancet* 1963, 1: 1081-1082.
48. Mallett, B.L. and Veall, N. "Measurement of Regional Cerebral Clearance Rates in Man Using ^{133}Xe Inhalation and Extracranial Recording." *Clinical Science* 1965, 29: 179-191.
49. Mathie, R.T.(editor) *Blood Flow Measurement in Man* Kent, England: Castle House Publications Ltd., 1982.
50. McHenry, L.C. *Cerebral Circulation and Stroke* St. Louis: Warren H. Green Incorporated, 1978.
51. Meier, P. and Zierler, K.L. "On the Theory of the

Indicator-Dilution Method for Measurement of Blood Flow and Volume." *Journal of Applied Physiology* 1954, 6: 731.

52. Menon, D. and Weir, B. "Evaluation of Cerebral Blood Flow in Arteriovenous Malformations by the ^{133}Xe Inhalation Method." *The Canadian Journal of Neurological Sciences* 1979, 6(4): 411-416.

53. Menon, D., Weir, B., and Overton, T. "Ventricular Size and Cerebral Blood Flow Following Subarachnoid Hemorrhage." *Journal of Computer Assisted Tomography* 1981, 5(3): 328-333.

54. Meric, P. and Seylaz J. "Radiation Scattering and the Determination of Regional Cerebral Blood Flow by Radioisotope Clearance." *Medical Progress through Technology* 1977, 5: 41-46.

55. Meric, P., Seylaz, J., Correze, J., Luft, A. and Mamo, H. "Measurement of Regional Cerebral Blood Flow by Intravenous Injection of ^{133}Xe ." *Medical Progress through Technology* 1979, 6: 53-63.

56. Namon, R., Reinmuth, O.M. and Schwelm, R. "Cerebral Blood Flow Studies in Man Using Recirculation Corrected Height/Area Computations for Intravenous Injection of ^{133}Xe ." *Stroke* 1982, 13(2): 208-219.

57. Nilsson, B.G., Ryding, E. and Ingvar, D.H. "Quantitative Airway Artefact Compensation at Regional Cerebral Blood Flow Measurements with Radioactive Gases." *Journal of Cerebral Blood Flow and Metabolism* 1982, 2: 73-78.
58. Obrist, W.D., Thompson, H.K., King, C.H. and Wang, H.S. "Determination of Regional Cerebral Blood Flow by Inhalation of $^{133}\text{Xenon}$." *Circulation Research* 1967, 20: 124-135.
59. Obrist, W.D., Thompson, H.K., et al. "Regional Cerebral Blood Flow Estimated by $^{133}\text{Xenon}$ Inhalation." *Stroke* 1975, 6: 245-256.
60. Oleson, J., Paulson, O.B. and Lassen, N.A. "Regional Cerebral Blood Flow in Man Determined by the Initial Slope of the Clearance of Intra-arterially Injected $^{133}\text{Xenon}$." *Stroke* 1971, 2: 519-540.
61. Orlando, R.V. and Anderson, T.L. "An Overview of the 9900 Microprocessor Family." *IEEE Micro* August 1981, 1: 38-44.
62. Phelps, M.E., Mazziotta, J.C. and Huang, S.C. "Study of Cerebral Function with Positron Computed Tomography - Review." *Journal of Cerebral Blood Flow and Metabolism* 1982, 2(2): 113-157.
63. Philipson, L., Bulow, B. and Ingvar, D.H. "High

- Resolution Inhalation rCBF Technique with Miniaturized CdTe Detectors." In Cerebral Blood Flow and Metabolism *Acta Neurologica Scandinavica* 1979, 60(Supplement 72): 212-213.
64. Potchen, E.J., Davis, D.O., Wharton, T., Mill, R., and Traveras, J.M. "Regional Cerebral Blood Flow in Man." *Archives of Neurology* 1969, 20: 378-383.
65. Risberg, J. "Regional Cerebral Blood Flow Measurements by ¹³³Xenon Inhalation: Methodology and Applications in Neuropsychology and Psychiatry." *Brain and Language* 1980, 9: 9-34.
66. Risberg, J., Ali, Z., Wilson, E.M., Wills, E.L. and Halsey, J.H. "Regional Cerebral Blood Flow by ¹³³Xenon Inhalation." *Stroke* 1975, 6: 142-148.
67. Risberg, J and Prohovnik, I. "rCBF Measurements by ¹³³Xenon Inhalation: Recent Methodological Advances." *Progress in Nuclear Medicine* 1981, 7: 70-81.
68. Risberg, J., Uzzell, B.P. and Obrist, W.D. "Spectrum Subtraction Technique for Minimizing Extracranial Influence on Cerebral Blood Flow Measurements by ¹³³Xenon Inhalation." *Stroke* 1977, 8(3): 380-382.
69. Rowan, J.O. "Atraumatic ¹³³Xenon Techniques and the Measurement of Cerebral Blood Flow in the

Investigation Room, Operating Theatre and Intensive Care Unit." *Progress in Nuclear Medicine* 1981, 7: 57-69.

70. Scheinberg, P., Meyer, J., Reivich, M., Sundt, T., and Waltz, A. "Cerebral Circulation and Metabolism in Stroke - A Review." *Stroke* 1976, 7(2): 212-234.
71. Seylaz, J., Meric, P., Correze, J.L. and Luft, A. "Analytical Problems Associated with the Noninvasive Measurements of Cerebral Blood Flow in Cerebrovascular Diseases." *Medical and Biological Engineering and Computing* 1980, 18(1): 39-47.
72. Stump, D. and Williams, R. "The Noninvasive Measurement of Regional Cerebral Circulation." *Brain and Language* 1980, 9: 35-46.
73. Teasdale, G. and Mendelow, D. "Cerebral Blood Flow Measurements in Clinical Neurosurgery." *Journal of Cerebral Blood Flow and Metabolism* 1981, 1: 357-359.
74. Tektronix, Inc. Tektronix 4010 Computer Display Terminal Users Manual, 1972.
75. Texas Instruments, Inc. Data Manuals for TMS 9900 microprocessor and related components, 1978.
76. Texas Instruments, Inc. Users Guide for TM 990/101A Microcomputer, 1981.

77. Toong, H.D. and Gupta, A. "An Architectural Comparison of Contemporary 16-bit Microprocessors." *IEEE Micro* May 1981, 1: 26-37.
78. Veall, N and Mallett, B.L. "The Partition of Trace Amounts of Xenon Between Human Blood and Brain Tissues at 37 Degrees Centigrade." *Physical Medicine and Biology* 1965, 10(3): 375-380.
79. Veall, N. and Mallett, B.L. "Regional Cerebral Blood Flow Determination by ^{133}Xe Inhalation and External Recording: the Effect of Arterial Recirculation." *Clinical Science* 1966, 30: 353-369.
80. Waltz, A.G., Wanek, A.R. and Anderson, R.E. "Comparison of Analytic Methods for Calculation of Cerebral Blood Flow After Intracarotid Injections of ^{133}Xe ." *Journal of Nuclear Medicine* 1972, 13(1): 66-72.
81. Weir, B., DeLeo, R., and Menon, D. "Effect of Therapy on Cerebral Blood Flow Following Aneurysm Surgery." *Canadian Journal of Neurological Sciences* 1981, 8: 27-30.
82. Weir, B., Menon, D., and Overton, T. "Regional Cerebral Blood Flow in Patients with Aneurysms: Estimation by ^{133}Xe Inhalation." *The Canadian Journal of Neurological Sciences* 1978, 5(3): 301-305.

83. Whitmore, K.D. "Microprocessor Controlled Gamma-Ray CT Scanner for Measurement of Bone Density." M.Sc. Thesis, University of Alberta, Edmonton, 1981.
84. Wilkinson, I., Bull, J., Du Bouley, G., Marshall, J., Russell, R.W.R., and Symon, L. "Regional Blood Flow in the Normal Cerebral Hemisphere." *Journal of Neurology, Neurosurgery, and Psychiatry* 1969, 32: 367-378.
85. Wilson, E.M., Wills, E.L., Risberg, J., et al. "Measurement of Regional Blood Flow by the ¹³³Xenon Inhalation Method with an On-Line Computer." *Computers in Biology and Medicine* 1976, 7: 143-157.
86. Wyper, D.J. and Rowan, J.O. "An On-Line System for Acquisition and Processing of Cerebral Blood Flow Data." *Computers in Biology and Medicine* 1972, 3: 55-62.
87. Yamamoto, Y.L., Meyer, E. and Feindel, W. "Multichannel Miniature Semiconductor Detector System with On-Line Computer Analysis for Measurement of Miniregional Cerebral Blood Flow." *IEEE Transactions on Nuclear Science* February 1975, 22: 384-387.
88. Younkin, D.P., Reivich, M., Jaggi, J., Obrist, W. and Delivoria-Papadopoulos, M. "Noninvasive Method of Estimating Human Newborn Regional Cerebral Blood Flow." *Journal of Cerebral Blood Flow and*

Metabolism 1982, 2: 415-420.

89. York, E.L., Jones, R.L., Menon, D., and Sproule, B.J.

"Effects of Secondary Polycythemia on Cerebral
Blood Flow in Chronic Obstructive Pulmonary
Disease." *American Review of Respiratory Disease*
1980, 121(5): 813-818.

90. Zierler, K.L. "Equations for Measuring Blood Flow by
External Monitoring of Radioisotopes." *Circulation*
Research 1965, 16(4): 309-321.

Appendix A. Radiation Dosage and Decay Scheme of ^{133}Xe

The primary radioisotope that is used in cerebral blood flow studies is ^{133}Xe . ^{133}Xe has a physical half-life of 5.27 days, and it decays by the emission of a beta particle (i.e. an electron) to the stable state of ^{133}Cs . The decay scheme of ^{133}Xe is shown in figure A.1 and table A.1 [45]. In general, the emission of the original electron will be followed by the emission of a photon (with energy of 81 KeV) or an internal conversion electron; the latter of which is followed by the emission of K characteristic X-ray radiation with energies of approximately 31 KeV. Thus, a spectral analysis of the radioisotope ^{133}Xe shows two main energy peaks: an 81 KeV γ -ray peak, and a 31 KeV X-ray peak. The inert gas is colourless and odorless, and is readily available commercially.

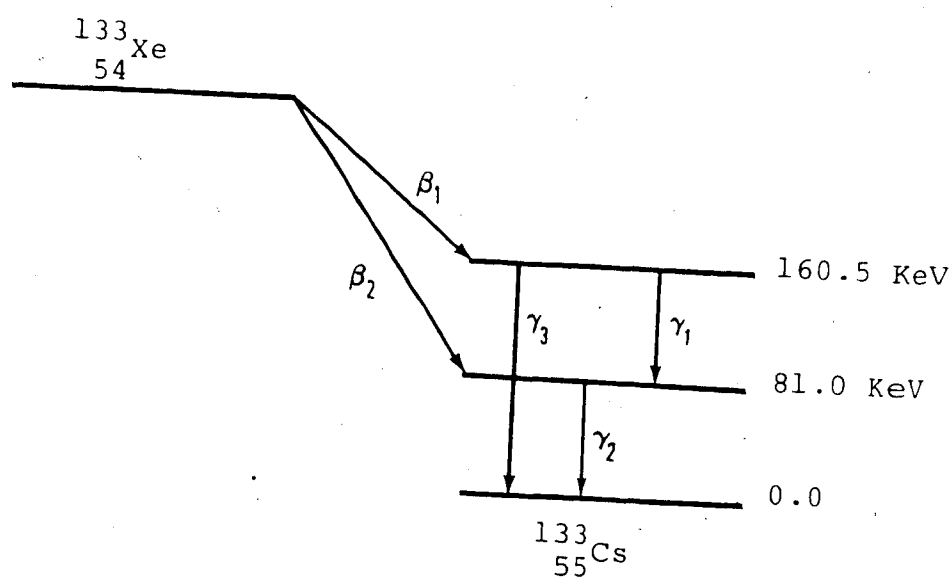


Figure A.1 Decay Scheme of ^{133}Xe

Table A.1 Emissions in the Decay Scheme of ^{133}Xe

Radiation	Mean Number per Disintegration	Mean Energy (KeV)
Beta-1	0.007	75.3
Beta-2	0.993	100.6
Gamma-1	0.00225	79.6
K internal conversion electron, γ_1	0.00225	43.6
L internal conversion electron, γ_1	0.00150	74.2
M internal conversion electron, γ_1	0.00050	78.6
Gamma-2	0.3499	81.0
K internal conversion electron, γ_2	0.4724	45.0
L internal conversion electron, γ_2	0.07874	75.7
M internal conversion electron, γ_2	0.09842	80.0
Gamma-3	0.00040	160.5
$K\alpha_1$ X-rays	0.22669	31.0
$K\alpha_2$ X-rays	0.11731	30.6
$K\beta_1$ X-rays	0.06325	35.0
$K\beta_2$ X-rays	0.01337	36.0
L X-rays	0.07366	4.3
KLL Auger electron	0.03577	25.4
KLX Auger electron	0.01574	29.7
KXY Auger electron	0.00262	34.0
LMM Auger electron	0.43786	3.3
MXY Auger electron	1.13252	0

There have been several investigations made regarding the tissue radiation doses to primary involved organs when using ^{133}Xe . In general, they show that there is no significant radiation hazard to the patient, even for several repeated measurements. The amount of ^{133}Xe administered to the patient varies, but, typically, for inhalation studies, the patient inhales a concentration of three to ten millicuries per litre of air¹⁴. When using the intravenous injection method, an injection of ten to twenty millicuries of ^{133}Xe is usually made into a peripheral vein, over a period of less than thirty seconds. With the intra-arterial injection method, three to five millicuries of ^{133}Xe dissolved in saline is rapidly injected into the internal carotid artery.

Estimates of radiation dosage levels by several authors are tabulated below (values are given in millirads¹⁵).

¹⁴ The SI (Système International) unit for radiation activity is the becquerel (Bq); 1 curie (Ci) = $3.7 \cdot 10^{10}$ Bq.
¹⁵ The SI unit for radiation dosage levels is the gray (Gy); 1 Gy = 100 rads.

Table A.2 Radiation Dosage Levels

Gonads	Blood	Lungs	Airway Mucosa	Total Body	Reference
3.7	3.7	39	642		75 ¹
7	9	65		0.9	76 ¹
	3.3	127			38 ²
	14.1	415			38 ³

¹Rebreathing 3 to 5 minutes and washout with 1 mCi/liter.

²Rebreathing 1 minute and washout with 10 mCi/liter.

³Rebreathing for 5 minutes with 10 mCi/liter (not including washout).

Appendix B. ¹³³Xenon Filling and Measuring Procedure

B.1 Filling Procedure

The following is the recommended procedure to fill the administration system with the proper radiation activity level of ¹³³Xenon. It is based on the procedure as set forth in the Inhamatic users manual but with some modifications.

1. Decide what activity level is required for the measurement.
2. Measure the activity remaining in the rebreathing system. This can be done by filling the rebreathing system with air, switching the air detector valve to the "bag" position and noting on the air detector ratemeter the count rate:

1 mCi/l = 740 counts/second

3 mCi/l = 2220 counts/second

5 mCi/l = 3700 counts/second

3. Calculate how much additional ¹³³Xenon is required.
4. Make room for the amount of ¹³³Xenon and oxygen which is to be added (the entire rebreathing system holds 5.25 litres). Room can be made by setting the air detector valve to the "bag" position and waiting for some of the air-xenon mixture to be vacated from the breathing bag (which can be viewed through the lead glass window).
5. Add the estimated amount of ¹³³Xenon from the 300 cc. tank pressurized to 120 psi. This is done by connecting the pressurized tank of ¹³³Xenon and depressing black switch on the front panel of the Inhamatic system

momentarily (see figure 3.7). This will pressurize the tubing up to the switch marked "Xenon". Depressing this switch will allow the ^{133}Xe gas to enter the rebreathing system.

6. Add 0.5 litre oxygen (approximately 0.5 litre of oxygen is required for each minute of ^{133}Xe administration).
7. Add air to fill the breath bag.
8. Measure the activity in the rebreathing system.
9. Set the air detector valve to the "mask" position.
10. Should the activity be lower than required, repeat the procedure from item 4.

B.2 Measuring Procedure

The following is the recommended procedure to acquire cerebral blood flow data:

1. Power up Inhamatic and microprocessor systems.
2. If the terminal being used is a Tektronix 4010 terminal, use the TTYPE command to change the terminal type flag.
3. If the floppy disk is a new disk, format it by issuing the FORMAT command. If the disk has been previously formatted, but new data is to be written over old data, issue the FRESH command.
4. Fill the administration system with ^{133}Xe and position the patient.
5. Measure the background activity level by using the BKGD command. When the microprocessor replies with a READY message, press the RUN switch on the Inhamatic system.

If the Inhamatic system is in the automatic mode, it will collect data for thirty seconds and then stop. The user will have to press the control and S keys on the terminal, simultaneously, to terminate data acquisition. If the Inhamatic system is in the manual mode, it will collect data for as long as the user wishes. The user, then, must depress the STOP switch on the Inhamatic system, and the space bar on the terminal, to terminate data acquisition.

6. Clear the memory buffer by issuing the CLEAR command.
7. To begin the data acquisition, use the DA n command, where n is the disk unit being used (ie. 0 or 1). The microprocessor will then request some patient data, such as blood pressure, PaCO₂, etc. To ignore this request, press the RETURN key for each information item. When the microprocessor system replies with a READY message, press the RUN switch to initiate the administration of ¹³³Xenon. The Inhamatic system will then administer ¹³³Xenon to the patient for one minute before switching to room air. If it is in the automatic mode, it will collect data for an additional nine minutes and stop. If it is in the manual mode, it will collect data indefinitely. Termination of data acquisition is the same as the background measurement procedure.
8. Store the data on disk using the STORE command. The data may now be displayed or analyzed at the users discretion.